

**RADIAL BASIS FUNCTIONS BASED SCHEMES FOR
FRACTIONAL DIFFERENTIAL EQUATIONS**

Thesis

Submitted in partial fulfillment of the requirements for the degree of

DOCTOR OF PHILOSOPHY

by

PRASHANTHI K. S.



DEPARTMENT OF MATHEMATICAL AND COMPUTATIONAL SCIENCES

NATIONAL INSTITUTE OF TECHNOLOGY KARNATAKA,

SURATHKAL, MANGALORE - 575025

DECEMBER 2018

Dedicated to my father, my husband and son

DECLARATION

By the Ph.D. Research Scholar

I hereby declare that the Research Thesis entitled “ **RADIAL BASIS FUNCTIONS BASED SCHEMES FOR FRACTIONAL DIFFERENTIAL EQUATIONS** ” which is being submitted to the **National Institute of Technology Karnataka, Surathkal** in partial fulfillment of the requirements for the award of the Degree of **Doctor of Philosophy in Mathematical and Computational Sciences** is a *bonafide report of the research work carried out by me*. The material contained in this Research Thesis has not been submitted to any University or Institution for the award of any degree.

Place : NITK, Surathkal

Date : 03-01-2019

Prashanthi K. S.

Reg. No. 135047MA13F02

Department of MACS

NITK, Surathkal

CERTIFICATE

This is to *certify* that the Research Thesis entitled “**RADIAL BASIS FUNCTIONS BASED SCHEMES FOR FRACTIONAL DIFFERENTIAL EQUATIONS**” submitted by **PRASHANTHI K. S.** (Register No.: 135047MA13F02), as the record of the research work carried out by her, is *accepted as the Research Thesis submission* in partial fulfillment of the requirements for the award of degree of **Doctor of Philosophy**.

Dr. Chandhini G.
Research Guide

Chairman - DRPC

ACKNOWLEDGMENTS

I take this opportunity to thank all those who have directly or indirectly helped me to make this work possible.

I would like to offer my heart full thanks to my guide *Dr. Chandhini G*, for her constant support, guidance, and encouragement in my research journey. She is the source of inspiration for my research work and demonstrated the correct way towards research. Whenever I was muddled with my issues and struggling to come out of it, she used to bring back my focus onto my mainstream responsibilities. Also my sincere thanks to *Dr. Antony Vijesh V*, School of Basic Sciences, Indian Institute of Technology Indore, for his help and valuable suggestions given throughout my research.

I would like to extend my sincere gratitude to *Dr. Ajay Kumar Yadav*, Department of Mechanical Engineering and *Prof. Santhosh George*, Department of Mathematical and Computational Sciences, National Institute of Technology Karnataka, for their scholarly advice, continuous support and consistent encouragement as my RPAC members.

My special thanks are due to the Head of the Department *Prof. B. R. Shankar* and previous HoDs *Prof. Murulidhar N. N* and *Prof. Santhosh George*, for providing all the required facilities during my research period. I am happy to acknowledge all the faculty members, non-teaching staffs and research scholars of the department of MACS, for their kind co-operation, continuous support and encouragement.

Finally, I would like to thank my dear husband, son and other family members for their moral support, love and encouragement during my research journey.

Place: NITK, Surathkal

PRASHANTHI K. S.

Date:03-01-2019

ABSTRACT

The primary objective of the present thesis is to explore on radial basis functions based numerical schemes for certain types of fractional differential equations. Unlike classical derivatives, non-local nature of the fractional derivatives makes extension of the existing schemes to fractional models complex and computationally expensive. In addition, compared to time fractional differential equations, attempts on RBF schemes for space and space-time fractional differential equations are less in the literature. This may be due to the difficulty in handling multidimensional space fractional derivatives because of the vector integral representation.

Two approaches, namely, direct and integrated RBF collocation methods (DRBF and IRBF) are extended to approximate fractional order derivatives. In particular, we have proposed these schemes for nonlinear fractional models: fractional nonlinear ODEs (both initial and boundary value problems) and fractional Darboux problem. These nonlinear fractional DEs are appropriately approximated by a sequence of linear fractional DEs that converges to the solutions of the problem. The proposed sequences are generated via either generalised quasilinearisation or successive approximation techniques. In all these cases, existence and uniqueness of the solution and convergence of the proposed sequences are proved for continuous case. The numerical solutions thus obtained are extensively studied and analysed in terms of accuracy, convergence, time complexity as well as shape parameter dependency.

While being capable to provide highly accurate approximations with exponential convergence rate, these characteristics of RBF based schemes are overwhelmed by infamous instability due to ill-conditioning of the governing system. Hence another important contribution to the thesis includes putting forth two algorithms based on Tikhonov regularisation and RBF-QR method to approximate fractional order derivatives. Using Chebyshev-Gauss quadrature, RBF-QR method is generalised to include all types of radial functions, wherein the algorithm was earlier restricted to Gaussian RBF. Then the proposed algorithms are validated using various fractional

models by computing solutions for significantly small shape parameters. Also they are analysed to see the effect of increase in nodal points.

Keywords: Fractional nonlinear differential equations; Fractional Darboux problem; Radial basis functions; Global numerical schemes; Successive approximation; Generalised quasilinearisation; Stable computation; Tikhonov regularisation; RBF-QR; Gauss-Chebyshev quadrature

CONTENTS

ABSTRACT	i
LIST OF TABLES	v
LIST OF FIGURES	viii
1 INTRODUCTION	1
1.1 HISTORICAL REVIEW	1
1.2 FRACTIONAL INTEGRALS AND DERIVATIVES	2
1.2.1 Riemann-Liouville(R-L) operators	3
1.2.2 Grünwald-Letnikov(G-L) operators	4
1.2.3 Caputo operator	4
1.2.4 Mittag-Lefler function	5
1.3 FRACTIONAL DIFFERENTIAL EQUATIONS	6
1.3.1 Applications	7
1.3.2 Analytical, semi-analytical and numerical methods	7
1.4 RADIAL BASIS FUNCTIONS	10
1.5 RBF FOR DIFFERENTIAL EQUATIONS	13
1.5.1 RBF for fractional differential equations	14
1.6 ORGANISATION OF THE THESIS	15
2 DIRECT AND INTEGRATED RADIAL FUNCTIONS BASED QUASILINEARISATION SCHEMES FOR NONLINEAR FRACTIONAL DIFFERENTIAL EQUATIONS	17
2.1 INTRODUCTION	17
2.2 CONVERGENCE ANALYSIS	18
2.3 DIFFERENTIAL AND INTEGRATED RBF SCHEMES	23

2.3.1	DRBF scheme	23
2.3.2	IRBF scheme	24
2.3.3	Gauss-Jacobi quadrature rule	25
2.4	NUMERICAL ILLUSTRATIONS	26
2.5	CONCLUSIONS	31
3	A RADIAL BASIS FUNCTION METHOD FOR FRACTIONAL DARBOUX PROBLEMS	46
3.1	INTRODUCTION	46
3.2	PARTIAL FRACTIONAL INTEGRALS AND DERIVATIVES	48
3.3	SUCCESSIVE APPROXIMATION	49
3.4	A FRACTIONAL RBF APPROXIMATION	50
3.4.1	Mixed Caputo derivative of radial basis functions	52
3.5	NUMERICAL ILLUSTRATIONS	53
3.5.1	Implementation of Rippa's optimisation algorithm	56
3.5.2	Effect of variable shape parameters	57
3.6	CONCLUSIONS	58
4	ON STABILISATION OF RADIAL BASIS FUNCTIONS BASED SCHEMES FOR FRACTIONAL DERIVATIVES	79
4.1	INTRODUCTION	79
4.2	METHODOLOGY	81
4.2.1	A direct RBF collocation space fractional diffusion model	81
4.2.2	RBF-QR method	83
4.2.3	Tikhonov Regularisation	87
4.3	NUMERICAL ILLUSTRATIONS	89
4.4	CONCLUSIONS	91
5	CONCLUSIONS	100
5.1	SCOPE FOR THE FUTUTE RESEARCH	102
	REFERENCES	103

PUBLICATIONS 116

LIST OF TABLES

1.1	Comparison of R-L and Caputo differential operators.	6
1.2	Examples for RBFs.	10
2.1	RMS and L_∞ error of Example 2.4.1 ($n = 11$).	38
2.2	Rate of convergence of Example 2.4.1.	38
2.3	Rate of convergence for $q = 0.1$ of Example 2.4.1 by IRBF and DRBF.	39
2.4	RMS and L_∞ error of Example 2.4.2 ($n = 11$).	39
2.5	Comparison of absolute error of Example 2.4.2 at $t = 1$	40
2.6	Rate of convergence of Example 2.4.2.	40
2.7	Rate of convergence of Example 2.4.2 by IRBF and DRBF for $q = 1.1$ and 0.1	41
2.8	RMS and L_∞ error of Example 2.4.3 ($n = 11$).	41
2.9	Comparison of solutions of Example 2.4.3 using IRBF, DRBF and Neural Networks (Qu and Liu, 2015) with exact solutions.	42
2.10	Rate of convergence of Example 2.4.3.	43
2.11	Rate of convergence for $q = 0.1$ of Example 2.4.3 by IRBF and DRBF.	43
2.12	Comparison of numerical results of Example 2.4.4 for various q ($K=0.5$).	44
2.13	Comparison of the numerical solution of Example 2.4.5 at $q = 0.9$ ($T =$ 0.1).	44
2.14	Comparison of the numerical solution of Example 2.4.6 at $q = 0.9$ ($T =$ 1).	44
2.15	L_∞ error of Example 2.4.7.	45
2.16	Rate of convergence of Example 2.4.7.	45
3.1	Comparison of errors for Example 3.5.1 using MQ, GA, PS ($\beta = 8$) and PS+polynomial ($\beta = 8$) for various q_1 and q_2 (11×11).	67

3.2	Rate of convergence of Example 3.5.1 for $\bar{q} = (1, 1)$	68
3.3	Rate of convergence of Example 3.5.1 for $\bar{q} = (0.7, 0.7)$	69
3.4	Rate of convergence of Example 3.5.1 for $\bar{q} = (0.5, 0.5)$	70
3.5	Rate of convergence of Example 3.5.1 for $\bar{q} = (0.3, 0.3)$	71
3.6	Comparison of errors for Example 3.5.2 using MQ, GA, PS ($\beta=12$), PS+polynomial ($\beta=12$), CS1 (Cheung, 1977) and CS2 (Cheung, 1977) with uniform collocation nodes (25×25) ($q_1 = q_2 = 1$).	72
3.7	Comparison of errors for Example 3.5.2 (21×21) using MQ, GA, PS ($\beta=12$), PS+polynomial ($\beta=12$) ($q_1 = q_2 = 1$).	72
3.8	Rate of convergence of Example 3.5.2.	73
3.9	Comparison of solutions of Example 3.5.3 using MQ, GA, PS ($\beta=12$) and PS+polynomial ($\beta=12$) with uniform collocation points (21×21) and Cubature method (Jain and Sharma, 1968) with exact solutions ($q_1 = q_2 = 1$).	74
3.10	Comparison of errors in the solutions of Example 3.5.3 (21×21) using MQ, GA, PS ($\beta=12$), PS+polynomial ($\beta=12$) ($q_1 = q_2 = 1$).	74
3.11	Rate of convergence of Example 3.5.3.	75
3.12	Comparison of range for ' ε ' using MQ, GA with initial approximation $u \equiv 0$	76
3.13	Comparison of errors using MQ, GA for various q_1 and q_2 with LOOCV algorithm.	77
3.14	Comparison of errors using MQ, GA for various q_1 and q_2 with trigonometric variable shape parameter.	78
4.1	L_∞ error and rate of convergence for Example 4.3.1 ($\Delta x = \Delta t$)	95
4.2	L_∞ error for Example 4.3.1 ($\Delta t = 0.0025$)	95
4.3	Absolute error for Example 4.3.1 ($\Delta x = 0.1, \Delta t = 0.0025$)	96
4.4	L_∞ error for Example 4.3.2 ($\Delta t = 0.0025$)	96
4.5	Absolute error for Example 4.3.2 ($\Delta x = 0.1, \Delta t = 0.0025$)	97
4.6	Comparison of L_∞ error for Example 4.3.3	97
4.7	Absolute error for Example 4.3.3 ($n=11$)	98

4.8	L_∞ error for Example 4.3.4	98
4.9	L_∞ error for Example 4.3.4.	99
4.10	Absolute error for Example 4.3.4.	99

LIST OF FIGURES

2.1	Solutions of Example 2.4.1 for various q by IRBF.	32
2.2	Errors at each iteration for Example 2.4.1 for various ε at $q = 0.5$ ($n = 21$) (a)IRBF, (b)DRBF	32
2.3	Solutions of Example 2.4.2 for various q by IRBF.	33
2.4	Error at each iteration for Example 2.4.2 (a) IRBF, (b) DRBF for $q = 0.5$ and (c) IRBF, (d) DRBF for $q = 1.5$	34
2.5	Solutions of Example 2.4.3 for various q by IRBF.	35
2.6	Errors at each iteration for Example 2.4.3 for various ε at $q = 0.5$ ($n = 21$):- (a) IRBF, (b) DRBF	35
2.7	Solutions of Example 2.4.4 for various q ($K=0.5$).	36
2.8	Comparison of Solutions of Example 2.4.5 for various q	36
2.9	Solutions of Example 2.4.6 for various q	37
2.10	Solutions of Example 2.4.7 for various q by IRBF.	37
3.1	Schematic of nodal distributions. (a) uniform, (b) nonuniform	58
3.2	Surface plots of Example 3.5.1 with (a) uniform (b) nonuniform node distributions. Row 1-3: Exact Solutions, RBF solutions, Error plots. . .	59
3.3	Surface plots of Example 3.5.2 with (a) uniform (b) nonuniform node distributions. Row 1-3: Exact Solutions, RBF solutions, Error plots. . .	60
3.4	Solutions of Example 3.5.2 (a) $x = 0.1, 0 \leq y \leq 0.5$ (b) $y = 0.1, 0 \leq x \leq 0.5$ (c) $x = 0.3, 0 \leq y \leq 0.5$ (d) $y = 0.3, 0 \leq x \leq 0.5$, for $q_1 = 1$ and various values of q_2	61
3.5	Solutions of Example 3.5.2 (a) $x = 0.1, 0 \leq y \leq 0.5$ (b) $y = 0.1, 0 \leq x \leq 0.5$ (c) $x = 0.3, 0 \leq y \leq 0.5$ (d) $y = 0.3, 0 \leq x \leq 0.5$, for $q_1 = 0.3$ and various values of q_2	61

3.6	Surface plots of Example 3.5.3 with (a) uniform (b) nonuniform node distributions. Row 1-3: Exact Solutions, RBF solutions, Error plots. . .	62
3.7	Solutions of Example 3.5.3 (a) $x = 0.1, 0 \leq y \leq 1$ (b) $y = 0.1, 0 \leq x \leq 1$ (c) $x = 0.5, 0 \leq y \leq 1$ (d) $y = 0.5, 0 \leq x \leq 1$ (e) $x = 0.9, 0 \leq y \leq 1$ (f) $y = 0.9, 0 \leq x \leq 1$, for $q_1 = 1$ and various values of q_2	63
3.8	Solutions of Example 3.5.3 (a) $x = 0.1, 0 \leq y \leq 1$ (b) $y = 0.1, 0 \leq x \leq 1$ (c) $x = 0.5, 0 \leq y \leq 1$ (d) $y = 0.5, 0 \leq x \leq 1$ (e) $x = 0.9, 0 \leq y \leq 1$ (f) $y = 0.9, 0 \leq x \leq 1$, for $q_1 = 0.3$ and various values of q_2	64
3.9	Example 3.5.1: Convergence of ε using Rippa's algorithm-iteration Vs ε_{opt} for GA (left) and MQ (right): (a) & (b) $(q_1, q_2) = (1, 1)$, (c) & (d) $(q_1, q_2) = (0.9, 0.1)$, (e) & (f) $(q_1, q_2) = (0.1, 0.1)$	65
3.10	Example 3.5.2: Convergence of ε using Rippa's algorithm - iteration Vs ε_{opt} for GA and MQ: $(q_1, q_2) = (1, 1)$	66
3.11	Example 3.5.3: Convergence of ε using Rippa's algorithm - iteration Vs ε_{opt} for GA and MQ: $(q_1, q_2) = (1, 1)$	66
4.1	Solutions using MQ-QR-CH method for Example 4.3.1.	92
4.2	Example 4.3.1: n Vs L_∞ error for different ε (a) uniform and (b) nonuniform nodes. Row 1: MQ-QR-CH; Row 2: MQ-TR ($\Delta t = 0.0025$).	92
4.3	Example 4.3.2: n Vs L_∞ error for different ε (a) uniform and (b) nonuniform nodes. Row 1: MQ-QR-CH; Row 2: MQ-TR ($\Delta t = 0.0025$).	93
4.4	Comparison of L_∞ error for Example 4.3.3	94
4.5	Solutions using MQ-QR-CH method for Example 4.3.4.	94

NOMENCLATURE

q	Fractional order
m	$\lceil q \rceil$
D^q	Liouville's fractional differential operator
D_a^q	for $q > 0$ Riemann-Liouville fractional differential operator
I_a^q	for $q > 0$ Riemann-Liouville fractional integral operator
\tilde{D}_a^q	Grünwald-Letnikov fractional differential operator
\tilde{I}_a^q	Grünwald-Letnikov fractional integral operator
${}^c D_a^q$	Caputo fractional differential operator
$E_{p,q}$	Mittag Leffler function with two parameters
Γ	Gamma function
$\ \cdot\ _p$	P-norm
$L_p[a, b]$	Set of measurable functions on $[a, b]$ with $\int_a^b f(x) ^p dx < \infty$
ϕ	Radial function
ε	Shape parameter of infinitely smooth RBFs
c	$1/\varepsilon$ (Chapter 1)
$s(\bar{x})$	Radial basis function interpolant
$\tilde{\lambda}$	Unknown coefficient vector of RBF interpolation
$\tilde{\gamma}$	Unknown coefficient vector of additional polynomial
M	Order of the radial basis function
d	Dimension of the space
n	Number of nodes
T	Upper limit for variable t
Δt	Steplength of variable t
Δx	Steplength of variable x
$P_N^{(S1, S2)}(x)$	Jacobi polynomial of degree N
$T_n(x)$	n^{th} Chebyshev polynomial
$\tilde{T}_n(x)$	n^{th} Shifted Chebyshev polynomial
A^*	Hermitian matrix of A
A^T	Transpose of the matrix A
\mathbb{R}	Set of real numbers
\mathbb{Z}	Set of integers
\mathbb{N}	Set of natural numbers

CHAPTER 1

INTRODUCTION

1.1 HISTORICAL REVIEW

The concept of “fractional derivative” was originated in the mind of de l’Hospital (derivative of order $\frac{1}{2}$) while responding to G.W. Leibniz’s (in 1695) letter introducing the notation $\frac{d^n}{dx^n}f(x)$ to denote the n^{th} derivative of a function ‘ f ’, where $n \in \mathbb{N}$. Leibniz thought of it as a “paradox” and was hopeful that some of the useful consequences will be drawn from this in the future. These historical records suggest that the idea of derivative of non-integer order stem at the time of the development of classical derivatives and integrals. Subsequently, many renowned mathematicians have shown interest in the idea, though in a subtle manner: Euler (1730), Lagrange (1772), Laplace (1812), Lacroix (1819) and Fourier (1822) (Oldham and Spanier, 1974; Miller and Ross, 1993).

Meanwhile, during 1823, it was N. H. Abel posed the solution of famous Tautochrone problem (Miller and Ross, 1993) in terms of integral equations, which was later identified in terms of Riemann-Liouville fractional integral. This work is treated as one of the remarkable achievement of Abel and referred it as an “elegant” work. It was Liouville (1832) who took up a detailed study on fractional derivatives. Started by discussing $\frac{d^{1/2}}{dx^{1/2}}e^{2x}$ and giving some examples from mechanics and geometry in his memoir, he went on to propose the existence of complementary functions for $\frac{d^q f}{dx^q} = 0$, $q > 0$. Basis of his work was the observations $D^n e^{ax} = a^n e^{ax}$ and its extensions to non-integer $q > 0$. Hence his focus was on functions that can be expressed as $f(x) = \sum_{n=0}^{\infty} C_n e^{a_n x}$, $Re(a_n) > 0$ and later for function of type x^{-a} , $a > 0$. The difference in the definition of fractional derivatives of Lacroix ($\frac{d^q x^m}{dx^q}$, $m \geq q$) and Liouville ($\frac{d^q x^{-a}}{dx^q}$, $a > 0$) with $q \in \mathbb{R}^+$ leads to lot of discussions ending up mathematicians taking sides between Liouville and Lacroix (1833-1846).

Second half of 19th century have seen a vast amount of discussions and work on formalising the definitions of fractional operators starting with Riemann's (1847) definition for fractional integration,

$$\frac{d^{-q}}{dx^{-q}}f(x) = \frac{1}{\Gamma(q)} \int_a^x (x-t)^{q-1} f(t) dt + \chi(x), \quad x \geq a, \quad q \in \mathbb{R}^+. \quad (1.1.1)$$

where $\chi(x)$ represents a complementary function according to Riemann. The works by: C. J. Hargreave (1848) on the generalisation of Leibniz rule of n^{th} derivative of product of two functions to fractional order, H. R. Greer (1858) on finding the finite differences of order $\frac{1}{2}$, H. Holmgren (1868) on some possible applications and possibility of $D^q y'' = D^{q+2} y$, $q \notin \mathbb{Z}^+$. Many more important works have transpired before settling with Riemann-Liouville definitions for fractional integrals and derivatives.

To add feather to the cap, many important contributions were made that accelerated the importance of fractional calculus. Grünward and Letnikov (1868) have developed an approach that define fractional integration and differentiation (a unified approach) and later it was shown that their integral definition coincides with that of Riemann's under appropriate conditions. Other works that followed were on the solutions of some fractional differential equations, connecting fractional integral with Laplace transforms etc. (E. Post (1919), H. T. Davis (1927), D. V. Widder (1941)) (Oldham and Spanier, 1974).

Riemann-Liouville (R-L) definition for differentiation is considered commonly for many theoretical analysis. However, R-L approach leads to initial conditions of the form $\lim_{t \rightarrow a} {}_a D_t^{q-1} f(t) = b_1$ and so on. Though differential equations with such types of initial conditions are solved mathematically, physical interpretations of them are still not understood. In 1967, Caputo proposed a variation to R-L derivative, which resolved this major concern and many more issues. Thereupon the journey from integer order to fractional order calculus witnessed many more definitions by Sonin & Letnikov, Liouville, Hadamard, Riesz, Riesz & Miller, Miller & Rose, Weyl, Chen & Machado and so on. (Oldham and Spanier, 1974; Miller and Ross, 1993).

1.2 FRACTIONAL INTEGRALS AND DERIVATIVES

For the completeness of the thesis we define most commonly considered definitions for fractional integration and differentiation. These definitions retain, in a generalised sense, one of the most important theorem in classical calculus (Diethelm, 2010).

Theorem 1.2.1. (Fundamental theorem of classical calculus) Let $f : [a, b] \rightarrow \mathbb{R}$ be a continuous function and let $F : [a, b] \rightarrow \mathbb{R}$ be defined by

$$F(x) = \int_a^x f(t)dt \quad (1.2.1)$$

Then, F is differentiable and $F' = f$.

Extending to Lebesgue space, fundamental theorem can be stated as,

Theorem 1.2.2. (Fundamental theorem in Lebesgue spaces). Let $f \in L_1[a, b]$. Then $I_a f$ is differentiable almost everywhere in $[a, b]$ and $DI_a f = f$ also holds almost everywhere on $[a, b]$, where $Df(x) = f'(x)$ and $I_a f(x) = \int_a^x f(t)dt$ for $a \leq x \leq b$.

1.2.1 Riemann-Liouville(R-L) operators

Definition 1.2.3. Let $q \in \mathbb{R}_+$ and $f \in L_1[a, b]$. The operator I_a^q , defined on $L_1[a, b]$ by

$$I_a^q f(x) = \frac{1}{\Gamma(q)} \int_a^x (x-t)^{q-1} f(t)dt$$

for $a \leq x \leq b$, is called the **Riemann-Liouville fractional integral operator of order q** . For $q = 0$ we set $I_a^0 = I$, the identity operator.

Some of the important characterisations of R-L integral operator are as given below.

Theorem 1.2.4. Let $f \in L_1[a, b]$ and $q > 0$, then the integral $I_a^q f(x)$ exists for almost every $x \in [a, b]$. Moreover, the function $I_a^q f$ itself is also an element of $L_1[a, b]$.

Theorem 1.2.5. (Commutative Property) Let $q_1, q_2 \geq 0$ and $f \in L_1[a, b]$. Then

$$I_a^{q_1} I_a^{q_2} f = I_a^{q_1+q_2} f = I_a^{q_2} I_a^{q_1} f$$

holds almost everywhere on $[a, b]$. If additionally $f \in C[a, b]$ or $q_1 + q_2 \geq 1$, then the identity holds everywhere on $[a, b]$.

Theorem 1.2.6. Let $q > 0$. Assume that $(f_k)_{k=1}^\infty$ is a uniformly convergent sequence of continuous functions on $[a, b]$. Then the fractional integral operator and the limit process can be interchanged. i.e., $(I_a^q \lim_{k \rightarrow \infty} f_k)(x) = (\lim_{k \rightarrow \infty} I_a^q f_k)(x)$. In particular, the sequence of functions $(I_a^q f_k)_{k=1}^\infty$ is uniformly convergent.

Definition 1.2.7. Let $q \in \mathbb{R}_+$ and $m = \lceil q \rceil$. The operator D_a^q defined by

$$D_a^q f = D^m I_a^{m-q} f$$

is called the **Riemann-Liouville fractional differential operator of order q** . For $q = 0$, we set $D_a^0 = I$, Identity operator.

The following theorem states that D_a^q is the left inverse of I_a^q .

Theorem 1.2.8. *Let $q \geq 0$. Then for every $f \in L_1[a, b]$, $D_a^q I_a^q f = f$ almost everywhere.*

1.2.2 Grünwald-Letnikov(G-L) operators

Definition 1.2.9. *Let $q > 0$, $m = [q]$ and $f \in C^m[a, b]$ (i.e. a set of functions with a continuous m^{th} derivative) and $a < x \leq b$. Then*

$$\tilde{D}_a^q f(x) = \lim_{n \rightarrow \infty} \frac{1}{h_n^q} \sum_{k=0}^n (-1)^k \binom{q}{k} f(x - kh_n)$$

with $h_n = \frac{(x-a)}{n}$ and $\binom{q}{k} = \frac{\Gamma(q+1)}{\Gamma(k+1)\Gamma(q-k+1)}$ is called the **Grünwald-Letnikov fractional derivative of order q** of the function f .

Definition 1.2.10. *Let $q > 0$, $f \in C[a, b]$ and $a < x \leq b$. Then*

$$\tilde{I}_a^q f(x) = \frac{1}{\Gamma(q)} \lim_{n \rightarrow \infty} h_n^q \sum_{k=0}^n \frac{\Gamma(q+k)}{\Gamma(k+1)} f(x - kh_n)$$

with $h_n = \frac{(x-a)}{n}$ is called the **Grünwald-Letnikov fractional integral of order q** of the function f .

Theorem 1.2.11. *Let $q > 0$, $m = [q]$ and $f \in C^m[a, b]$. Then, for $x \in (a, b]$, $\tilde{D}_a^q f(x) = D_a^q f(x)$.*

Due to this equivalence of R-L and G-L operators, G-L operator definition or its variants are utilised to obtain numerical approximation whenever R-L operators are used in the problem formulation (Podlubny, 1998; Diethelm, 2010).

1.2.3 Caputo operator

Definition 1.2.12. *Let $q \geq 0$ and $m = [q]$. Then we define the operator ${}^c D_a^q$ as*

$${}^c D_a^q f = I_a^{m-q} D^m f$$

whenever $D^m f \in L_1[a, b]$, is called **Caputo fractional differential operator**.

The relationship between R-L differential operator and Caputo operator is as below: Let $q \geq 0$ and $m = \lceil q \rceil$. Assuming that f is such that both $D_a^q f$ and ${}^c D_a^q f$ exist. Then

$${}^c D_a^q f(x) = D_a^q f(x) - \sum_{k=0}^{m-1} \frac{D^k f(a)}{\Gamma(k-q+1)} (x-a)^{k-q}$$

and ${}^c D_a^q f(x) = D_a^q f(x)$ holds if and only if $D^k f(a) = 0$ for $k = 0, 1, 2, \dots, m-1$.

Again, it can be seen that Caputo derivative is also the left inverse of R-L integral operator and need not be the right inverse.

Theorem 1.2.13. *If f is continuous and $q \geq 0$, Then ${}^c D_a^q I_a^q f = f$.*

Theorem 1.2.14. *Let $A^m[a, b]$ denotes the set of functions with an absolutely continuous $(m-1)^{th}$ derivative on $[a, b]$. Assume that $q \geq 0$, $m = \lceil q \rceil$, $f \in A^m[a, b]$, then*

$$I_a^q {}^c D_a^q f(x) = f(x) - \sum_{k=0}^{m-1} \frac{D^k f(a)}{k!} (x-a)^k \quad (1.2.2)$$

If $f(x) = c$, where c is a constant then $D_a^q(c) \neq 0$, but ${}^c D_a^q(c) = 0$. Due to this implication, Caputo operator is, in general, considered to model applications.

1.2.4 Mittag-Leffler function

Finally, we introduce the one parameter and two parameter Mittag-Leffler functions which play a crucial role in the solution of the following non-homogeneous linear fractional differential equation,

$${}^c D^q x(t) = \mu x(t) + f(t), \quad x(t_0) = x_0 \quad (1.2.3)$$

where μ is a real number and $f \in C([t_0, T] \times \mathbb{R}, \mathbb{R})$. Using the Laplace Transform technique, the solution for non-homogeneous initial value problem (1.2.3) is obtained as follows

$$x(t) = x_0 E_q(\mu(t-t_0)^q) + \int_{t_0}^t (t-s)^{q-1} E_{q,q}(\mu(t-s)^q) f(s) ds, \quad t \in [t_0, T] \quad (1.2.4)$$

where $E_q(t) = \sum_{k=0}^{\infty} \frac{t^k}{\Gamma(qk+1)}$ and $E_{q,q}(t) = \sum_{k=0}^{\infty} \frac{t^k}{\Gamma(qk+q)}$ are the Mittag-Leffler functions of one parameter and two parameter respectively. If $f(t) = 0$ then the solution

of the corresponding homogeneous initial value problem is given by

$$x(t) = x_0 E_q(\mu(t - t_0)^q), \quad t \in [t_0, T] \quad (1.2.5)$$

Few of the important similarities and differences between R-L and Caputo operators are given in the Table 1.1.

Property	Riemann-Liouville	Caputo
Definition	$D_a^q f(t) = D^m I_a^{m-q} f(t)$	${}^c D_a^q f(t) = I_a^{m-q} D^m f(t)$
Interpolation	$\lim_{q \rightarrow m} D_a^q f(t) = f^{(m)}(t)$ $\lim_{q \rightarrow m-1} D_a^q f(t) = f^{(m-1)}(t)$	$\lim_{q \rightarrow m} {}^c D_a^q f(t) = f^{(m)}(t)$ $\lim_{q \rightarrow m-1} {}^c D_a^q f(t) = f^{(m-1)}(t) - f^{(m-1)}(a)$
Linearity	$D_a^q(\lambda f(t) + \beta g(t)) = \lambda D_a^q f(t) + \beta D_a^q g(t)$	${}^c D_a^q(\lambda f(t) + \beta g(t)) = \lambda {}^c D_a^q f(t) + \beta {}^c D_a^q g(t)$
Commutativity	$D^m D_a^q f(t) = D_a^{m+q} f(t) \neq D_a^q D^m f(t)$	${}^c D_a^q D^m f(t) = {}^c D_a^{m+q} f(t) \neq D^m {}^c D_a^q f(t)$
Laplace transform	$L\{D_a^q f(t); s\} = s^q F(s) - \sum_{k=0}^{m-1} s^k [D_a^{q-k-1} f]_{t=0}$	$L\{{}^c D_a^q f(t); s\} = s^q F(s) - \sum_{k=0}^{m-1} s^{q-k-1} f^{(k)}(0)$
$f(t) = c = \text{constant}$	$D_a^q c = \frac{c}{\Gamma(1-q)} (t-a)^{-q}$	${}^c D_a^q c = 0$
$f(t) = t^p$	$\frac{\Gamma(p+1)}{\Gamma(p-q+1)} t^{p-q} \quad m-1 < q < m, \quad p > -1$	$\begin{cases} \frac{\Gamma(p+1)}{\Gamma(p-q+1)} t^{p-q} & m-1 < q < m, \quad p > m-1, \quad p \in \mathbb{R} \\ 0 & m-1 < q < m, \quad p \leq m-1, \quad p \in \mathbb{N} \end{cases}$
$f(t) = e^{\mu t}$	$t^{-q} E_{1,1-q}(\mu t)$	$\sum_{k=0}^{\infty} \frac{\mu^{k+m} t^{k+m-q}}{\Gamma(k+1+m-q)} = \mu^m t^{m-q} E_{1,m-q+1}(\mu t)$
$f(t) = \cos(\mu t)$	$\frac{1}{2} t^{-q} [E_{1,1-q}(i\mu t) + E_{1,1-q}(-i\mu t)]$	$\frac{1}{2} (i\mu)^m t^{m-q} [E_{1,m-q+1}(i\mu t) + (-1)^n E_{1,m-q+1}(-i\mu t)]$
$f(t) = \sin(\mu t)$	$-\frac{1}{2} i t^{-q} [E_{1,1-q}(i\mu t) - E_{1,1-q}(-i\mu t)]$	$-\frac{1}{2} i (i\mu)^m t^{m-q} [E_{1,m-q+1}(i\mu t) - (-1)^n E_{1,m-q+1}(-i\mu t)]$

Table 1.1 Comparison of R-L and Caputo differential operators.

1.3 FRACTIONAL DIFFERENTIAL EQUATIONS

Mathematical models of real-world problems are often represented in the form of various types of differential equations. In recent decades, scientists and mathematicians realised the efficiency of fractional differential equations (FDEs) as an appropriate model to describe any natural or complex phenomena of real-life problems, than using their classical counterparts. Unlike classical derivative which requires information about the function at a particular value and its neighbourhood, the fractional derivative of a function needs information about the function from the starting to the existing state. This non-local nature of the fractional derivatives makes it to be an excellent tool in describing the memory and hereditary properties of various materials and processes (Podlubny, 1998).

1.3.1 Applications

Oliver Heaviside (1892), an electrical engineer, has introduced fractional differentiation in the study of electrical transmission line theory (Oldham and Spanier, 1974). After a break of more than fifty years, modelling or studying problems in terms of fractional operators started gaining momentum. Nutting equations, which provides a deformation relations between stress and strain of materials were put into practice by G. W. Blair and Reiner (1951). Many other studies on materials also lead to fractional calculus approach: Caputo and Mainardi (1971) on relating stress and strain fields in viscoelastic materials, Bagley and Torvik (1983) in viscoelasticity and electro chemistry corrosion, Jaishankar and McKinley (2012) and Faber et al. (2017) have proposed a fractional constitutive frame work in rheology and so on. Oldham (1972), in his work on electro analysis has considered an integral of order $\frac{1}{2}$. Sugimoto's (1991) article discusses hereditary effects on nonlinear acoustic waves by adding fractional derivative term to Burgers equation. Many studies by Saichev and Zaslavsky (1997) focuses on understanding fractal Brownian motion and Lévy process by generalizing space and time diffusion equations. Experimental results obtained by Ciuchi et al. (2012) in the study of liquid-crystalline cells indicate that the process is anomalous in nature, which is described better by fractional diffusion. Other studies that motivate to understand fractional differential models are: i) Anomalous transport and wave propagations by West and Nonnenmacher (2001), ii) fractional telegraph equations model to describe transient sound wave propagations through inhomogeneous materials by Fella et al. (2006) iii) Magin (2006) in bioengineering and so on.

1.3.2 Analytical, semi-analytical and numerical methods

After reinventing the idea of generalised derivatives in the beginning of 19th century, significant efforts were made in obtaining the conditions on existence and uniqueness of the solutions of various classes of fractional differential and integral equations. Some of the results in terms of Riemann-Liouville definition can be found in articles by Al-Bassam (1965); Delbosco and Rodino (1996); Zhang (2000). Podlubny (1998) in his book also discussed conditions for the existence, uniqueness and well posedness of the linear and general initial value problems in terms of the Miller-Ross sequential fractional order derivatives where the cases of classical R-L, G-L and Caputo definitions can be deduced as special cases. Refer the book by Diethelm (2010) and a survey by Agarwal et al. (2010) for the results of many special cases of fractional initial and boundary value problems involving Caputo definition. Refer the articles by Devi et al.

(2010), Denton et al. (2011), Yakar (2012) and Roy et al. (2018) for results of some fractional models via quasilinearisation.

Ever since introducing mathematical definitions for fractional order derivatives and integrals, many attempts were made in obtaining solutions for fractional order model problems. Though the aim always is to obtain closed-form solutions, which generally gets restricted to linear problems with simple initial and boundary conditions. Following are some of works that can be classified into analytical or semi-analytical (expressed in terms of special functions or infinite series etc.) solutions. The book by Podlubny (1998) provides details of the work done based on Laplace transforms, fractional Green's function, Mellin transforms etc. and gave important references on operational calculus methods. His book focuses on Laplace transforms for linear fractional ODEs and PDEs using standard and sequential fractional derivatives and uses of other methods for single and multi-term initial value problems. Since then there are many works in this direction to obtain solutions for various classes of fractional model equations: Laplace transforms (Agrawal, 2002; Wang et al., 2017); Mellin transforms (Mainardi et al., 2001; Butera and Di Paola, 2015); Adomian decomposition (Shawagfeh, 1999; Jafari and Daftardar-Gejji, 2006); homotopy perturbation and homotopy analysis (Song and Zhang, 2007; Odibat and Momani, 2008; Cang et al., 2009; Ateş and Zegeling, 2017); variational iteration (He, 1998; Wu and Lee, 2010); differential transform method (Ertürk and Momani, 2008) etc. Though these methods yield accurate results they are applicable to a limited class of fractional differential equations. Hence we resort to numerical (discretisation) methods, in order to solve more class of problems using a single scheme with minor modifications.

Majority of the well-known numerical schemes for classical differential equations are being extended to FDEs. The traditional mesh-based local approximation methods like fractional linear multistep methods, finite difference (FD), finite element (FE), finite volume (FV), etc. are successfully modified in order to solve FDEs. In 1986, Lubich introduced fractional multistep method to solve fractional integral equations which yields higher order of convergence. Later Diethelm and Freed (1999) introduced fractional Adams-Bashforth-Moulton method to solve fractional IVPs with lesser computational cost than that of Lubich's scheme, however with slower convergence rate. In their work, Galeone and Garrappa (2008) obtained explicit formulation and stability properties of fractional Adams-Bashforth-Moulton method for fractional order IVPs.

It was Meerschaert and Tadjeran (2004), who has introduced finite difference method to space-fractional diffusion/dispersion equation, where formulation is based

on implicit Euler for time derivative and modified Grünwald approximation to the fractional diffusion term. Zhuang et al. (2008) introduced an implicit approach along with techniques for enhancing the convergence to an anomalous subdiffusion problem. Some important contributions are done by Sousa (2009), who also generalised central, upwind and Lax-Wendroff schemes to fractional advection-diffusion equation. Refer the article by Li et al. (2016) for finite difference discretisation on nonlinear fractional models. Liu et al. (2015) generalised point interpolation method for space fractional diffusion model. Some of the important works on generalising and analysing finite element and finite volume formulations are done by Ervin et al. (2007); Deng (2008); Li et al. (2011); Yang et al. (2011); Zhang et al. (2005); Liu et al. (2014a); Simmons et al. (2017). Since it is apparent that fractional derivatives are non-local operators, even simple material models or unified principles comes with a high computational cost in terms of storage, time and overall complexity in numerical algorithms. Due to this, these local schemes becomes less attractive as they loose the sparse nature of the coefficient matrices. Hence global methods appear to have certain advantages in numerical simulation of the fractional derivative models by virtue of their high accuracy using smaller set of discretisation points.

There are many spectrally convergent global collocation methods based on various polynomials and special functions: Polynomial splines (Blank, 1996), Chebyshev polynomials (Khader, 2011) for space fractional diffusion equations, Legendre polynomials (Zayernouri and Karniadakis, 2014) for FPDEs, Jacobi polynomials for fractional Fokker-Plank equations (Yang et al., 2018), Galerkin Chebyshev's pseudospectral method for space-time fractional diffusion models (Hanert and Piret, 2014). Similar to above developments, a surge of work is directed towards wavelet schemes on various fractional models. Interests are shown on obtaining solutions based on different wavelets such as Haar, Chebyshev, Legendre, Bernoulli and so on (Zhu and Fan, 2012; Saeed and ur Rehman, 2013; Mohammadi and Cattani, 2018). Galerkin reproducing kernel particle meshfree (Lin et al., 2018) and discontinuous Galerkin methods are another class where many important developments to solve fractional order PDEs are taking place (Mustapha and McLean, 2013; Mao and Karniadakis, 2017).

Though most of these methods are accurate and have higher order of convergence, but extension to higher dimensional problems becomes tedious and sometimes require appropriate reformulation of the method. So, in our work, naturally meshfree radial function based global schemes are proposed for some class of fractional differential equations. Like conventional spectral methods global radial basis function (RBF)

schemes promise higher order of convergence and accuracy. Additionally, extending RBF schemes to higher dimensions are, in general, simple.

1.4 RADIAL BASIS FUNCTIONS

On failure of Fourier and polynomial series approximation to fit data on topographic surfaces, Hardy (1971) constructed a method with basis $\{\sqrt{(\bar{x} - \bar{x}_j)^2 + c^2}\}_{j=1}^n$, with $c > 0$ and $\bar{x} \in \mathbb{R}^2$. Introduction of multiquadric (MQ) was followed by other two important radial functions, namely inverse multiquadric by Hardy and thin plate splines (TPS) by Duchon. Subsequently, other radial functions have also come into use for multidimensional interpolation (see Table 1.2, $r = \|\bar{x}\|_2$). In their work, Fornberg and Wright (2004) modified $c = 1/\varepsilon$ and we follow this notation throughout the thesis.

These efforts have received a further forward push with the numerical experiment by Franke (1982) on various approximation methods, to assess their advantages in terms of CPU time, storage, accuracy, qualitative representation and ease in implementation. From those trials, he concluded that MQ and TPS have produced best results in comparison with other methods considered. In the following, we provide some of the important definitions and results on radial functions based approximations.

Definition 1.4.1. *Let $X \subseteq \mathbb{R}^d$, $d \geq 1$ be a normed linear space. A function $\psi : X \rightarrow \mathbb{R}$ is said to be **radial** if there exists a univariate function $\phi : \mathbb{R}^+ \rightarrow \mathbb{R}$ such that $\psi(\bar{x}) = \phi(\|\bar{x}\|)$ for all $\bar{x} \in X$. Here $\|\cdot\|$, represents some norm in $X \subseteq \mathbb{R}^d$. Usually Euclidean norm is considered.*

Table 1.2 Examples for RBFs.

Name of the radial functions	$\phi(r)$, $r > 0$
Infinitely Smooth	
Gaussian (GA)	$e^{-\varepsilon^2 r^2}$
Multiquadric (MQ)	$\sqrt{1 + \varepsilon^2 r^2}$
Inverse multiquadric (IMQ)	$\frac{1}{\sqrt{1 + \varepsilon^2 r^2}}$
Inverse quadric (IQ)	$\frac{1}{1 + \varepsilon^2 r^2}$
Sech	$\text{sech}(\varepsilon r)$
Piecewise Smooth	
Polyharmonic splines (PS)	r^β , $0 < \beta \in (2\mathbb{N} - 1)$ $r^\beta \log r$, $\beta \in 2\mathbb{N}$

Conventional radial functions family can be classified into two types: Infinitely smooth and piecewise smooth functions (Refer Table 1.2 for examples).

Definition 1.4.2. *Radial function interpolation: Given a set of n distinct data $(\bar{x}_i, f_i)_{i=1}^n$, $\bar{x}_i \in \mathbb{R}^d$, $d \geq 1$, the RBF interpolant $s(\bar{x})$ of the unknown function $f(\bar{x})$ is expressed as a linear combination of translates of one particular radial function ϕ ,*

$$s(\bar{x}) = \sum_{j=1}^n \lambda_j \phi(\|\bar{x} - \bar{x}_j\|) \quad (1.4.1)$$

The interpolation condition,

$$s(\bar{x}_i) = f_i, \quad i = 1, \dots, n \quad (1.4.2)$$

leads to a $n \times n$ symmetric linear system $A\bar{\lambda} = \bar{f}$, where $A_{i,j} = \phi(\|\bar{x}_i - \bar{x}_j\|)$, $i, j = 1, 2, \dots, n$ and $\bar{f} = [f_1, f_2, \dots, f_n]^T$. $\bar{\lambda} = [\lambda_1, \lambda_2, \dots, \lambda_n]^T$ is an unknown vector, which has to be determined using interpolation condition (1.4.2). The set $\{\phi(\|\bar{x} - \bar{x}_j\|)\}_{j=1}^n$ is the basis, called radial basis functions (RBFs).

Infinitely smooth functions yield accurate results with exponential convergence rate. The shape parameter ε , as name suggests, effects the shape of those functions. While $\varepsilon \rightarrow 0$ provides flatter functions, $\varepsilon \rightarrow \infty$ makes it sharper. However, the ‘uncertainty principle’ suggested by Schaback (1995) and from other numerical experiments, it is understood that accuracy (ε close to 0) and stability (large ε - better condition number) are inversely proportional. Piecewise smooth radial functions possess algebraic rate of convergence and their accuracy and stability depends on space dimension and smoothness of the function (on ‘ β ’ in Table 1.2).

Consequently the existence of an RBF interpolant for an arbitrary given data, depends only on the invertibility of the interpolation matrix A defined in Definition 1.4.2. This is ensured by following theorems.

Definition 1.4.3. *A real valued continuous function $\phi : \mathbb{R}^+ \rightarrow \mathbb{R}$ is positive definite, if and only if it is even and the quadratic form $\sum_{j=1}^n \sum_{k=1}^n c_j c_k \phi(\|\bar{x}_j - \bar{x}_k\|) \geq 0$ for any n pairwise distinct points $\bar{x}_1, \bar{x}_2, \dots, \bar{x}_n \in \mathbb{R}^d$ and $c = [c_1, c_2, c_3, \dots, c_n]^T \in \mathbb{R}^n$. The function ϕ is strictly positive definite if the above quadratic form is zero only for $c = 0$.*

Definition 1.4.4. *A function $\phi : \mathbb{R}^+ \rightarrow \mathbb{R}$ which is in $C[0, \infty) \cap C^\infty(0, \infty)$ and that satisfies $(-1)^l \phi^{(l)}(r) \geq 0$, $r > 0$, $l = 0, 1, 2, \dots$ is called completely monotone on $[0, \infty)$.*

Gaussian and inverse multiquadrics are examples for complete monotone functions. In 1938, Schoenberg presented a characterisation theorem for the existence of the unique solution,

Theorem 1.4.5. *If the function $\phi : \mathbb{R}^+ \rightarrow \mathbb{R}$ is completely monotone, but not constant if and only if $\phi(\|\cdot\|^2)$ is strictly positive definite and radial on \mathbb{R}^d , for any $d \in \mathbb{N}$.*

Thus, if ϕ is completely monotone, then the corresponding RBF interpolation is uniquely solvable. This ensures that GA and IMQ produces invertible coefficient matrix A . But, these results fails to generalise the invertibility of the matrix for other popular RBFs like MQs and TPS. Micchelli (1986) generalised these results, by considering the notion of conditionally positive definite functions.

Definition 1.4.6. *A real-valued continuous even function ϕ is called conditionally positive definite of order M on \mathbb{R}^d if $\sum_{j=1}^n \sum_{k=1}^n c_j c_k \phi(\|\bar{x} - \bar{x}_j\|) \geq 0$ for any n pairwise distinct points $\bar{x}_1, \bar{x}_2, \dots, \bar{x}_n \in \mathbb{R}^d$ and $c = [c_1, c_2, \dots, c_n]^T \in \mathbb{R}^n$ satisfying $\sum_{j=1}^n c_j p(\bar{x}_j) = 0$ for any real-valued polynomial p of degree at most $(M - 1)$. The function ϕ is called strictly conditionally positive definite of order M if the quadratic form is zero only for $c = 0$.*

Thus according to Micchelli, the generalised form of RBF interpolation problem takes the following form,

Definition 1.4.7. *Given a set of n distinct data $(\bar{x}_i, f_i)_{i=1}^n$, $\bar{x}_i \in \mathbb{R}^d$, $d \geq 1$, the RBF interpolant in (1.4.1) has been modified to ,*

$$s(\bar{x}) = \sum_{j=1}^n \lambda_j \phi(\|\bar{x} - \bar{x}_j\|) + \sum_{j=1}^l \gamma_j p_j(\bar{x}), \quad \bar{x} \in \mathbb{R}^d. \quad (1.4.3)$$

where $p_j(\bar{x})_{j=1}^l$ is a basis for $\Pi_{(M-1)}^d$ (space of all d -variate polynomials with degree $\leq (M - 1)$) and $l = \binom{M-1+d}{M-1}$, is the dimension of $\Pi_{(M-1)}^d$. Here, M is called the order of the radial basis function, which represents the minimum degree of the polynomial to be appended to the interpolant to ensure the non-singularity of the interpolation matrix. However, to take care of the extra degrees of freedom in (1.4.3), l extra conditions are necessary along with the interpolation condition (1.4.2) i.e.,

$$\sum_{j=1}^n \lambda_j p_k(\bar{x}_j) = 0, \quad p_k \in \Pi_{M-1}^d, \quad k = 1, 2, \dots, l \quad (1.4.4)$$

This leads to an $(n+l) \times (n+l)$ system i.e.,

$$\begin{pmatrix} A & P \\ P^T & \mathbf{0} \end{pmatrix} \begin{pmatrix} \bar{\lambda} \\ \bar{\gamma} \end{pmatrix} = \begin{pmatrix} \bar{f} \\ \bar{0} \end{pmatrix} \quad (1.4.5)$$

where $A_{ij} = \phi(\|\bar{x}_i - \bar{x}_j\|)$, $i, j = 1, 2, \dots, n$, $P_{ij} = p_j(\bar{x}_i)$, $i = 1, 2, \dots, n$, $j = 1, 2, \dots, l$, $\mathbf{0}$ is the $l \times l$ zero matrix, $\bar{f} = [f_1, f_2, \dots, f_n]^T$, $\bar{0}$ is a zero vector of length l . $\bar{\lambda} = [\lambda_1, \lambda_2, \dots, \lambda_n]^T$ and $\bar{\gamma} = [\gamma_1, \gamma_2, \dots, \gamma_n]^T$ are unknown vectors to be determined.

In his work, Micchelli (1986) has also shown that it is not necessary to append polynomial to MQ for unique solvability, conjectured by Franke. Influenced by Micchelli, Buhmann (2003) proved the following,

Theorem 1.4.8. *Let $g \in C^\infty[0, \infty)$ be such that g' is completely monotonic but not constant, suppose further that $g(0) \geq 0$, then A is non-singular for $\phi(r) = g(r^2)$.*

1.5 RBF FOR DIFFERENTIAL EQUATIONS

Despite some of the shortcoming like exponential increasing in condition number as $\varepsilon \rightarrow 0$ or number of data increases, radial functions based approximations have received wide acceptance in practical applications. This is due to the efforts in stabilising the system by means of preconditioned or by changing the representation of the basis (Beatson et al. (1999); Ling and Kansa (2005), variable shape parameters (Kansa, 1990)). Since part of our work focuses on ‘stable computation’ of RBF solutions, a brief literature survey is provided in Chapter 4.

Considering the advantages of radial functions over traditional approximation methods, Kansa (1990) have proposed a collocation method, also known in the literature as symmetric/direct collocation method. In his work, the proposed scheme was applied to two dimensional BVP like Laplace equation as well as IBVPs like heat and wave equations. The method became highly successful due to the ease in implementation to any dimension, even though a detailed theoretical convergence analysis is missing in the literature. Following this, many other formulations are proposed, namely, integrated RBF (Mai-Duy and Tran-Cong, 2001), RBF-DQ (Wu and Shu, 2002), symmetric collocation, moving least square (Fasshauer, 2007) and finite difference type RBF schemes (RBF-FD) (Wright and Fornberg, 2006; Chandhini and Sanyasiraju, 2007). Refer books by Chen et al. (2014) and Fornberg and Flyer (2015) for application of these methods to many practical problems.

1.5.1 RBF for fractional differential equations

It was Chen et al. (2010b), who made the first attempt to use the Kansa's method in determining the solution of the time fractional diffusion equations. Thereafter RBF based collocations schemes were applied to some of the important time fractional partial differential equations such as anomalous sub-diffusion, fractional diffusion and advection-diffusion problems (Brunner et al., 2010; Chen et al., 2010a; Liu et al., 2011; Uddin and Haq, 2011; Shirzadi et al., 2012; Yan and Yang, 2015). Also, other equations for which RBF based methods have been considered are fractional variants of Schrödinger equation (Mohebbi et al., 2013) and telegraph equation (Hosseini et al., 2014), fractal mobile/immobile transport model (Liu et al., 2014b), Sine-Gordon and Klein-Gordon equations (Dehghan et al., 2015), nonlinear time fractional integro-differential equations (Aslefallah and Shivanian, 2015) and so on. All these time fractional differential equations were solved by discretising the time fractional derivative mentioned in the equation using finite difference method and then Kansa's method is applied to approximate the integer order spatial derivatives. Some other RBF formulations in terms of moving least squares and Galerkin approaches for time fractional problems (Yang et al., 2015; Dehghan et al., 2016) are reported in literature. These results again suggests RBF approximations are considered only for integer order space derivatives involved.

Compared to time fractional differential equations, space fractional differential equations were considered less in literature may be because multi-dimensional space fractional derivatives are difficult to handle due to vector integral representation. Piret and Hanert (2013) have extended RBF algorithm to space fractional diffusion problems with RBF-QR to overcome ill-conditioning of the discretised system. Also, Kansa's asymmetric collocation method was found successful in solving the space-fractional advection-dispersion equations (Pang et al., 2015), two-dimensional fractional evolution equations (Ghehsareh et al., 2015), spatiotemporal fractional diffusion equation (Sun et al., 2017). A recent work by Zhu et al. (2018) shows application of RBF-DQ method on space fractional diffusion equation. Further, there are a few attempts to solve fractional ordinary differential equations using Kansa's approach: Fakhr Kazemi and Ghoreishi (2013); Antunes and Ferreira (2015).

As discussed in earlier, only a few works have focused on developing schemes to approximate fractional order derivatives using radial functions. Apart from this, many natural phenomena are nonlinear in nature, which leads to nonlinear governing

equations. While dealing with the schemes for nonlinear equations, it is not only to be concerned about the accurate solution but also about the convergence of the algorithm. So, in our work, we made an attempt to develop radial basis functions based schemes for a class of fractional nonlinear differential equations both in one and two dimensions. Prior to RBF formulation, each fractional model is linearised to a sequence of linear fractional DEs either via generalised quasilinearisation or successive approximation. Then, the existence and uniqueness of the solutions of the chosen problems and convergence of the iterative techniques are also proved.

In spite of high accuracy and order of convergence, radial functions based schemes suffer instability due to ill-conditioning of the discretised system. i.e., RBFs are sensitive to both shape parameter and closeness of the nodal points in the domain. This disadvantage is observed even while approximating fractional order derivatives. Hence, in the thesis, we also propose two stabilisation methods based on Tikhonov regularisation as well as RBF-QR algorithms.

1.6 ORGANISATION OF THE THESIS

The thesis comprises of five chapters.

To make the thesis self-supportive, Chapter 1 gives a brief introduction on fractional order calculus, their applications and radial basis functions. Some preliminary results required and a detailed literature survey are also presented in this chapter.

In Chapter 2, the proposed radial basis functions based methods, differentiated (Kansa's) and integrated schemes, for nonlinear fractional order differential equations are derived in detail. Before discretisation, the nonlinear problem is linearised using generalised quasilinearisation. An interesting proof via generalised monotone quasilinearisation for the existence and uniqueness for fractional order initial value problem is given. This convergence analysis also proves quadratic convergence of the generalised quasilinearisation method. Variety of examples are provided to show the quadratic convergence of the proposed quasilinearisation. Through these examples, we also compare between the two RBF schemes as well as with the results available in some of the recent literature.

Chapter 3 details formulation of Kansa's differentiated RBF scheme to fractional Darboux problem, a fractional nonlinear partial differential equation. Unlike in

Chapter 2, linearisation is obtained through successive approximation. In addition, existence and uniqueness of the solution of fractional Darboux problem is proved via successive approximation. Many example problems are compared for accuracy, rate of convergence, optimal shape parameters and CPU time, wherever possible.

The focus of Chapter 4 is on stabilisation algorithms for fractional models, due to the inherent ill-conditioning issues pertains to RBF schemes. To overcome this, two algorithms, based on Tikhonov regularisation and RBF-QR methods are proposed to approximate fractional derivatives and fractional differential equation models. RBF-QR by Fornberg et al. (2011), which was restricted to Gaussian, is generalised to consider all infinitely smooth radial functions.

Finally, Chapter 5 summarises the work highlighting the observed advantages, issues and problems. Also the chapter suggests possible improvements on some of these issues to tackle in the future.

CHAPTER 2

DIRECT AND INTEGRATED RADIAL FUNCTIONS BASED QUASILINEARISATION SCHEMES FOR NONLINEAR FRACTIONAL DIFFERENTIAL EQUATIONS

2.1 INTRODUCTION

Many mathematical models of physical phenomena can be expressed as nonlinear ordinary differential equations (ODEs). Some of the well-known nonlinear ODEs are Riccati equation, Van der Pol oscillators problem, Lane-Emden equation and Painlevé equation. As discussed in the earlier chapter, fractional counterparts of many classical differential equations can be effective and accurate models to describe any physical phenomena. Though there are a few attempts of Kansa's radial functions method to fractional PDEs, efforts on solving fractional ODEs using Kansa's or even other RBF schemes are rare in the literature. Hence, in the work presented in this chapter, we extend two radial basis functions based schemes namely differentiated and integrated (DRBF and IRBF) methods, to nonlinear fractional initial and boundary value problems with governing equation,

$${}^c D_a^q x(t) = h(t, x) \quad (2.1.1)$$

Appropriate initial or boundary conditions are considered. Here, h is continuous and $(m-1) < q \leq m$, $m \in \mathbb{N}$.

Another important contribution in the present chapter is that it also proves the

existence and uniqueness of the solution of fractional order initial value problem via generalised monotone quasilinearisation method. Though a few results are available in the literature regarding generalised monotone quasilinearisation Devi et al. (2010); Denton et al. (2011), the convergence analysis is based on the comparison theorem for fractional order initial value problem. In contrast to the literature, the proposed proof is based on the fixed point theorem in Banach space (Lakshmikantham et al., 2009; Vijesh and Kumar, 2015) and also make use of some interesting properties of generalised Mittag-Leffler function (Miller and Samko, 2001; Schneider, 1996).

The remaining part of the chapter is organised as follows: Section 2.2 provides a detailed proof on the existence and uniqueness of the solution of fractional initial value problems and convergence of the quasilinearisation. In section 2.3, the RBF discretisations (DRBF and IRBF) for the fractional ODE (2.1.1) with initial condition is detailed when $0 < q \leq 1$. The proposed schemes are validated using variety of fractional problems in Section 2.4. Then the chapter is summarised in Section 2.5, citing various advantages and possible improvements.

2.2 CONVERGENCE ANALYSIS

Many interesting existence and uniqueness theorem for fractional order initial value problem discussed in the literature are proved using various fixed point theorems. In some cases, though they produce an iterative scheme to approximate the unique solution, the order of the convergence of the scheme is linear. Recently, Lakshmikantham et al. (2009) have proposed a fixed point theorem in Banach space and show its application to prove the existence and uniqueness theorem for classical initial value problem and semilinear parabolic initial boundary value problem via monotone quasilinearisation method. In contrast to the classical fixed point theorem, the iterative scheme, in their work, converges to the unique solution quadratically. An interesting extension of this fixed point theorem is studied by Vijesh and Kumar (2015), which is a key tool for the proposed proof on existence, uniqueness and convergence of fractional order DE given in (2.1.1) with $0 < q \leq 1$ and $x(0) = x_0$. Before providing the proof, we state the main results by Vijesh and Kumar (2015) in the following.

Theorem 2.2.1. *(Vijesh and Kumar, 2015) Let E be an ordered Banach space with a normal order cone E_+ . Assume that $\widehat{T} : E \rightarrow E$ satisfies the following hypotheses*

1. *There exists $v^0, w^0 \in E$ such that $v^0 \leq \widehat{T}v^0$, $\widehat{T}w^0 \leq w^0$ and $v^0 \leq w^0$; $F, G :$*

$[v^0, w^0] \rightarrow E$ are compact where, $\widehat{T} = F + G$;

2. The Frechet derivative F'_u and G'_u exist for every $u \in [v^0, w^0]$; $u \rightarrow F'_u v$ and $u \rightarrow G'_u v$ are increasing and decreasing, respectively, on $[v^0, w^0]$ for all $v \in E_+$;
- 3.

$$Fu^0 - Fu^1 \leq F'_{u^0}(u^0 - u^1) \text{ whenever } v^0 \leq u^0 \leq u^1 \leq w^0. \quad (2.2.1)$$

$$Gu^0 - Gu^1 \leq G'_{u^1}(u^0 - u^1) \text{ whenever } v^0 \leq u^0 \leq u^1 \leq w^0. \quad (2.2.2)$$

4. $(I - F'_v - G'_w)^{-1}$ exists and it is a bounded positive operator for all $v, w \in [v^0, w^0]$.
Then for $k \in \mathbb{N}$, relations

$$v^{k+1} = \widehat{T}v^k + (F'_{v^k} + G'_{w^k})(v^{k+1} - v^k) \quad (2.2.3)$$

$$w^{k+1} = \widehat{T}w^k + (F'_{v^k} + G'_{w^k})(w^{k+1} - w^k) \quad (2.2.4)$$

define an increasing sequence $\{v^k\}$ and a decreasing sequence $\{w^k\}$ which converges to the solutions of the operator equation $\widehat{T}x = x$. These fixed points are equal if $\widehat{T}u^1 - \widehat{T}u^0 < u^1 - u^0$ for all $v^0 \leq u^0 < u^1 \leq w^0$.

Proposition 2.2.2. (Vijesh and Kumar, 2015) Let \widehat{T} satisfy all the hypotheses of Theorem 2.2.1 and

1. $\|F'_u - F'_v\| \leq L_1 \|u - v\|$ and $\|G'_u - G'_v\| \leq L_2 \|u - v\|$ for all $u, v \in [v^0, w^0]$ for some L_1 and $L_2 > 0$.
2. $M = \sup\{\|(I - F'_u - G'_v)^{-1}\| : u, v \in [v^0, w^0]\} < \infty$.

Then the sequences $\{v^k\}$ and $\{w^k\}$ converge quadratically to the same fixed point of \widehat{T} .

To proceed further, we consider following definitions and assumptions: Let $v^0, w^0 \in C[0, T]$ said to be a ordered lower and upper solution of (2.1.1), if $v^0 \leq w^0$ and ${}^c D^q v^0 \leq h(t, v^0), v^0(0) \leq x_0$ and ${}^c D^q w^0 \geq h(t, w^0), w^0(0) \geq x_0$.

Assume that h has the decomposition as $f + g$. For the function f , f_2 denotes the partial derivative of f with respect to the second variable. Assume,

- (I₁) Let $v^0, w^0 \in C[0, T]$ be an ordered lower and upper solution for (2.1.1). Define $m_1 = \inf_{t \in [0, T]} \{v^0, w^0\}$ and $m_2 = \sup_{t \in [0, T]} \{v^0, w^0\}$

- (I₂) For some $\delta > 0$, the functions f, g, f_2, g_2 are in $C([0, T] \times [m_1 - \delta, m_2 + \delta])$

(a) Let $\mu \geq 0$ be such that for all $t \in [0, T]$ and $s_1, s_2 \in [m_1 - \delta, m_2 + \delta]$

$$f_2(t, s_1) + g_2(t, s_2) + \mu \geq 0 \quad (2.2.5)$$

(b) For each $t \in [0, T]$, $f_2 : [0, T] \times [m_1, m_2] \rightarrow \mathbb{R}$ are increasing in second variable;

(c) For each $t \in [0, T]$, $g_2 : [0, T] \times [m_1, m_2] \rightarrow \mathbb{R}$ are decreasing in second variable;

(d) For each $t \in [0, T]$, $|f_2(t, x) - f_2(t, y)| \leq L_1|x - y|$, $L_1 \geq 0$ and $x, y \in [m_1, m_2]$;

(e) For each $t \in [0, T]$, $|g_2(t, x) - g_2(t, y)| \leq L_2|x - y|$, $L_2 \geq 0$ and $x, y \in [m_1, m_2]$.

Using the lower solution v^0 and the upper solution w^0 as initial guess one can construct two sequences $\{v^k\}$ and $\{w^k\}$ using the generalised quasilinearisation iterative scheme as follows

$${}^c D^q v^{k+1} = h(t, v^k) + f_2(t, v^k)(v^{k+1} - v^k) + g_2(t, w^k)(v^{k+1} - v^k); \quad (2.2.6)$$

$$v^{k+1}(0) = x_0$$

$${}^c D^q w^{k+1} = h(t, w^k) + f_2(t, v^k)(w^{k+1} - w^k) + g_2(t, w^k)(w^{k+1} - w^k); \quad (2.2.7)$$

$$w^{k+1}(0) = x_0$$

The following theorem, ensures the well defined property, monotone property of (2.2.6) and (2.2.7) as well as their quadratic convergence to the unique solution of (2.1.1).

Theorem 2.2.3. *Let the hypotheses I_1 and I_2 be satisfied then the initial value problem (2.1.1) has a unique solution in the sector $[v^0, w^0]$. Moreover the sequences $\{v^k\}$ and $\{w^k\}$ converges uniformly, monotonically and quadratically to the unique solution of (2.1.1).*

Proof The initial value problem (2.1.1) can be rewritten as

$${}^c D^q x(t) + \mu x(t) = h(t, x(t)) + \mu x(t), \quad x(0) = x_0 \quad (2.2.8)$$

The above initial value problem (2.2.8) is equivalent to the integral equation

$$x(t) = x_0 E_q(-\mu t^q) + \int_0^t (t-s)^{q-1} E_{q,q}(-\mu(t-s)^q) (h(s, x(s)) + \mu x(s)) ds \quad (2.2.9)$$

Define an operator $\widehat{T} : C[0, T] \rightarrow C[0, T]$ by

$$\widehat{T}x(t) = x_0 E_q(-\mu t^q) + \int_0^t (t-s)^{q-1} E_{q,q}(-\mu(t-s)^q) (h(s, x(s)) + \mu x(s)) ds \quad (2.2.10)$$

It is easy to verify that the operator is well defined and the solution of the initial value problem (2.1.1) is nothing but the solution of the operator equation $\widehat{T}x = x$. Note that the operator \widehat{T} can be decomposed as $F + G$ where F and G are given by

$$\begin{aligned} Fx(t) &= x_0 E_q(-\mu t^q) + \int_0^t (t-s)^{q-1} E_{q,q}(-\mu(t-s)^q) (f(s, x(s)) + \mu x(s)) ds \\ Gx(t) &= \int_0^t (t-s)^{q-1} E_{q,q}(-\mu(t-s)^q) g(s, x(s)) ds \end{aligned}$$

According to the Lemma 2.1 given by Vijesh and Kumar (2015), the Frechet derivative of F and G exists for all $u \in [v^0, w^0]$ and the Frechet derivative is given by

$$\begin{aligned} F'_u(h) &= \int_0^t (t-s)^{q-1} E_{q,q}(-\mu(t-s)^q) (f_2(s, u(s)) + \mu) h(s) ds \\ G'_u(h) &= \int_0^t (t-s)^{q-1} E_{q,q}(-\mu(t-s)^q) g_2(s, u(s)) h(s) ds \end{aligned}$$

For any $u, v \in [v^0, w^0]$ define $\mathcal{T}(u, v)$ by

$$\mathcal{T}(u, v)h(t) = \int_0^t (t-s)^{q-1} E_{q,q}(-\mu(t-s)^q) [f_2(s, u(s)) + g_2(s, v(s)) + \mu] h(s) ds.$$

Using the results by Schneider (1996), It is easy to see that $E_{q,q}(-t)$, $t \geq 0$ is a completely monotone function. Moreover the completely monotone function cannot vanish for any positive value (see Miller and Samko, 2001). Thus $E_{q,q}(-t) > 0$, $t \geq 0$. Consequently $E_{q,q}(-\mu t^q) \geq 0$ for any positive μ and $t \geq 0$. Combining with this choice of μ it can be conclude that for any u and v in $[v^0, w^0]$, the operator $\mathcal{T}(u, v)$ is positive bounded operator. Define a norm on $C[0, T]$ by $\|h\|_\rho = \sup_{t \in [0, T]} \left| \frac{h(t)}{E_q(\rho t^q)} \right|$. Clearly $\|\cdot\|_\rho$ is equivalent to $\|\cdot\|_\infty$. For any $u, v \in [v^0, w^0]$ and $h \in C[0, T]$ with $\|h\|_\rho = 1$,

$$\begin{aligned} |\mathcal{T}(u, v)h(t)| &= \left| \int_0^t (t-s)^{q-1} E_{q,q}(-\mu(t-s)^q) [f_2(s, u(s)) + g_2(s, v(s)) + \mu] h(s) ds \right| \\ &\leq \frac{M\Gamma(q)}{\Gamma(q)} \int_0^t (t-s)^{q-1} |h(s)| ds, \quad M \geq 0, \text{ a constant} \\ &\leq \frac{M\Gamma(q)}{\Gamma(q)} \int_0^t (t-s)^{q-1} E_q(\rho s^q) \left| \frac{h(s)}{E_q(\rho s^q)} \right| ds \\ &\leq \frac{M\Gamma(q)}{\rho} \|h\|_\rho E_q(\rho t^q) \end{aligned}$$

$$\left| \frac{\mathcal{F}(u, v)h(t)}{E_q(\rho t^q)} \right| \leq \frac{M\Gamma(q)}{\rho}$$

Thus $\|\mathcal{F}(u, v)\| \leq \frac{M\Gamma(q)}{\rho}$. Now choose $\rho > M\Gamma(q)$. Hence $\|\mathcal{F}(u, v)\| \leq \rho < 1$ where $\rho = \frac{M\Gamma(q)}{\rho}$. Note that for any $h \in C[0, T]$ with $\|h\|_\rho = 1$ and $u, v \in [v^0, w^0]$

$$\begin{aligned} (G'_u - G'_v)h &= \int_0^t (t-s)^{q-1} E_{q,q}(-\mu(t-s)^q) [g_2(s, u(s)) - g_2(s, v(s))] h(s) ds \\ |(G'_u - G'_v)h| &\leq L_2 \int_0^t (t-s)^{q-1} [E_q(\rho s^q)]^2 \left| \frac{u(s) - v(s)}{E_q(\rho s^q)} \right| \left| \frac{h(s)}{E_q(\rho s^q)} \right| ds \\ &\leq L_2 E_q(\rho T^q) \int_0^t (t-s)^{q-1} E_q(\rho s^q) \left| \frac{u(s) - v(s)}{E_q(\rho s^q)} \right| \left| \frac{h(s)}{E_q(\rho s^q)} \right| ds \\ &\leq L_2 E_q(\rho T^q) \|u(s) - v(s)\| \int_0^t (t-s)^{q-1} E_q(\rho s^q) ds \\ \left| \frac{(G'_u - G'_v)h}{E_q(\rho t^q)} \right| &\leq \frac{L_2 \Gamma(q) E_q(\rho T^q)}{\rho} \|u - v\| \end{aligned}$$

Thus $\|G'_u - G'_v\| \leq \frac{L_2 \Gamma(q) E_q(\rho T^q)}{\rho} \|u - v\|$. Consequently $u \rightarrow G'_u$ is Lipschitz continuous. Similarly it can be seen that $u \rightarrow F'_u$ is Lipschitz continuous. For any $h \in C[0, T]$ with $\|h\|_\rho = 1$ and $u^0, u^1 \in [v^0, w^0]$ with $u^0 \leq u^1$

$$\begin{aligned} Gu^0 - Gu^1 &= \int_0^t (t-s)^{q-1} E_{q,q}(-\mu(t-s)^q) [g(s, u^0(s)) - g(s, u^1(s))] ds \\ &= \int_0^t (t-s)^{q-1} E_{q,q}(-\mu(t-s)^q) \int_0^1 g_2(s, u^0 + \theta(u^1 - u^0)) \\ &\quad (u^0 - u^1) d\theta ds \\ &\leq \int_0^t (t-s)^{q-1} E_{q,q}(-\mu(t-s)^q) g_2(s, u^1(s)) (u^0 - u^1) ds \\ Gu^0 - Gu^1 &\leq G'_{u^1}(u^0 - u^1) \end{aligned}$$

Similarly one can show $Fu^0 - Fu^1 \leq F'_{u^0}(u^0 - u^1)$ whenever $v^0 \leq u^0 \leq u^1 \leq w^0$. Thus all the hypotheses of Theorem 2.2.1 and Proposition 2.2.2 are satisfied. Consequently the operator equation $\widehat{T}x = x$ has a unique solution in $[v^0, w^0]$ and hence the fractional differential equation (2.1.1) with initial condition $x(0) = x_0$, $0 < q \leq 1$ has a unique solution in $[v^0, w^0]$. In this case, it is also easy to verify that (2.2.3) and (2.2.4) becomes (2.2.6) and (2.2.7), respectively. Thus the generalised quasilinearisation iterative scheme converges monotonically and quadratically to the unique solution of the initial value problem (2.1.1).

Remark 2.2.4. *Generalisation of the above theorem to corresponding initial value*

problems with $q > 1$ is straightforward.

2.3 DIFFERENTIAL AND INTEGRATED RBF SCHEMES

In the following, we derive both Kansa's method (DRBF) and integrated scheme (IRBF) for the linearised fractional problems (2.2.6) and (2.2.7). Let v^k and w^k represent k^{th} iterates of lower and upper solutions, respectively.

2.3.1 DRBF scheme

In this method, the solution is represented as linear combination of radial basis functions as follows. i.e., the solutions can be expressed as,

$$v^{k+1}(t) = \sum_{j=1}^n (\lambda_v)_j^{k+1} \phi(\|t - t_j\|) + \sum_{j=1}^l (\gamma_v)_j^{k+1} p_j(t) \quad (2.3.1)$$

$$w^{k+1}(t) = \sum_{j=1}^n (\lambda_w)_j^{k+1} \phi(\|t - t_j\|) + \sum_{j=1}^l (\gamma_w)_j^{k+1} p_j(t) \quad (2.3.2)$$

where t_j , $j = 1, 2, \dots, n$, are collocation points distributed in the given interval. Assuming sufficient smoothness of ϕ , (2.3.1) is substituted in both governing equation (2.2.6) and corresponding initial condition at each node t_i . These equations along with l extra conditions given in (1.4.4) leads to an $(n + l) \times (n + l)$ linear system,

$$\begin{pmatrix} A^k & B^k \\ P & \mathbf{0} \end{pmatrix} \begin{pmatrix} \bar{\lambda}_v^{k+1} \\ \bar{\gamma}_v^{k+1} \end{pmatrix} = \begin{pmatrix} \bar{F}^k \\ \bar{0} \end{pmatrix} \quad (2.3.3)$$

where A^k , B^k and P are matrices of sizes $n \times n$, $n \times l$ and $l \times n$, respectively. $\mathbf{0}$ is a zero matrix of order l . The components of these submatrices are

$$P_{sj} = p_s(t_j)$$

$$A_{ij}^k = \begin{cases} {}^c D_a^q \phi(\|t_i - t_j\|) - (f_2(t_i, v_i^k) + g_2(t_i, w_i^k)) \phi(\|t_i - t_j\|) & \text{if } t_i \in (a, b], \\ \phi(\|t_i - t_j\|) & \text{if } t_i = a \end{cases}$$

$$B_{is}^k = \begin{cases} {}^c D_a^q p_s(t_i) - (f_2(t_i, v_i^k) + g_2(t_i, w_i^k)) p_s(t_i) & \text{if } t_i \in (a, b]. \\ p_s(t_i) & \text{if } t_i = a \end{cases}$$

where $i, j = 1, 2, \dots, n$, $s = 1, 2, \dots, l$ and $\bar{\lambda}_v^{k+1} = [(\lambda_v)_1^{k+1}, (\lambda_v)_2^{k+1}, \dots, (\lambda_v)_n^{k+1}]^T$,

$\bar{\gamma}_v^{k+1} = [(\gamma_v)_1^{k+1}, (\gamma_v)_2^{k+1}, \dots, (\gamma_v)_l^{k+1}]^T$ are the column vectors containing unknowns. On the RHS of the matrix equation, $\bar{0}$ is a zero vector of length l and $\bar{F}^k = [F_1^k, F_2^k, \dots, F_n^k]^T$ is a vector with the entries,

$$F_i^k = \begin{cases} h(t_i, v_i^k) - v_i^k (f_2(t_i, v_i^k) + g_2(t_i, w_i^k)) & \text{if } t_i \in (a, b). \\ x_0 & \text{if } t_i = a \end{cases}$$

A similar derivation is obtained for (2.2.7) using (2.3.2), which gives the upper solution w^{k+1} .

2.3.2 IRBF scheme

In this method, the formulation of the problem starts with the decomposition of the highest order derivative under consideration as a linear combination of RBFs. The obtained derivative expression is then integrated to yield expressions for lower order derivatives and finally for the original function itself.

To derive the scheme, both ${}^c D_a^q v^{k+1}(t)$ and ${}^c D_a^q w^{k+1}(t)$, respectively in (2.2.6) and (2.2.7) are represented as,

$${}^c D_a^q v^{k+1}(t) = \sum_{j=1}^n (\lambda_v)_j^{k+1} \phi(\|t - t_j\|) \quad (2.3.4)$$

$${}^c D_a^q w^{k+1}(t) = \sum_{j=1}^n (\lambda_w)_j^{k+1} \phi(\|t - t_j\|) \quad (2.3.5)$$

where $t_j, j = 1, 2, \dots, n$, are collocation points distributed in the given interval. Applying the fractional integral operator I_a^q on both the sides of (2.3.4) leads to

$$v^{k+1}(t) = \sum_{j=1}^n (\lambda_v)_j^{k+1} I_a^q \phi(\|t - t_j\|) + (\gamma_v)_1^{k+1} \quad (2.3.6)$$

Equation (2.3.6) is analogous to (2.3.1), however linear combination of fractional integral of RBFs. Extra constant term is due to integration, while in (2.3.1) a polynomial term is appended. The integration leads to a higher order polynomial according to the order of the equation q . We can use Theorem 1.2.14 for initial value problems, however incorporation of initial conditions at $t = 0$ leads to singular system. Discretizing the fractional DE in (2.2.6) and (2.2.7) and the corresponding initial conditions using

(2.3.4)-(2.3.6) and taking care of extra degrees of freedom using the normal equation

$$\sum_{j=1}^n (\lambda_v)_j^{k+1} = 0 \quad (2.3.7)$$

leads to a linear system of order $(n+1) \times (n+1)$,

$$\begin{pmatrix} A^k & B^k \\ P & 0 \end{pmatrix} \begin{pmatrix} \bar{\lambda}_v^{k+1} \\ \bar{\gamma}_v^{k+1} \end{pmatrix} = \begin{pmatrix} \bar{F}^k \\ 0 \end{pmatrix} \quad (2.3.8)$$

where A , B and P are matrices of sizes $n \times n$, $n \times 1$ and $1 \times n$, respectively. The components of these submatrices are: $P_{sj} = (t_j - a)^{s-1}$

$$A_{ij}^k = \begin{cases} \phi(\|t_i - t_j\|) - (f_2(t_i, v_i^k) + g_2(t_i, w_i^k)) I_a^q \phi(\|t_i - t_j\|) & \text{if } t_i \in (a, b]. \\ I_a^q \phi(\|t_i - t_j\|) & \text{if } t_i = a \end{cases}$$

$$B_{is}^k = \begin{cases} -(f_2(t_i, v_i^k) + g_2(t_i, w_i^k)) & \text{if } t_i \in (a, b]. \\ 1 & \text{if } t_i = a. \end{cases}$$

where $i, j = 1, 2, \dots, n$ and $s = 1$. The vector \bar{F}^k in the RHS of the matrix equation (2.3.8) has entries same as that in the case of DRBF equation. A similar system is obtained for sequence of upper solutions $\{w^k\}$.

The obtained systems (in both the schemes) are to be solved at each iteration so that both $\{v^k\}$ and $\{w^k\}$ converge to the solution of (2.1.1) with $x(0) = x_0$, $0 < q \leq 1$.

2.3.3 Gauss-Jacobi quadrature rule

The linear systems (2.3.3) and (2.3.8) have components involving fractional derivatives or integrals of radial functions. Gauss-Jacobi quadrature rule is employed to calculate those integrals, where integral takes a general form $\int_a^t (t - \tau)^\beta F(\tau) d\tau$. Substitution $\tau = \left(\frac{t+a}{2} - \frac{t-a}{2} \xi \right)$ reduces the integral in the form $\int_{-1}^1 (1 + \xi)^\beta F(\xi) d\xi$, which is suitable form to use Gauss-Jacobi method for which the integral must be of the form $\int_{-1}^1 W(\xi) F(\xi) d\xi$, where $W(\xi) = (1 - \xi)^{s_1} (1 + \xi)^{s_2}$ with $s_1, s_2 > -1$. In the present case $s_1 = 0$ and $s_2 = \beta$. Then the integral is approximated as,

$$\int_{-1}^1 (1 - \xi)^{s_1} (1 + \xi)^{s_2} F(\xi) d\xi \approx \sum_{p=1}^N W_p F(\xi_p) \quad (2.3.9)$$

where N is the number of quadrature points chosen for the evaluation. The quadrature points $\{\xi_p\}_1^N$ are the roots of the Jacobi polynomial $P_N^{(s_1, s_2)}$ of degree N and $\{W_p\}_1^N$ are the corresponding weights computed using the algorithm by Hale and Townsend (2013):

$$W_p = \frac{\Gamma(N + s_1 + 1)\Gamma(N + s_2 + 1)}{\Gamma(N + s_1 + s_2 + 1)N!} \frac{2^{s_1 + s_2 + 1}}{(1 - \xi_p^2)[(P_N^{(s_1, s_2)})'(\xi_p)]^2}, \quad p = 1, 2, \dots, N. \quad (2.3.10)$$

2.4 NUMERICAL ILLUSTRATIONS

This section provides illustration of the schemes discussed through various fractional ODE models. The results are obtained using MATLAB2014a. Multiquadric radial function is chosen for all the computations for which the optimal shape parameter for each case has been obtained by trial and error. Both uniform and nonuniform nodal distributions are considered. Unless specified, Chebyshev-Gauss-Lobatto nodes, $\left(\frac{1 - \cos(i\pi/n)}{2}\right)$, $i = 0, 1, \dots, n$ are chosen to distribute points nonuniformly. Accuracy of the schemes are compared by calculating both root mean square as well as maximum error using the formulae,

$$RMS \text{ error} = \sqrt{\frac{1}{n} \sum_{j=1}^n [x(t_j) - x_{app}(t_j)]^2}; \quad L_\infty \text{ error} = \max_{1 \leq j \leq n} |x(t_j) - x_{app}(t_j)|$$

Also, numerical rate of convergence of the schemes are obtained by making nodal distribution coarser to finer to see how fast the solution converges to analytical solution (As $\Delta t \rightarrow 0$).

Example 2.4.1. Consider ${}^c D^q x + x + x^2 = [E_q(-t^q)]^2$, $0 < t < 1$, $0 < q \leq 1$, $x(0) = 1$

Analytical solution is $x(t) = E_q(-t^q)$, where E_q represent one parameter Mittag-Leffler function defined by $E_q(z) = \sum_{k=0}^{\infty} \frac{z^k}{\Gamma(qk + 1)}$. According to the decomposition of $h(t, x) = f(t, x) + g(t, x)$ discussed in Section 2.2, $f \equiv 0$, $g(t, x) = [E_q(-t^q)]^2 - x - x^2$. Initial approximation for the lower and upper solutions v^0 and w^0 , respectively are 0 and $E_q(-t^q)$. Hence, it is not necessary to use iteration (2.2.6) and iteration for upper solution (2.2.7) leads to

$${}^c D^q w^{k+1} = (-w^k - (w^k)^2) + [E_q(-t^q)]^2 - (1 + 2w^k)(w^{k+1} - w^k); \quad w^{k+1}(0) = x(0) = 1$$

IRBF solutions along with exact solutions are plotted in Figure 2.1 for various

values of q . It can be seen that the solutions are visually indistinguishable from each other. For a detailed study we have compared the accuracy, rate of convergence etc. between the two proposed RBF schemes. Table 2.1 gives both RMS and L_∞ errors obtained using both uniform and nonuniform nodes ($n = 11$) with corresponding optimal shape parameter ε . Clearly, IRBF solution shows better accuracy, especially as q decreases.

Table 2.2 and 2.3 present numerical rate of convergence obtained by varying n from 21 to 81 set of nodes, for q ranging from 0.1 to 1. The results are given for $\varepsilon = 8$. For $q = 1, 0.75$, IRBF methods shows good rate of convergence. Gauss-Jacobi integration requires only 8 quadrature points in IRBF scheme, whereas DRBF shows similar accuracy only when $q = 1$. For $q < 1$, rate of convergence is very low and also requires more number of quadrature points to obtain converged solutions. i.e., For the DRBF scheme, number of quadrature points are increased to 20, 30 and 40, respectively for $q = 0.5, 0.25$ and 0.1 to have a positive rate of convergence. This increases the required computational time. Further, Table 2.3 also reveals the effect of quadrature points on convergence and accuracy for both the schemes. Integrated RBF scheme is saturated with 8 points, however improvements (nonconvergence to convergence) are seen in DRBF performance with respect to the increase in quadrature points. One reason for such a scenario is the effect of ill-conditioning of the collocation matrix, which is handled better in integrated RBF schemes.

Figure 2.2 illustrate the convergence of the generalised quasilinearisation to the exact solution by plotting error with respect to iteration. As proved in Section 2.2, it can be seen that convergence is monotone.

Example 2.4.2. *The problem ${}^c D^q x(t) = g_1(t) - x^2(t)$, $0 < t < 1$ with IC(s) $x(0) = 0$ ($x'(0) = 0$ if $1 < q \leq 2$) has analytic solution $x(t) = t^5 + \frac{3}{2}t^4 - 2t^{(2+q)}$, where $g_1(t) = \frac{\Gamma(6)}{\Gamma(6-q)}t^{(5-q)} + \frac{36}{\Gamma(5-q)}t^{(4-q)} - \Gamma(3+q)t^2 + (t^5 + \frac{3}{2}t^4 - 2t^{(2+q)})^2$. Using finite difference schemes, Li et al. (2016) has solved the example.*

For this example also, $f \equiv 0$, hence $g(t, x) = g_1(t) - x^2$. i.e., To obtain the converged solution, it is not required to compute $\{v^k\}$. Initial approximation required for evaluating $\{v^k\}$ and $\{w^k\}$ are $v^0 = 0$ and $w^0 = 3$, according to Theorem 2.2.3.

This problem is solved for both the cases $0 < q \leq 1$ and $1 < q \leq 2$. Both the schemes are compared (See Tables 2.4 and 2.6) and further they are compared with the finite difference schemes proposed by Li et al. (2016) in Table 2.5. Figure 2.3

shows a qualitative comparison of IRBF solutions with exact solutions. Unlike in Example 2.4.1, performance of both the schemes are equally good. When the accuracy is compared to that of the methods by Li et al. (2016) at $t = 1$, RBF collocation schemes provides better accuracy using far lesser set of nodes. Influence of quadrature points on convergence/accuracy is also validated in Table 2.7 for both $q = 0.1$ and 1.1 . Like in earlier examples, as q decreases $2 \geq q > 1$ (or) $1 \geq q > 0$, it is noticed that the number of quadrature points required for effective implementation of DRBF also increases. However, IRBF is not constrained with such a condition, hence computationally robust. Like in earlier example, Figure 2.4 shows that the sequence $\{w^k\}$ obtained using (2.2.6) are monotone.

Example 2.4.3. Consider the IVP ${}^cD^q x = t^6 + \frac{\Gamma(3.5)}{\Gamma(3.5-q)}t^{(2.5-q)} - tx^2$, $0 < t < 1$, $0 < q < 1$, $x(0) = 0$, solved using a neural network approach by Qu and Liu (2015). The exact solution is given by $x(t) = t^{(5/2)}$.

This example also has $g(t, x) = h(t, x)$ and $f \equiv 0$, which makes computation of lower solution $\{v^k\}$ not necessary. However, initial approximations are $v^0 = 0$ and $w^0 = t^{5/2} + 1$ to use the iterative formulae (2.2.6) and (2.2.7). Using them the solutions are obtained and monotonicity is shown through Figure 2.6.

Analytical solution for this example does not depend on q . As observed through Figure 2.5 and Tables 2.8-2.11, both the schemes provide good accuracy and rate of convergence. Comparing to the solutions obtained by Qu and Liu (2015), it is found that RBF solutions are much superior in terms of accuracy.

Example 2.4.4. Consider the fractional order logistic differential equation

$${}^cD^q x(t) = K^q x(t)(1 - x(t)), t > 0, 0 < q \leq 1; x(0) = x_0$$

that is discussed by West (2015), Area et al. (2016) and Hamarshah et al. (2017). Exact solution (for $q = 1$) is $x(t) = \frac{x_0}{x_0 + (1 - x_0)e^{-Kt}}$, where K is a constant.

Remark: For any $0 < q < 1$, a series solution was proposed by B. J. West (2015):

$x(t) = \sum_{j=0}^{\infty} \left(\frac{x_0 - 1}{x_0} \right)^j E_q(-jK^q t^q)$. But in 2016, Iván Area et al. (2016) have shown that this function does not represent the solution of above fractional logistic model.

For the choice $0 \leq x_0 \leq 1$, $v^0 = 0$, $w^0 = 1$, $f(t, x) = K^q x(t)$ and $g(t, x) = -K^q x^2(t)$, one can easily verify that ${}^cD^q v^0 \leq h(t, v^0)$ and ${}^cD^q w^0 \geq h(t, w^0)$, for $t \in [0, \infty)$. Thus v^0 and w^0 are ordered lower and upper solutions, respectively. Clearly from the definition

$m_1 = 0$ and $m_2 = 1$. Also note that $f_2(t, x) = K^q$, $g_2(t, x) = -2K^q x$ are increasing and decreasing in the second variable, respectively, for each $(t, y) \in [0, T] \times [m_1, m_2]$. Moreover both f_2 and g_2 satisfy the Lipschitz condition with respect to the second variable in $[0, T] \times [m_1, m_2]$. Hence by proposed theorem, the fractional order logistic equation has an unique solution in the sector $[v^0, w^0]$. To compare with the results by Hamarsheh et al. (2017), we have chosen $0 < t \leq 3$ and $x_0 = 0.85$. For the chosen f and g , the solution is obtained by iterating using following monotone iterative procedure with either DRBF or IRBF discretisation.

$${}^c D^q w^{k+1} = K^q w^k - K^q (w^k)^2 + (K^q - 2K^q w^k)(w^{k+1} - w^k); \quad w^{k+1}(0) = x_0$$

The DRBF and IRBF solutions computed are plotted in Figure 2.7 for various values of q . These methods are further compared with a semi-analytical approach optimal homotopy asymptotic method (OHAM) by Hamarsheh et al. (2017) and fractional Adams-Bashforth-Moulton (FABM) method by Diethelm (2010). FABM solution is obtained using the step size $\Delta t = 0.003$, whereas step sizes for proposed RBF schemes are $\Delta t = 0.3$ and 0.03 . Between two RBF schemes, IRBF shows better performances, both in terms of accuracy and convergence.

Example 2.4.5. Consider the example ${}^c D^q x(t) + e^{x(t)} = 0$, $t > 0$, $0 < q \leq 1$; $x(0) = 0$ given by Jang (2014). Obtaining analytical solution for $q = 1$ is straightforward, while not explicit for fractional case. A semi analytical approach called generalised differential transform method (GDTM) is proposed by Jang (2014).

If $v^0 = -E_q(t^q)$, $w^0 \equiv 1$, $h(t, x) \equiv g(t, x) = -e^x$ and $f(t, x) \equiv 0$, it is straightforward to verify that the required conditions are satisfied, for any $t > 0$. This implies proposed theorem is applicable and hence, solutions are obtained using DRBF and IRBF methods combined with following monotone iterative scheme,

$${}^c D^q w^{k+1}(t) = -e^{w^k} - e^{w^k} (w^{k+1} - w^k); \quad w^{k+1}(0) = 0.$$

Computed IRBF and DRBF solutions are plotted in Figures 2.8. A comparison of the present schemes with (GDTM) (Jang, 2014) and FABM (Diethelm, 2010; Jang, 2014) are detailed in Table 2.13 for $q = 0.9$. Solutions obtained using IRBF method matches excellently with that of GDTM and FABM solutions. Though GDTM and FABM are comparable for initial values of t , RBF and FABM solutions start getting closer as t increases. While both the RBF schemes are simple and efficient, IRBF yields better results with $\Delta t = T/10$ and 8 quadrature points whereas DRBF demands smaller Δt and more quadrature points for better accuracy and convergence.

Example 2.4.6. Consider the example ${}^c D^q x(t) + \sin(x(t)) = 0$, $t > 0$, $0 < q \leq 1$; $x(0) = 3\pi/4$ given by Jang (2014). Similar to Example 2.4.5, obtaining analytical solution for $q = 1$ is straightforward, while not explicit for fractional case. Jang (2014) has solved the problem using GDTM.

For the choices $v^0 \equiv 0$, $w^0 \equiv \pi$, $h \equiv f = -\sin x$ and $g \equiv 0$ one can easily check whether all assumptions in the main Theorem 2.2.3, are satisfied and hence above problem has a unique solution in the sector $[v^0, w^0]$. Further, following iteration ensures convergence to the solution.

$${}^c D^q v^{k+1} = -\sin(v^k) - \cos(v^k)(v^{k+1} - v^k); \quad v^{k+1}(0) = 3\pi/4$$

Comparisons between two RBF formulations and these schemes with GDTM and FABM are presented in the Figure 2.9 and Table 2.14), respectively. They show a similar behaviour as in earlier example.

Remark: Though our results are primarily for fractional initial value problems, as a numerical illustration, we include the following boundary value problem using the proposed RBF schemes based on the quasilinearisation (2.2.6) and (2.2.7). The representation of the IRBF solution (2.3.4) and (2.3.5) can be suitably modified to incorporate the boundary conditions.

Example 2.4.7. Consider the boundary value problem, which is solved using Haar wavelet scheme by Saeed and ur Rehman (2013).

${}^c D^q x + a(t)x'^2 + b(t)xx' = g_1(t)$, $1 < q \leq 2$; $x(0) = x(1) = 0$. Exact solution is given by $x(t) = t^q - t^{70-q}$ and g_1 is defined as

$$g_1(t) = \Gamma(q+1) - \frac{\Gamma(71-q)}{\Gamma(71-2q)} t^{70-2q} + a(t)(qt^{q-1} - (70-q)t^{69-q})^2 + b(t)(qt^{q-1} - (70-q)t^{69-q})(t^q - t^{70-q})$$

Extending Theorem 2.2.3 to the problem and we obtained solutions for $a(t) = e^t$ and $b(t) = t$ using the iterative scheme (2.2.6) and (2.2.7).

From the Figure 2.10, it can be seen that the solution x has high gradients near $x = 0.95$. Apart from uniform nodes of various sizes, as done by Saeed and ur Rehman (2013), we have divided the interval $[0, 1]$ into two parts, say $[0, 0.94]$ and $[0.94, 1]$. Then distributed the nodes uniformly as: $[0, 0.94]$ is described with stepsize $\Delta t_1 = \frac{(0.94-0)}{\frac{3m}{2}}$ and $[0.94, 1]$ with the stepsize $\Delta t_2 = \frac{(1-0.94)}{\frac{m}{2}}$, where $n = 2m$.

Apart from Figure 2.10, the methods are compared in Tables 2.15 and 2.16. To capture the high gradient solution accurately, finer nodal distributions are chosen. Nonuniform distribution did not yield any better accuracy, unlike in the Haar wavelet solution discussed by Saeed and ur Rehman (2013). Despite using uniform nodes, the RBF solutions with lesser nodes are as accurate as the corresponding non-uniform solution by Saeed and ur Rehman (2013). Comparing each other, it is observed that integrated RBF collocation is marginally better than its differential RBF counterpart (See Table 2.15). While observing the convergence order in Table 2.16, it is found that IRBF behaves better for q close to 1 and DRBF when $q = 2$. This may be due to high ill-conditioning effect inherent in radial basis function based schemes, since number of nodes are very high (this makes nodal spacing very small) when compared to earlier examples.

2.5 CONCLUSIONS

Present work focuses on two aspects: 1) Proves existence and uniqueness of the solution of fractional order IVP via generalised monotone quasilinearisation, which proposes the sequences (2.2.6), (2.2.7) and 2) Based on this iterative procedures two RBF based schemes, namely, integrated as well as differentiated RBF collocation schemes to solve nonlinear fractional ordinary differential equations are proposed. Variety of examples are provided to illustrate the results thus proved and also to make a detailed comparison between intergrated RBF scheme with Kansa's differential RBF method. Further, merits and demerits of the schemes are analysed using various examples and obtained solutions are also compared with available results in some of the recent literature. In terms of accuracy and convergence, RBF schemes are found to be superior. However, these advantages are crippled due to the instability caused by ill-conditioning as the nodes becomes finer. Hence, the decrease in error using non-uniform nodal distribution is marginal when compared to same number of uniform nodes in most of the examples chosen. For collocation schemes, this issue needs further attention.

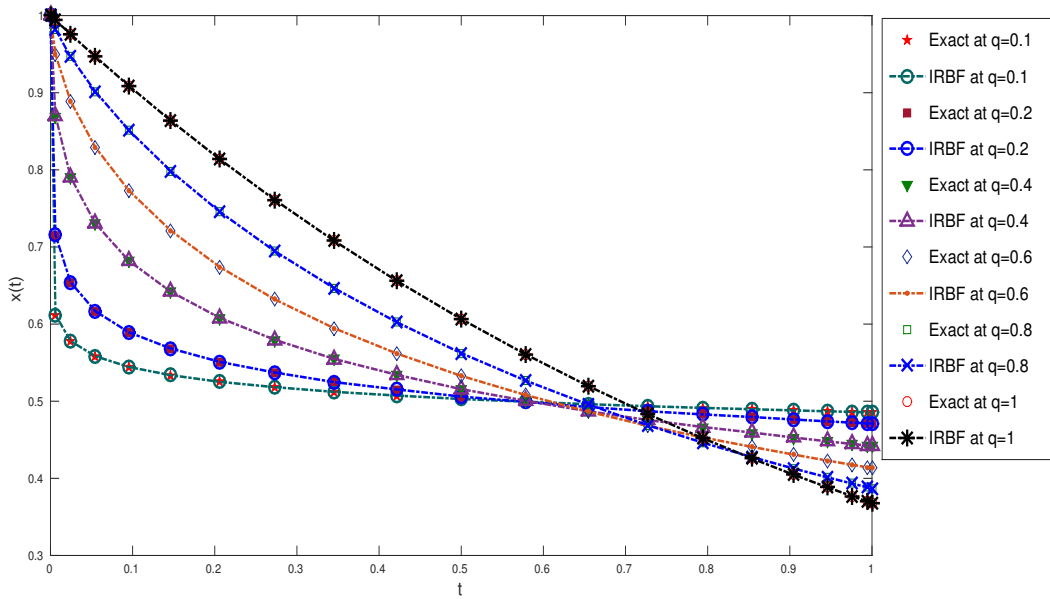
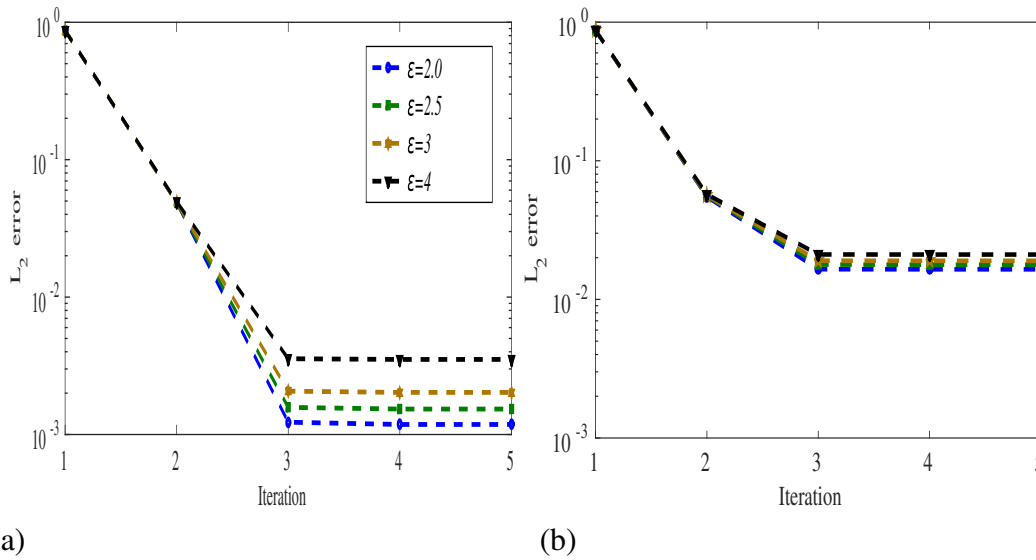


Figure 2.1 Solutions of Example 2.4.1 for various q by IRBF.



(a) (b)
 Figure 2.2 Errors at each iteration for Example 2.4.1 for various ϵ at $q = 0.5$ ($n = 21$)
 (a)IRBF, (b)DRBF

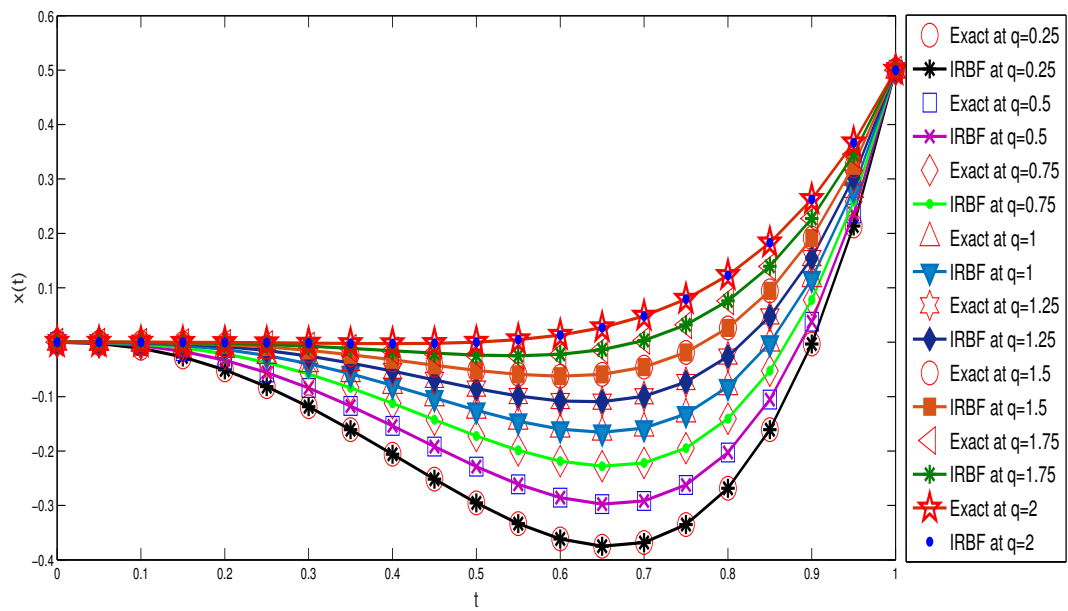


Figure 2.3 Solutions of Example 2.4.2 for various q by IRBF.

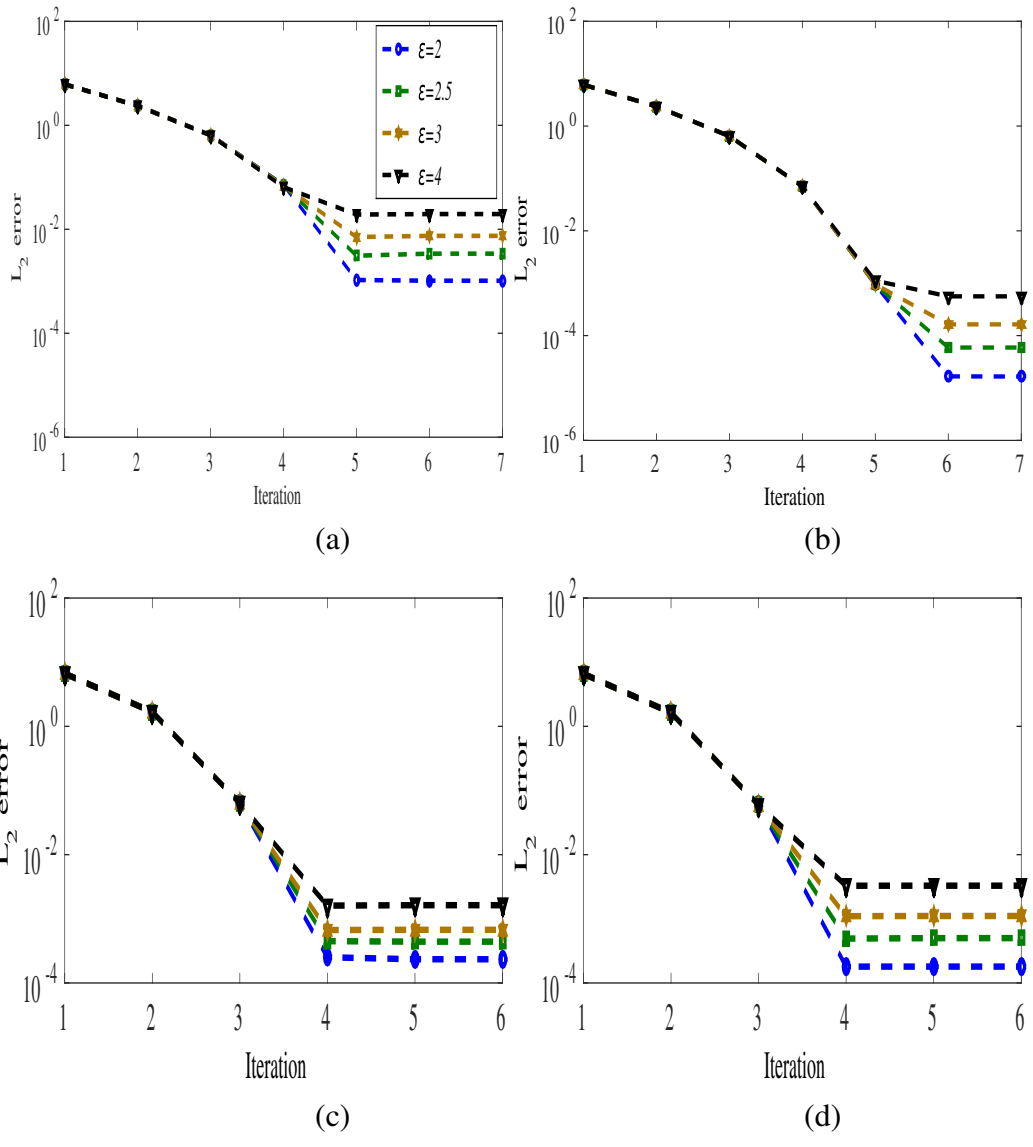


Figure 2.4 Error at each iteration for Example 2.4.2 (a) IRBF, (b) DRBF for $q = 0.5$ and (c) IRBF, (d) DRBF for $q = 1.5$.

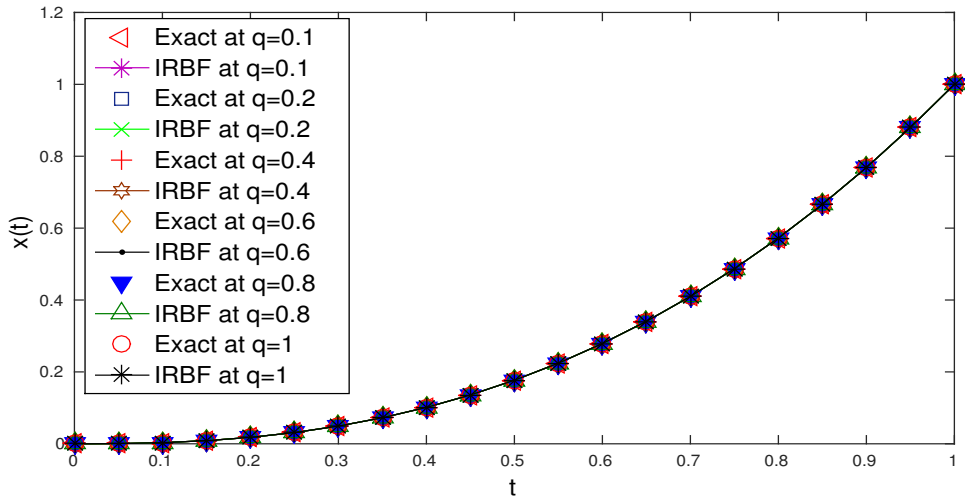


Figure 2.5 Solutions of Example 2.4.3 for various q by IRBF.

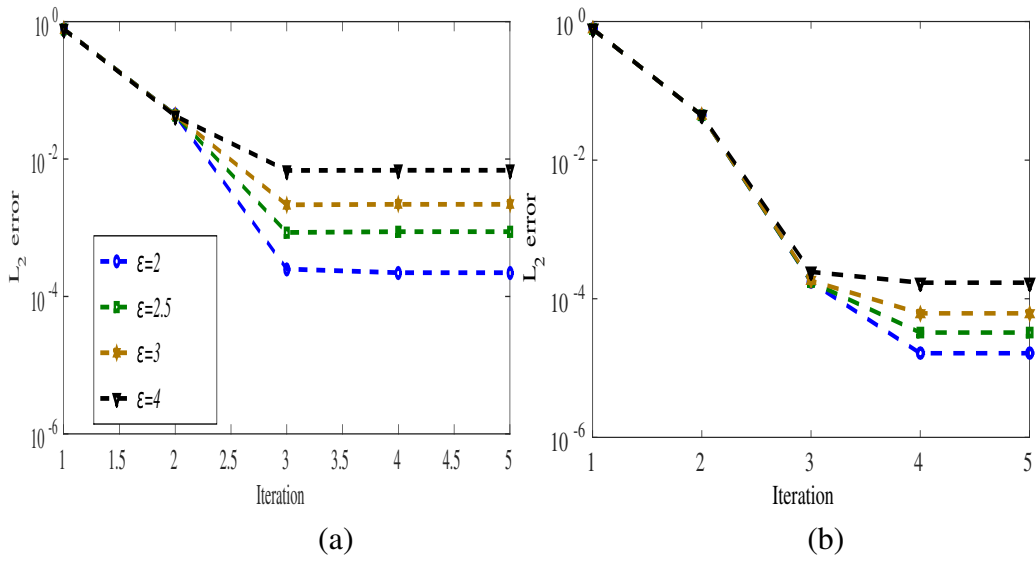


Figure 2.6 Errors at each iteration for Example 2.4.3 for various ϵ at $q = 0.5$ ($n = 21$):- (a) IRBF, (b) DRBF

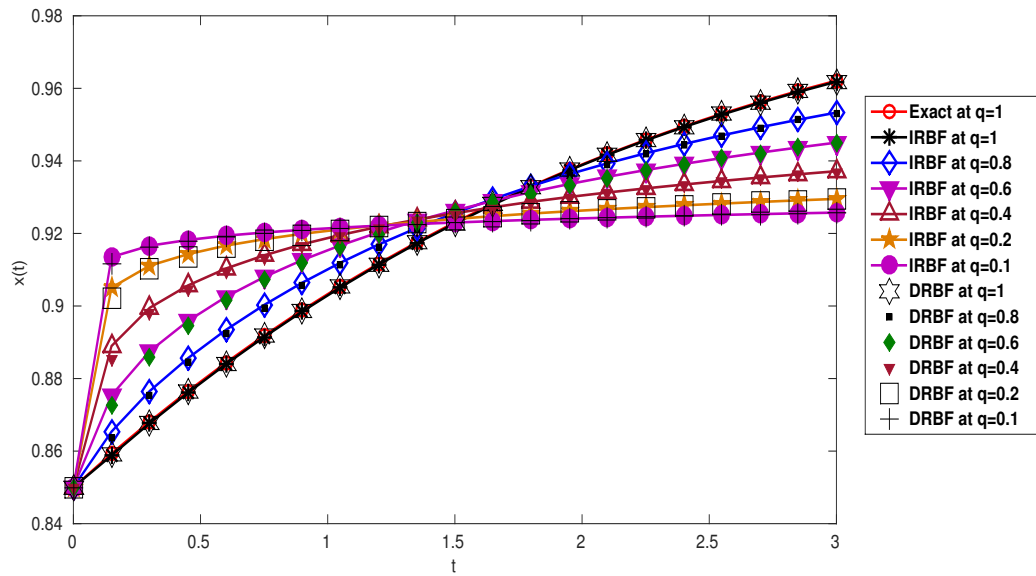


Figure 2.7 Solutions of Example 2.4.4 for various q ($K=0.5$).

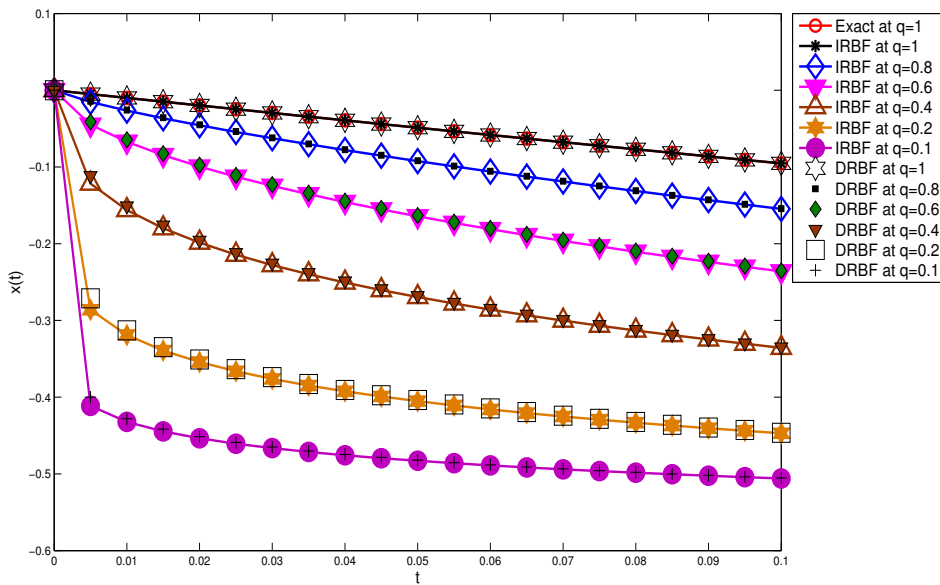


Figure 2.8 Comparison of Solutions of Example 2.4.5 for various q .

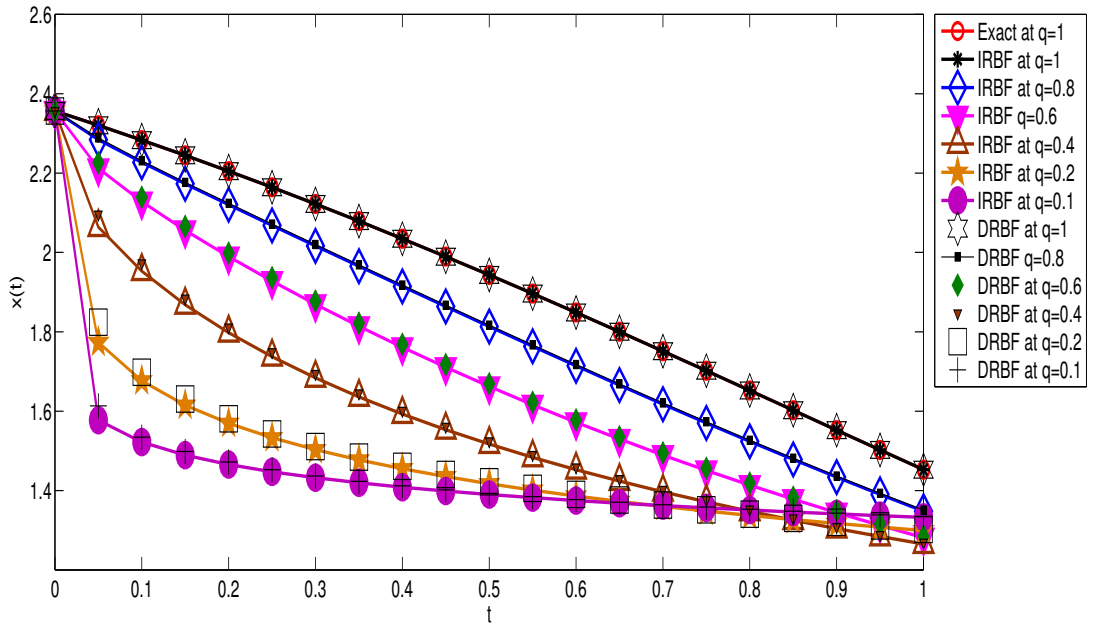


Figure 2.9 Solutions of Example 2.4.6 for various q .

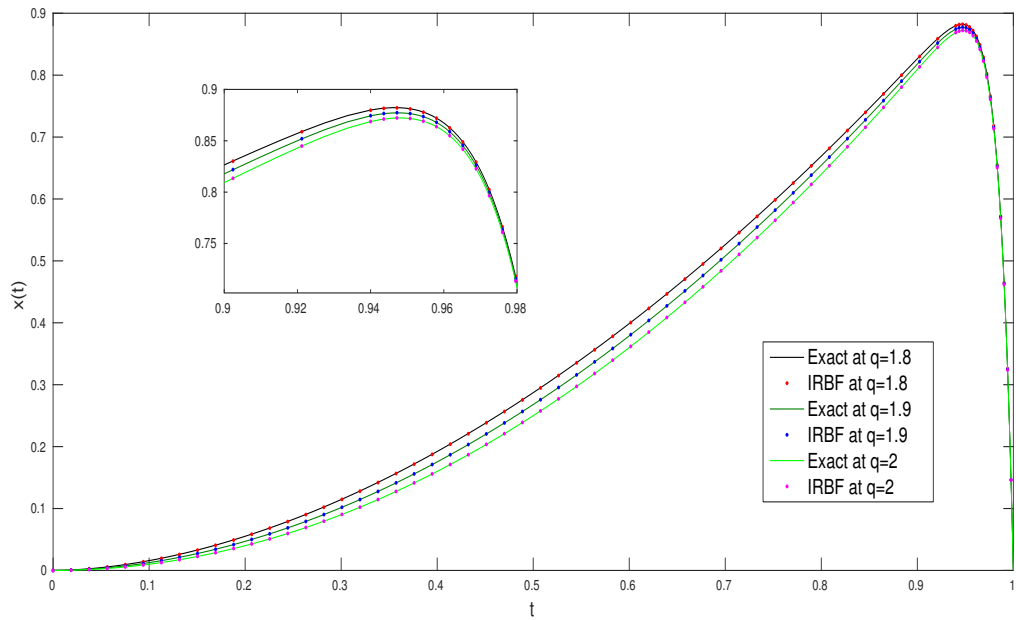


Figure 2.10 Solutions of Example 2.4.7 for various q by IRBF.

Table 2.1 RMS and L_∞ error of Example 2.4.1 ($n = 11$).

q	IRBF			DRBF		
	ε	RMS error	L_∞ error	ε	RMS error	L_∞ error
Uniform Nodes						
1	0.4	7.63E-07	1.49E-06	0.49	1.35E-07	2.88E-07
0.75	0.6	1.67E-04	4.42E-04	0.68	3.21E-03	8.49E-03
0.5	0.65	4.59E-04	1.32E-03	0.68	5.47E-03	1.59E-02
0.25	0.65	3.92E-04	1.13E-03	0.75	4.88E-03	1.46E-02
Nonuniform Nodes						
1	0.59	3.24E-08	6.81E-08	0.49	7.83E-09	1.52E-08
0.75	0.55	6.15E-05	1.94E-04	0.75	2.06E-03	6.45E-03
0.5	0.65	3.55E-04	1.16E-03	0.75	5.90E-03	1.83E-02
0.25	0.66	5.10E-04	1.68E-03	0.85	7.84E-03	2.22E-02

Table 2.2 Rate of convergence of Example 2.4.1.

Δt	IRBF				DRBF			
	RMS error	ROC	L_∞ error	ROC	RMS error	ROC	L_∞ error	ROC
$q=1$								
1/20	2.21E-03		4.95E-03		1.42E-03		3.48E-03	
1/40	1.68E-04	3.7129	3.71E-04	3.7366	1.11E-04	3.6827	2.69E-04	3.6925
1/60	1.83E-05	5.4742	3.59E-05	5.7618	1.10E-05	5.6950	2.63E-05	5.7345
1/80	1.94E-06	7.7954	3.88E-06	7.7304	1.22E-06	7.6569	2.89E-06	7.6859
$q=0.75$								
1/20	2.62E-03		8.87E-03		3.42E-03		1.16E-02	
1/40	2.39E-04	3.4560	9.60E-04	3.2074	1.40E-03	1.2869	5.60E-03	1.0450
1/60	3.58E-05	4.6778	1.60E-04	4.4201	8.23E-04	1.3159	3.62E-03	1.0766
1/80	1.07E-05	4.1843	4.68E-05	4.2679	5.74E-04	1.2512	2.68E-03	1.0457
$q=0.5$								
1/20	3.02E-03		1.22E-02		5.80E-03		2.34E-02	
1/40	3.97E-04	2.9254	2.11E-03	2.5329	2.77E-03	1.0662	1.47E-02	0.6771
1/60	1.08E-04	3.2051	6.72E-04	2.8272	1.77E-03	1.1022	1.10E-02	0.7177
1/80	5.37E-05	2.4391	3.50E-04	2.2700	1.29E-03	1.0973	8.93E-03	0.7116
$q=0.25$								
1/20	2.33E-03		9.92E-03		5.26E-03		2.24E-02	
1/40	4.11E-04	2.5071	2.35E-03	2.0794	2.93E-03	0.8454	1.69E-02	0.4034
1/60	1.63E-04	2.2859	1.10E-03	1.8736	2.04E-03	0.8839	1.41E-02	0.4412
1/80	1.00E-04	1.6791	7.58E-04	1.2913	1.58E-03	0.8928	1.24E-02	0.4454

Table 2.3 Rate of convergence for $q = 0.1$ of Example 2.4.1 by IRBF and DRBF.

Δt	RMS error	ROC	L_∞ error	ROC	RMS error	ROC	L_∞ error	ROC
IRBF								
	with 8 quadrature points				with 30 quadrature points			
1/10	3.80E-03		1.20E-02		3.80E-03		1.20E-02	
1/20	1.06E-03	1.8413	4.52E-03	1.4043	1.06E-03	1.8430	4.52E-03	1.4043
1/40	1.65E-04	2.6815	9.50E-04	2.2504	1.65E-04	2.6784	9.50E-04	2.2503
1/60	6.16E-05	2.4353	4.18E-04	2.0268	6.16E-05	2.4331	4.18E-04	2.0268
1/80	3.93E-05	1.5559	3.01E-04	1.1391	3.92E-05	1.5715	3.01E-04	1.1391
DRBF								
	with 40 quadrature points				with 50 quadrature points			
1/10	4.04E-03		1.27E-02		4.04E-03		1.27E-02	
1/20	2.57E-03	0.6530	1.10E-02	0.2100	2.57E-03	0.6530	1.10E-02	0.2100
1/40	1.52E-03	0.7548	8.87E-03	0.3045	1.52E-03	0.7548	8.87E-03	0.3045
1/60	1.11E-03	0.7871	7.74E-03	0.3347	1.10E-03	0.7878	7.74E-03	0.3347
1/80	8.79E-04	0.7942	7.02E-03	0.3383	8.79E-04	0.7952	7.02E-03	0.3386

Table 2.4 RMS and L_∞ error of Example 2.4.2 ($n = 11$).

q	IRBF			DRBF		
	ε	RMS error	L_∞ error	ε	RMS error	L_∞ error
Uniform Nodes						
2	0.48	2.52E-06	5.75E-06	0.42	5.01E-05	8.46E-05
1.75	0.46	3.66E-05	5.78E-05	0.42	1.21E-04	1.80E-04
1.5	0.47	5.59E-05	7.89E-05	0.45	8.14E-05	1.12E-04
1.25	0.42	1.96E-05	6.43E-05	0.46	2.56E-05	3.89E-05
1	0.71	3.24E-04	3.65E-04	0.46	6.34E-06	1.02E-05
0.75	0.76	4.50E-04	6.60E-04	0.52	2.98E-05	4.21E-05
0.5	0.76	3.94E-04	7.56E-04	0.6	2.75E-05	5.33E-05
0.25	0.85	4.60E-04	1.03E-03	0.72	1.02E-05	2.27E-05
Nonuniform Nodes						
2	0.52	5.78E-07	1.10E-06	0.42	1.07E-06	2.38E-06
1.75	0.52	5.72E-06	9.04E-06	0.45	3.60E-06	5.52E-06
1.5	0.47	3.46E-06	5.69E-06	0.47	9.33E-07	1.73E-06
1.25	0.48	1.84E-06	2.87E-06	0.48	1.97E-06	3.29E-06
1	0.64	4.27E-06	7.26E-06	0.46	1.12E-06	1.99E-06
0.75	0.64	6.87E-06	1.48E-05	0.72	4.19E-06	7.67E-06
0.5	0.66	1.22E-05	2.95E-05	0.72	4.55E-06	1.09E-05
0.25	0.68	1.63E-05	4.03E-05	0.68	4.15E-06	6.76E-06

Table 2.5 Comparison of absolute error of Example 2.4.2 at $t = 1$.

q	IRBF			DRBF			Rectangle Sch. (Li et al., 2016)		Trapezoidal Sch. (Li et al., 2016)	
	n	ϵ	Error	n	ϵ	Error	n	Error	n	Error
0.25	11	0.53	1.35E-05	11	0.57	1.24E-06	160	3.95E-02	160	2.14E-04
	21	0.92	1.27E-07	21	0.91	1.31E-06	320	1.85E-02	320	5.66E-05
0.75	11	0.53	7.90E-06	11	0.48	7.33E-06	160	3.15E-02	160	2.90E-04
	21	0.68	7.15E-07	21	0.79	3.24E-06	320	1.56E-02	320	7.30E-05
1.25	11	0.42	8.67E-06	11	0.46	5.88E-06	160	2.53E-02	160	2.25E-04
	21	0.79	4.17E-07	21	0.91	3.95E-07	320	1.28E-02	320	5.65E-05
1.75	11	0.46	4.95E-05	11	0.39	1.69E-04	160	1.85E-02	160	1.44E-04
	21	1.3	6.70E-06	21	0.82	1.15E-05	320	9.35E-03	320	3.62E-05

Table 2.6 Rate of convergence of Example 2.4.2.

Δt	IRBF				DRBF			
	RMS error	ROC	L_∞ error	ROC	RMS error	ROC	L_∞ error	ROC
$q=2$								
1/20	2.32E-04		9.46E-04		4.08E-02		6.71E-02	
1/40	6.17E-06	5.2328	1.91E-05	5.6337	5.36E-03	2.9280	9.00E-03	2.8980
1/60	4.25E-07	6.5974	1.10E-06	7.0314	7.80E-04	4.7518	1.32E-03	4.7348
1/80	5.67E-08	7.0026	1.11E-07	7.9866	1.14E-04	6.6871	1.93E-04	6.6751
$q=1.5$								
1/20	8.47E-04		3.38E-03		4.68E-03		7.28E-03	
1/40	1.86E-05	5.5072	6.49E-05	5.7011	3.74E-04	3.6446	6.55E-04	3.4729
1/60	2.80E-06	4.6765	1.34E-05	3.8934	3.72E-05	5.6942	5.01E-05	6.3425
1/80	2.42E-07	8.5134	7.35E-07	10.0873	4.02E-06	7.7394	6.12E-06	7.3092
$q=1.25$								
1/20	2.58E-03		1.17E-02		3.03E-03		1.19E-02	
1/40	1.29E-04	4.3197	8.22E-04	3.8362	1.80E-04	4.0753	9.75E-04	3.6045
1/60	1.10E-05	6.0764	8.36E-05	5.6383	1.51E-05	6.1109	9.89E-05	5.6453
1/80	5.50E-07	10.4125	4.14E-06	10.4467	1.49E-06	8.0436	1.09E-05	7.6557
$q=1$								
1/20	3.05E-02		4.03E-02		2.60E-02		3.10E-02	
1/40	2.25E-03	3.7608	2.83E-03	3.8339	1.92E-03	3.7640	2.11E-03	3.8770
1/60	1.72E-04	6.3413	2.54E-04	5.9464	1.89E-04	5.7115	2.06E-04	5.7415
1/80	1.58E-05	8.2975	2.66E-05	7.8398	2.07E-05	7.6906	2.24E-05	7.7028
$q=0.5$								
1/20	1.75E-02		4.61E-02		9.13E-04		3.38E-03	
1/40	1.45E-03	3.5914	4.95E-03	3.2191	3.32E-05	4.7799	1.94E-04	4.1235
1/60	1.38E-04	5.8104	6.02E-04	5.1980	1.14E-06	8.3121	6.68E-06	8.3099
1/80	1.50E-05	7.7083	7.68E-05	7.1596	1.55E-07	6.9385	1.32E-06	5.6333
$q=0.25$								
1/20	1.01E-02		3.43E-02		4.27E-04		1.68E-03	
1/40	9.44E-04	3.4171	4.39E-03	2.9678	1.48E-05	4.8486	8.90E-05	4.2371
1/60	1.00E-04	5.5311	5.91E-04	4.9465	9.31E-07	6.8241	7.10E-06	6.2365
1/80	1.18E-05	7.4232	8.10E-05	6.9041	7.16E-08	8.9198	5.64E-07	8.8061

Table 2.7 Rate of convergence of Example 2.4.2 by IRBF and DRBF for $q = 1.1$ and 0.1 .

Δt	RMS error	ROC	L_∞ error	ROC	RMS error	ROC	L_∞ error	ROC
IRBF for $q = 1.1$								
	with 14 quadrature points				with 30 quadrature points			
1/10	3.16E-02		1.04E-01		3.16E-02		1.04E-01	
1/20	4.35E-03	2.8600	1.98E-02	2.3947	4.56E-03	2.7953	2.08E-02	2.3270
1/40	2.23E-04	4.2850	1.43E-03	3.7967	2.39E-04	4.2511	1.53E-03	3.7672
1/60	2.13E-05	5.7973	1.65E-04	5.3231	1.88E-05	6.2683	1.46E-04	5.7845
1/80	1.31E-06	9.6935	1.15E-05	9.2474	1.77E-06	8.2135	1.60E-05	7.7032
IRBF for $q = 0.1$								
	with 6 quadrature points				with 30 quadrature points			
1/10	1.67E-02		4.27E-02		1.69E-02		4.25E-02	
1/20	4.70E-03	1.8305	1.61E-02	1.4063	4.46E-03	1.9269	1.61E-02	1.4001
1/40	4.24E-04	3.4697	2.32E-03	2.7966	4.54E-04	3.2960	2.32E-03	2.7963
1/60	4.97E-05	5.2872	3.32E-04	4.7891	5.33E-05	5.2792	3.33E-04	4.7893
1/80	6.16E-06	7.2596	4.72E-05	6.7804	6.57E-06	7.2791	4.72E-05	6.7917
DRBF for $q = 1.1$								
	with 30 quadrature points				with 40 quadrature points			
1/10	2.21E-02		7.10E-02		2.21E-02		7.10E-02	
1/20	3.57E-03	2.6293	1.59E-02	2.1589	3.57E-03	2.6293	1.59E-02	2.1589
1/40	2.01E-04	4.1479	1.26E-03	3.6534	2.09E-04	4.0923	1.31E-03	3.5989
1/60	1.65E-05	6.1776	1.26E-04	5.6847	1.73E-05	6.1453	1.33E-04	5.6492
1/80	2.34E-06	6.7754	2.08E-05	6.2698	1.62E-06	8.2440	1.43E-05	7.7494
DRBF for $q = 0.1$								
	with 30 quadrature points				with 40 quadrature points			
1/10	1.48E-03		3.72E-03		1.48E-03		3.72E-03	
1/20	1.55E-04	3.2553	5.96E-04	2.6419	1.55E-04	3.2553	5.96E-04	2.6419
1/40	4.22E-06	5.1989	2.54E-05	4.5524	5.35E-06	4.8566	3.21E-05	4.2147
1/60	6.93E-07	4.4555	3.22E-06	5.0938	3.69E-07	6.5950	2.80E-06	6.0159
1/80	3.42E-07	2.4549	1.87E-06	1.8890	1.94E-08	10.2388	1.49E-07	10.1968

Table 2.8 RMS and L_∞ error of Example 2.4.3 ($n = 11$).

q	IRBF Sol.			DRBF Sol.		
	ε	RMS error	L_∞ error	ε	RMS error	L_∞ error
Uniform Nodes						
1	0.6	1.54E-04	1.78E-04	0.48	1.31E-04	1.51E-04
0.75	0.63	6.69E-05	1.14E-04	0.61	4.69E-05	8.11E-05
0.5	0.65	1.39E-05	3.18E-05	0.6	1.39E-05	3.27E-05
0.25	0.69	3.16E-06	9.04E-06	0.6	3.61E-06	1.03E-05
Nonuniform Nodes						
1	0.51	1.32E-05	2.26E-05	0.49	1.29E-05	2.22E-05
0.75	0.51	5.48E-06	1.47E-05	0.68	4.85E-06	1.28E-05
0.5	0.53	2.11E-07	5.66E-07	0.66	2.85E-06	5.90E-06
0.25	0.7	1.22E-06	3.92E-06	0.6	1.37E-06	2.38E-06

Table 2.9 Comparison of solutions of Example 2.4.3 using IRBF, DRBF and Neural Networks (Qu and Liu, 2015) with exact solutions.

t	Exact	IRBF DRBF	IRBF DRBF	IRBF DRBF
		NW (Qu and Liu, 2015) $q = 1$	NW (Qu and Liu, 2015) $q = 0.7$	NW (Qu and Liu, 2015) $q = 0.5$
0.1	0.003162	0.002993 0.003014 0.0022	0.003104 0.003091 0.0055	0.003148 0.003134 0.0066
0.2	0.017889	0.017722 0.017747 0.0133	0.017845 0.017834 0.0234	0.017880 0.017868 0.0266
0.5	0.176777	0.176613 0.176629 0.1773	0.176746 0.176741 0.1783	0.176772 0.176770 0.1772
0.6	0.278855	0.278696 0.278720 0.2797	0.278827 0.278816 0.2733	0.278850 0.278848 0.2711
0.9	0.768433	0.768306 0.768320 0.767	0.768418 0.768410 0.7832	0.768432 0.768421 0.7847
1	1.000000	0.999895 0.999905 1.0064	0.999988 0.999987 1.0105	0.999998 1.000007 1.0056

Table 2.10 Rate of convergence of Example 2.4.3.

Δt	IRBF				DRBF			
	RMS error	ROC	L_∞ error	ROC	RMS error	ROC	L_∞ error	ROC
$q=1$								
1/20	9.72E-03		1.14E-02		7.31E-03		9.11E-03	
1/40	7.16E-04	3.7628	9.36E-04	3.6082	5.61E-04	3.7025	6.53E-04	3.8023
1/60	5.94E-05	6.1400	8.87E-05	5.8130	5.73E-05	5.6296	6.48E-05	5.6972
1/80	6.18E-06	7.8689	1.02E-05	7.5030	7.10E-06	7.2551	7.91E-06	7.3091
$q=0.75$								
1/20	9.09E-03		1.87E-02		8.81E-04		1.67E-03	
1/40	6.94E-04	3.7124	1.61E-03	3.5411	4.81E-05	4.1937	1.14E-04	3.8683
1/60	6.22E-05	5.9465	1.72E-04	5.5170	4.80E-06	5.6839	1.04E-05	5.8965
1/80	6.29E-06	7.9694	2.00E-05	7.4694	6.30E-07	7.0619	1.45E-06	6.8672
$q=0.5$								
1/20	8.33E-03		2.55E-02		2.66E-04		6.71E-04	
1/40	6.74E-04	3.6282	2.57E-03	3.3098	1.16E-05	4.5176	4.15E-05	4.0165
1/60	6.59E-05	5.7344	2.99E-04	5.3088	8.57E-07	6.4315	3.92E-06	5.8177
1/80	7.10E-06	7.7417	3.68E-05	7.2781	1.10E-07	7.1357	5.48E-07	6.8389
$q=0.25$								
1/20	6.36E-03		2.44E-02		8.93E-05		2.78E-04	
1/40	5.69E-04	3.4835	2.89E-03	3.0781	3.39E-06	4.7193	1.47E-05	4.2474
1/60	6.06E-05	5.5223	3.68E-04	5.0839	2.32E-07	6.6153	1.17E-06	6.2249
1/80	6.97E-06	7.5168	4.82E-05	7.0623	2.40E-08	7.8850	1.61E-07	6.9103

Table 2.11 Rate of convergence for $q = 0.1$ of Example 2.4.3 by IRBF and DRBF.

Δt	RMS error	ROC	L_∞ error	ROC	RMS error	ROC	L_∞ error	ROC
IRBF								
	with 8 quadrature points				with 30 quadrature points			
1/10	1.28E-02		3.94E-02		1.28E-02		3.94E-02	
1/20	3.37E-03	1.9188	1.39E-02	1.4970	3.37E-03	1.9197	1.39E-02	1.4980
1/40	3.26E-04	3.3726	1.82E-03	2.9393	3.26E-04	3.3722	1.82E-03	2.9378
1/60	3.65E-05	5.3969	2.45E-04	4.9486	3.66E-05	5.3902	2.45E-04	4.9485
1/80	4.35E-06	7.3947	3.32E-05	6.9375	4.35E-06	7.4012	3.31E-05	6.9544
DRBF								
	with 30 quadrature points				with 40 quadrature points			
1/10	2.38E-04		5.33E-04		2.38E-04		5.33E-04	
1/20	2.76E-05	3.1067	8.48E-05	2.6512	2.76E-05	3.1067	8.48E-05	2.6512
1/40	9.04E-07	4.9317	4.17E-06	4.3450	1.00E-06	4.7811	4.46E-06	4.2485
1/60	6.41E-08	6.5288	3.50E-07	6.1121	6.91E-08	6.6006	3.79E-07	6.0816
1/80	1.25E-08	5.6875	6.18E-08	6.0314	6.33E-09	8.3079	4.74E-08	7.2310

Table 2.12 Comparison of numerical results of Example 2.4.4 for various q ($K=0.5$).

t	IRBF		DRBF		OHAM (Hamarshah et al.) (2017)	FABM (Diethelm, 2010) $\Delta t = 3/1000$
	$\Delta t = 3/10$	$\Delta t = 3/100$	$\Delta t = 3/10$	$\Delta t = 3/100$		
$q = 0.95$						
0.30	0.8701496556	0.8701607496	0.8698139719	0.8700861931	0.8695174678	0.87016114741
2.40	0.9484783173	0.9484816402	0.9483566631	0.9484589100	0.9465598493	0.94848145599
2.70	0.9546218276	0.9546299562	0.9545176912	0.9546260834	0.9527358459	0.95462642429
3.00	0.9599748015	0.9599790186	0.9598850429	0.9599602222	0.9581461009	0.95997935080
$q = 0.499$						
0.30	0.8935988613	0.8941906750	0.8898782160	0.8939290047	0.8835393627	0.89419679205
2.40	0.9363750943	0.9364460766	0.9359190358	0.9365393519	0.9214213883	0.93644696415
2.70	0.9388860644	0.9389519304	0.9384762587	0.9390915930	0.9238740100	0.93895245078
3.00	0.9411188793	0.9411644995	0.9407859851	0.9411096275	0.9263917529	0.94117011121
$q = 0.155$						
0.30	0.9136791640	0.9138517467	0.9111921475	0.9137007203	0.8932334396	0.9138566224
2.40	0.9264872996	0.9265023991	0.9262895044	0.9264853427	0.9039197368	0.9265037573
2.70	0.9272092854	0.9272211649	0.9270072508	0.9272199315	0.9045401707	0.9272245219
3.00	0.9278574319	0.9278694469	0.9277664045	0.9278735326	0.9054430750	0.9278689008

Table 2.13 Comparison of the numerical solution of Example 2.4.5 at $q = 0.9$ ($T = 0.1$).

t	IRBF $(\Delta t = T/10)$	DRBF $(\Delta t = T/10)$	DRBF $(\Delta t = T/20)$	DRBF $(\Delta t = T/30)$	FABM (Jang, 2014) $(\Delta t = T/100)$	GDTM (Jang, 2014)
0.01	-0.016327	-0.015784	-0.016074	-0.016163	-0.016331	-0.016331
0.02	-0.030238	-0.029755	-0.030004	-0.030113	-0.030241	-0.030238
0.05	-0.067560	-0.067145	-0.067363	-0.067386	-0.067564	-0.067531
0.1	-0.122265	-0.121895	-0.122083	-0.122096	-0.122267	-0.122072

Table 2.14 Comparison of the numerical solution of Example 2.4.6 at $q = 0.9$ ($T = 1$).

t	IRBF $(\Delta t = T/10)$	IRBF $(\Delta t = T/20)$	DRBF $(\Delta t = T/10)$	DRBF $(\Delta t = T/20)$	DRBF $(\Delta t = T/30)$	FABM Jang (2014) $(\Delta t = T/1000)$	GDTM Jang (2014)
0.1	2.25883	2.25889	2.26248	2.26049	2.26007	2.25891	2.25891
0.2	2.16704	2.16710	2.17063	2.16870	2.16829	2.16712	2.16712
0.5	1.88159	1.88165	1.88539	1.88334	1.88291	1.88168	1.88168
1	1.39668	1.39674	1.40027	1.39833	1.39793	1.39676	1.39620

Table 2.15 L_∞ error of Example 2.4.7.

q	IRBF			DRBF			Haar-wavelet (Saeed and ur Rehman, 2013)	
	n	ε	L_∞ error	n	ε	L_∞ error	n	L_∞ error
Uniform Nodes								
2	201	26.4	1.31E-04	201	17.1	7.46E-05		
	401	54	2.28E-05	401	33.3	8.33E-06	512	1.02E-02
	501	70	9.17E-06	501	39.4	4.42E-06	1024	2.40E-03
1.9	201	26.3	3.68E-05	201	16	7.19E-05		
	401	54	1.26E-05	401	30.7	1.35E-05	512	6.43E-02
	501	70.3	8.39E-06	501	38.8	1.36E-05	1024	2.28E-02
1.8	201	32.9	6.93E-05	201	29	7.21E-04		
	401	54	1.06E-05	401	48.1	1.71E-04	512	8.29E-02
	501	70.9	1.24E-05	501	40	6.10E-05	1024	2.28E-02
Nonuniform Nodes								
2	201	116	4.47E-05	201	80	2.78E-04		
	401	243	2.55E-05	401	148	6.00E-05	512	8.08E-05
	501	300	2.64E-05	501	170	3.61E-05	1024	2.04E-05
1.9	201	200	1.80E-04	201	79	6.72E-03		
	401	431	3.51E-05	401	135	3.14E-03	512	2.74E-04
	501	560	2.77E-05	501	170	2.62E-03	1024	1.11E-04
1.8	201	205	7.79E-04	201	110	6.37E-03		
	401	587	7.86E-05	401	151	2.34E-03	512	5.44E-04
	501	679	2.27E-04	501	178	2.12E-03	1024	2.54E-04

Table 2.16 Rate of convergence of Example 2.4.7.

Δt	IRBF				DRBF			
	RMS error	ROC	L_∞ error	ROC	RMS error	ROC	L_∞ error	ROC
$q=2$								
1/200	1.94E-04		1.07E-03		3.47E-03		4.82E-03	
1/400	1.72E-04	0.1726	2.86E-04	1.8997	2.90E-04	3.5812	3.94E-04	3.6119
1/600	4.28E-05	3.4286	6.09E-05	3.8165	2.07E-05	6.5088	2.79E-05	6.5286
1/800	1.84E-05	2.9386	3.37E-05	2.0613	1.46E-06	9.2273	1.98E-06	9.2069
$q=1.9$								
1/200	1.81E-03		3.66E-03		7.57E-04		9.84E-04	
1/400	1.37E-04	3.7280	4.05E-04	3.1754	2.67E-04	1.5000	3.14E-04	1.6491
1/600	2.94E-05	3.7898	5.91E-05	4.7422	2.92E-05	5.4627	3.40E-05	5.4825
1/800	5.36E-06	5.9105	1.37E-05	5.0871	9.12E-06	4.0449	1.07E-05	4.0110
$q=1.8$								
1/200	9.32E-03		1.64E-02		1.24E-03		3.63E-03	
1/400	5.42E-05	7.4259	7.42E-04	4.4675	3.35E-04	1.8896	3.85E-04	3.2394
1/600	1.52E-05	3.1423	7.18E-05	5.7599	6.68E-05	3.9757	7.65E-05	3.9824
1/800	1.60E-06	7.8150	1.65E-05	5.1145	3.48E-05	2.2712	4.00E-05	2.2520

CHAPTER 3

A RADIAL BASIS FUNCTION METHOD FOR FRACTIONAL DARBOUX PROBLEMS

3.1 INTRODUCTION

Darboux problems, where the governing equation is of hyperbolic (in nature), in general arises in wave phenomena, has in the following form:

$$\begin{aligned} D_{xy}u(x,y) &= \frac{\partial^2 u}{\partial x \partial y} = f(x,y,u(x,y)), \quad (x,y) \in J & (3.1.1) \\ u(x,0) &= g(x); \quad x \in [0,a] \\ u(0,y) &= h(y); \quad y \in [0,b] \end{aligned}$$

where $a, b > 0$, $J := [0, a] \times [0, b]$ and g and h are continuously differentiable functions.

Sometimes the Darboux problem is also referred as the Goursat problem. Certain classical problems of mathematical physics and rigid body dynamics are expressed in terms of Darboux problems. They can also be considered as a limiting case of tricomi problem. Efforts to solve (3.1.1) numerically is dated back to 1960's. These attempts are made by J. T. Day (1966), M. K. Jain and Sharma (1968) and A. R. Gourlay (1970). They are based on Trapezoidal or other quadrature formulae and Runge-Kutta type methods. Later a nonlinear trapezoidal formula based on geometric means (Evans and Sanugi, 1988) and harmonic means (Wazwaz, 1993) are also considered in solving Goursat problems. In a work by Człapiński (1999), a general class of difference schemes for this problem have been attempted. In 2011, Gou and Sun have solved the problem in a triangular domain with mixed Dirichlet and impedance boundary conditions, based on Runge-Kutta and trapezoidal methods.

The literature on numerical schemes for fractional partial differential equations majorly covers models that are fractional counterparts of parabolic differential equations. Further, these models do not involve mixed fractional partial derivatives. Hence, the work reported in this chapter is an attempt to extend Kansa's asymmetric RBF collocation method to fractional Darboux problem in the following form,

$$\begin{aligned} {}^c D^{\bar{q}} u(x,y) &= \frac{\partial^{q_1+q_2} u}{\partial x^{q_1} \partial y^{q_2}} = f(x,y,u(x,y)), \quad (x,y) \in J, \\ u(x,0) &= g(x) \quad x \in [0,a]; \\ u(0,y) &= h(y); \quad y \in [0,b], \end{aligned} \quad (3.1.2)$$

where $a, b > 0$, $J := (0, a] \times (0, b]$, $\bar{q} = (q_1, q_2) \in (0, 1] \times (0, 1]$ and g and h are continuously differentiable functions with $g(0) = h(0)$. The function $f : J \times \mathbb{R} \rightarrow \mathbb{R}$ is a continuous function and satisfies Lipschitz condition with respect to the third variable u with Lipschitz constant L .

Researchers, namely, S. Abbas, M. Benchohra and A. Vityuk have worked extensively on the existence and uniqueness of various classes of fractional Darboux problem; Refer the book by Abbas et al. (2012) and the references therein for the detailed proof. The problems considered were fractional equations or inclusions with and without delay terms in various forms. Results are also established for equations that involves impulsive effect. Vityuk and Mykhailenko (2011) have obtained the sufficient conditions of the existence and uniqueness of the solution of implicit fractional Darboux problem and also provided some numerical solutions.

Even for integer order Darboux model, there are only a few efforts to obtain numerical solutions as briefed in earlier paragraph. In addition, there are no efforts based on RBF schemes. Hence our main contribution is extending the direct RBF collocation schemes to both integer and fractional order Darboux problem (3.1.2). Further, to linearise the Darboux model, successive approximation is considered.

The remaining part of the chapter is organised as follows: Section 3.2 provides some of the basic definitions on mixed fractional derivatives and Section 3.3 proves a theorem that ensures the existence and uniqueness of the solution of Darboux problem (3.1.2) and the convergence of successive approximation to the solution of (3.1.2). Derivation of Kansa's collocation (Kansa, 1990) for fractional Darboux equations are detailed in Section 3.4. For some of the radial functions, strategies such as optimisation of shape

parameter and variable shape parameters are employed. The scheme then tested on variety of example problems and these results are analysed in Section 3.5. Finally, the chapter is concluded by summarising both advantages and disadvantages with some suggestions for possible future improvements.

3.2 PARTIAL FRACTIONAL INTEGRALS AND DERIVATIVES

Since we are considering fractional order Darboux problem as in Eqn. (3.1.2), which requires the definition of mixed (partial) fractional derivative, the extension of the definition for fractional integrals and derivatives to partial fractional integrals and derivatives are considered in the following (Kilbas et al., 1993).

Definition 3.2.1. *The Riemann–Liouville fractional integral of order $q \in (0, \infty)$ of a function $u \in L_1(J)$ with respect to x is defined by*

$$I_{0,x}^q u(x,y) = \frac{1}{\Gamma(q)} \int_0^x (x-s)^{q-1} u(s,y) ds,$$

for $x \in [0, a]$ and $y \in [0, b]$. Analogously, $I_{0,y}^q u(x,y)$ can also be defined.

Definition 3.2.2. *The Caputo fractional derivative of order $q \in (0, 1]$ of a function u , where $\frac{\partial u}{\partial x} \in L_1(J)$, with respect to x is defined by*

$${}^c D_{0,x}^q u(x,y) = I_{0,x}^{1-q} \frac{\partial}{\partial x} u(x,y),$$

for $x \in [0, a]$ and $y \in [0, b]$. Analogously, ${}^c D_{0,y}^q u(x,y)$ can also be defined.

Definition 3.2.3. *Let $\bar{q} = (q_1, q_2) \in (0, \infty) \times (0, \infty)$, $\theta = (0, 0)$ and $u \in L_1(J)$. The mixed Riemann-Liouville integral of order \bar{q} of u is defined by*

$$I_{\theta}^{\bar{q}} u(x,y) = I_0^{q_1} I_0^{q_2} u(x,y) = \frac{1}{\Gamma(q_1)\Gamma(q_2)} \int_0^x \int_0^y (x-s)^{q_1-1} (y-t)^{q_2-1} u(s,t) dt ds$$

for $(x,y) \in J$. In particular,

$$I_{\theta}^{\theta} u(x,y) = u(x,y); \quad I_{\theta}^{\sigma} u(x,y) = \int_0^x \int_0^y u(s,t) dt ds; \quad (3.2.1)$$

for $(x,y) \in J$, where $\sigma = (1, 1)$.

Definition 3.2.4. *Let $\bar{q} \in (0, 1] \times (0, 1]$. The mixed fractional Caputo derivative of order \bar{q} of u is defined by the expression ${}^c D_{\theta}^{\bar{q}} u(x,y) = I_{\theta}^{1-\bar{q}} D_{xy} u(x,y)$, where $1 - \bar{q} = (1 -$*

$q_1, 1 - q_2$) and $D_{xy}u = \frac{\partial^2 u}{\partial x \partial y} \in L_1(J)$. In particular, ${}^c D_{\theta}^{\sigma} u(x, y) = D_{xy}u(x, y)$ for $(x, y) \in J$, where $\sigma = (1, 1)$.

3.3 SUCCESSIVE APPROXIMATION

The following theorem establishes the existence of the solution of (3.1.2) and the convergence of successive approximation to the solution.

Theorem 1. *The fractional Darboux problem (3.1.2) has a unique solution. Moreover, the following successive approximation scheme*

$${}^c D_{\theta}^{\bar{q}} u^{k+1}(x, y) = f(x, y, u^k(x, y)) \quad (3.3.1)$$

$$u^{k+1}(x, 0) = g(x) \quad ; \quad u^{k+1}(0, y) = h(y); \quad g(0) = h(0) \quad (3.3.2)$$

converges uniformly to the unique solution of (3.1.2), for any continuous function as initial guess.

Proof: It is easy to show that Eqn. (3.1.2) is equivalent to the integral equation

$$u(x, y) = \eta(x, y) + \frac{1}{\Gamma(q_1)\Gamma(q_2)} \int_0^x \int_0^y (x-s)^{q_1-1} (y-t)^{q_2-1} f(s, t, u(s, t)) dt ds \quad (3.3.3)$$

where $\eta(x, y) = g(x) + h(y) - g(0)$. Note that $C([0, a] \times [0, b])$ is a Banach space with the norm defined $\|u\|_{\rho} = \sup_{(x, y) \in [0, a] \times [0, b]} \frac{1}{E_{q_1}(\rho x^{q_1})} |u(x, y)|$, $\rho > 0$. Define an operator $\widehat{T} : C([0, a] \times [0, b]) \rightarrow C([0, a] \times [0, b])$ by

$$\widehat{T}u(x, y) = \eta(x, y) + \frac{1}{\Gamma(q_1)} \frac{1}{\Gamma(q_2)} \int_0^x \int_0^y (x-s)^{q_1-1} (y-t)^{q_2-1} f(s, t, u(s, t)) dt ds \quad (3.3.4)$$

Note that

$$\begin{aligned} & |(\widehat{T}u_1 - \widehat{T}u_2)(x, y)| \\ & \leq \frac{L}{\Gamma(q_1)\Gamma(q_2)} \int_0^x \int_0^y (x-s)^{q_1-1} (y-t)^{q_2-1} |u_1(s, t) - u_2(s, t)| dt ds \\ & = \frac{L}{\Gamma(q_1)\Gamma(q_2)} \int_0^x \int_0^y (x-s)^{q_1-1} (y-t)^{q_2-1} \frac{E_{q_1}(\rho s^{q_1})}{E_{q_1}(\rho s^{q_1})} |u_1(s, t) - u_2(s, t)| dt ds \\ & \leq L \|u_1 - u_2\| \frac{1}{\Gamma(q_1)\Gamma(q_2)} \int_0^x \int_0^y (x-s)^{q_1-1} (y-t)^{q_2-1} E_{q_1}(\rho s^{q_1}) dt ds \\ & \leq \frac{Lb^{q_2}}{\Gamma(q_2+1)} \|u_1 - u_2\| \frac{1}{\Gamma(q_1)} \int_0^x (x-s)^{q_1-1} E_{q_1}(\rho s^{q_1}) ds \end{aligned}$$

$$= \frac{Lb^{q_2}}{\Gamma(q_2 + 1)} \|u_1 - u_2\| \frac{E_{q_1}(\rho x^{q_1})}{\rho}$$

Thus

$$\frac{|(\widehat{T}u_1 - \widehat{T}u_2)(x, y)|}{E_{q_1}(\rho x^{q_1})} \leq \frac{Lb^{q_2}}{\Gamma(q_2 + 1)\rho} \|u_1 - u_2\| \quad (3.3.5)$$

Hence

$$\|\widehat{T}u_1 - \widehat{T}u_2\| \leq \frac{Lb^{q_2}}{\Gamma(q_2 + 1)\rho} \|u_1 - u_2\| \quad (3.3.6)$$

Thus \widehat{T} is a contraction for sufficiently large ρ . Consequently the successive iteration $u^{k+1} = \widehat{T}u^k$ converge to the unique fixed point of \widehat{T} . Consequently the iterative scheme (3.3.1) converge to the unique solution.

Example: The Sine-Gordon equation ${}^c D_0^{\bar{q}} u(x, y) = \sin u$, $(x, y) \in [0, a] \times [0, b]$ where $\bar{q} = (q_1, q_2) \in (0, 1] \times (0, 1]$, $u(x, 0) = g(x)$, $u(0, y) = h(y)$, $g(0) = h(0)$ has a unique solution. Moreover the following iterative scheme converge to the unique solution.

$${}^c D_0^{\bar{q}} u^{k+1}(x, y) = \sin(u^k) \quad (3.3.7)$$

$$u^{k+1}(x, 0) = g(x); \quad u^{k+1}(0, y) = h(y); \quad g(0) = h(0) \quad (3.3.8)$$

Equivalently

$$u^{k+1}(x, y) = \eta(x, y) + \frac{1}{\Gamma(q_1)\Gamma(q_2)} \int_0^x \int_0^y (x-s)^{q_1-1} (y-t)^{q_2-1} \sin(u^k(s, t)) ds dt \quad (3.3.9)$$

converge to the unique solution for any continuous function as initial guess.

In the following section, we describe an RBF scheme for fractional Darboux equation.

3.4 A FRACTIONAL RBF APPROXIMATION

Consider the linearised Darboux problem (3.3.1)-(3.3.2). Assume that the function $u^{k+1}(\bar{x})$ represents the solution of the linearised problem at $(k+1)^{th}$ iteration and can be represented in terms of RBFs as

$$u^{k+1}(\bar{x}) = \sum_{j=1}^n \lambda_j^{k+1} \phi(\|\bar{x} - \bar{x}_j\|) + \sum_{j=1}^l \gamma_j^{k+1} p_j(\bar{x}) \quad (3.4.1)$$

where $\bar{x}_j = (x_j, y_j)$, $j = 1, 2, \dots, n$, are collocation points distributed in the given domain. Assuming that ϕ is sufficiently smooth, the operator ${}^c D_0^{\bar{q}}$ is acted on both the sides of

the Eqn.(3.4.1), we obtain

$${}^c D_0^{\bar{q}} u^{k+1}(\bar{x}) = \sum_{j=1}^n \lambda_j^{k+1} {}^c D_0^{\bar{q}} \phi(\|\bar{x} - \bar{x}_j\|) + \sum_{j=1}^l \gamma_j^{k+1} {}^c D_0^{\bar{q}} p_j(\bar{x}) \quad (3.4.2)$$

For each node $\bar{x}_i = (x_i, y_i)$, $i = 1, 2, \dots, n$, the problem (3.3.1)-(3.3.2) is discretised by substituting (3.4.1) and (3.4.2) for the governing equation and the initial conditions appropriately. This leads to the following system of equations. i.e., For each $i = 1, 2, \dots, n$.

$$\sum_{j=1}^n \lambda_j^{k+1} {}^c D_0^{\bar{q}} \phi(\|\bar{x}_i - \bar{x}_j\|) + \sum_{j=1}^l \gamma_j^{k+1} {}^c D_0^{\bar{q}} p_j(\bar{x}_i) = f(x_i, y_i, u_i^k), \quad (3.4.3)$$

if $x_i, y_i > 0$

$$\sum_{j=1}^n \lambda_j^{k+1} \phi(\|\bar{x}_i - \bar{x}_j\|) + \sum_{j=1}^l \gamma_j^{k+1} p_j(\bar{x}_i) = g(x_i), \quad \text{if } y_i = 0 \quad (3.4.4)$$

$$\sum_{j=1}^n \lambda_j^{k+1} \phi(\|\bar{x}_i - \bar{x}_j\|) + \sum_{j=1}^l \gamma_j^{k+1} p_j(\bar{x}_i) = h(y_i), \quad \text{if } x_i = 0 \quad (3.4.5)$$

with l extra conditions,

$$\sum_{j=1}^n \lambda_j^{k+1} p_i(\bar{x}_j) = 0, \quad i = 1, 2, \dots, l \quad (3.4.6)$$

Eqns. (3.4.3)-(3.4.6) together can be written in the matrix form,

$$\begin{pmatrix} A & B \\ P & \mathbf{0} \end{pmatrix} \begin{pmatrix} \bar{\lambda}^{k+1} \\ \bar{\gamma}^{k+1} \end{pmatrix} = \begin{pmatrix} \bar{f} \\ \bar{0} \end{pmatrix} \quad (3.4.7)$$

where A , B and P are matrices of sizes $n \times n$, $n \times l$ and $l \times n$, respectively. $\mathbf{0}$ is a zero matrix of order l . The components of these submatrices are

$$A_{ij} = \begin{cases} {}^c D_0^{\bar{q}} \phi(\|\bar{x}_i - \bar{x}_j\|), & \text{if } x_i, y_i > 0 \\ \phi(\|\bar{x}_i - \bar{x}_j\|), & \text{if } x_i = 0 \text{ or } y_i = 0. \end{cases}$$

$$B_{is} = \begin{cases} {}^c D_0^{\bar{q}} p_s(\bar{x}_i), & \text{if } x_i, y_i > 0 \\ p_s(\bar{x}_i), & \text{if } x_i = 0 \text{ or } y_i = 0. \end{cases}$$

$$P_{sj} = p_s(\bar{x}_j), \quad \text{if } x_j, y_j \geq 0 \text{ and } s = 1, 2, \dots, l.$$

Also, $\bar{\lambda}^{k+1} = [\lambda_1^{k+1}, \lambda_2^{k+1}, \dots, \lambda_n^{k+1}]^T$, $\bar{\gamma}^{k+1} = [\gamma_1^{k+1}, \gamma_2^{k+1}, \dots, \gamma_l^{k+1}]^T$, are the column

vectors containing unknown coefficients. On the right hand side of the matrix equation $\bar{0}$ is a zero vector of length l and $\bar{f} = [f_1, f_2, \dots, f_n]^T$ is a vector with following entries.

$$f_i = \begin{cases} f(x_i, y_i, u_i^k) & \text{if } x_i, y_i > 0, \\ g(x_i) & \text{if } y_i = 0 \\ h(y_i) & \text{if } x_i = 0 \end{cases}$$

The solution u at each node is updated using Eqn. (3.4.1) after solving the system (3.4.7) at each iteration. It is observed that only \bar{f} needs to be corrected for each iteration k , whereas the coefficient matrix remains unaltered in any iteration. This significantly reduces the computation.

3.4.1 Mixed Caputo derivative of radial basis functions

It is seen in the above description that the discretisation of the fractional Darboux problem further requires the evaluation of the mixed (partial) fractional derivatives of the radial basis functions. For each $j = 1, 2, \dots, n$, if $\phi = \phi(\|\bar{x} - \bar{x}_j\|)$, then

$${}^c D_0^{\bar{q}} \phi = \frac{1}{\Gamma(1-q_1)\Gamma(1-q_2)} \int_0^x \int_0^y (x-s)^{-q_1} (y-t)^{-q_2} \frac{\partial^2 \phi(\|\bar{s} - \bar{x}_j\|)}{\partial s \partial t} dt ds \quad (3.4.8)$$

where $\bar{x} = (x, y)$, $\bar{x}_j = (x_j, y_j)$ and $\bar{s} = (s, t)$.

An accurate evaluation of ${}^c D_0^{\bar{q}} \phi$ is important in achieving the overall accuracy in the solution. Obtaining analytic fractional derivative is a tedious task and such efforts lead to infinite series in terms of hypergeometric functions (Mohammadi and Schaback). Effective evaluation of such series is again time consuming, hence Gauss-Jacobi rule (Pang et al., 2015) is chosen for the computation of (3.4.8).

3.4.1.1 Gauss-Jacobi quadrature rule

As discussed in chapter 2, Gauss-Jacobi quadrature rule is considered for calculating the numerical integral of the form $\int_{-1}^1 W(\xi) F(\xi) d\xi$, where $W(\xi) = (1-\xi)^{\mu_1} (1+\xi)^{\mu_2}$ with $\mu_1, \mu_2 > -1$. It has been proved that Gauss-Jacobi rules are exact for polynomials of degree less than or equal to $2N+1$. Extending Gauss-Jacobi quadrature rule to two dimensions over a rectangle $[-1, 1] \times [-1, 1]$ and using iterated integral, we can write

$$\int_{-1}^1 \int_{-1}^1 (1-\xi)^{\mu_1} (1+\xi)^{\mu_2} (1-\zeta)^{\mu_3} (1+\zeta)^{\mu_4} F(\xi, \zeta) d\xi d\zeta$$

$$\begin{aligned}
&= \int_{-1}^1 (1-\xi)^{\mu_1} (1+\xi)^{\mu_2} \left(\int_{-1}^1 (1-\zeta)^{\mu_3} (1+\zeta)^{\mu_4} F(\xi, \zeta) d\zeta \right) d\xi \\
&\approx \sum_{p_1=1}^{N_1} \sum_{p_2=1}^{N_2} W_{p_1} V_{p_2} F(\xi_{p_1}, \zeta_{p_2})
\end{aligned} \tag{3.4.9}$$

Here, $\{\xi_{p_1}\}$ and $\{W_{p_1}\}$, $p_1 = 1, 2, \dots, N_1$ are Gauss-Jacobi quadrature points and weights corresponds to the variable ξ , while $\{\zeta_{p_2}\}$ and $\{V_{p_2}\}$, $p_2 = 1, 2, \dots, N_2$ corresponds to ζ . Further, $\mu_i > -1$, $i = 1, 2, 3, 4$.

To implement the quadrature rule on (3.4.8), convert the integral from $[0, x] \times [0, y]$ to the interval $[-1, 1] \times [-1, 1]$ using the change of variable $\bar{s}(\xi, \zeta) = [\frac{x}{2}(1-\xi), \frac{y}{2}(1-\zeta)]$. The integral (3.4.8) then becomes,

$${}^c D_0^{\bar{q}} \phi = \frac{(\frac{x}{2})^{(-q_1+1)} (\frac{y}{2})^{(-q_2+1)}}{\Gamma(1-q_1)\Gamma(1-q_2)} \int_{-1}^1 \int_{-1}^1 (1+\xi)^{-q_1} (1+\zeta)^{-q_2} \frac{\partial^2 \phi(\|\bar{s} - \bar{x}_j\|)}{\partial s \partial t} \Big|_{\bar{s}(\xi, \zeta)} d\xi d\zeta \tag{3.4.10}$$

Applying quadrature rule to (3.4.10)

$${}^c D_0^{\bar{q}} \phi \approx \frac{(\frac{x}{2})^{(-q_1+1)} (\frac{y}{2})^{(-q_2+1)}}{\Gamma(1-q_1)\Gamma(1-q_2)} \sum_{p_1=1}^{N_1} \sum_{p_2=1}^{N_2} w_{p_1} v_{p_2} F(\xi_{p_1}, \zeta_{p_2})$$

$$\text{where } F(\xi_{p_1}, \zeta_{p_2}) = \frac{\partial^2 \phi(\|\bar{s} - \bar{x}_j\|)}{\partial s \partial t} \Big|_{\bar{s}(\xi_{p_1}, \zeta_{p_2})}.$$

3.5 NUMERICAL ILLUSTRATIONS

This section provides various examples of fractional Darboux problem to illustrate the proposed RBF scheme. For an exhaustive comparison among various RBFs we have considered MQ, GA and PS. The shape parameter ε in MQ and GA has been varied numerically to improve the solution. The exponent in PS have been varied to study the effect of the parameter on accuracy and stability of the method. Nodes have been distributed both uniformly and nonuniformly in the domain. Nonuniform nodal distribution has been done using Chebyshev-Gauss-Lobatto point distribution in both x and y directions $\left(\frac{1-\cos(i\pi/n)}{2}, i = 0, 1, \dots, n \right)$. Chosen nodal distributions are shown in Figure 3.1. Whenever exact solution is available, accuracy has been compared by obtaining RMS and L_∞ errors using the formula,

$$RMS\ error = \sqrt{\frac{1}{n} \sum_{j=1}^n [u(\bar{x}_j) - u_{app}(\bar{x}_j)]^2}; \quad L_{\infty}error = \max_{1 \leq j \leq n} |u(\bar{x}_j) - u_{app}(\bar{x}_j)|$$

where n is the total number of nodes in the given domain. Error tolerance for successive approximation is fixed as 10^{-04} , unless otherwise specified.

Example 3.5.1. Consider \bar{q}^{th} order nonlinear fractional Darboux problem:

$${}^c D_0^{\bar{q}} u = u - u^2 - xy + (xy)^2 + \frac{x^{1-q_1} y^{1-q_2}}{\Gamma(2-q_1)\Gamma(2-q_2)}, \quad (x,y) \in [0,1] \times [0,1],$$

subject to the conditions, $u(x,0) = u(0,y) = 0, 0 \leq x,y \leq 1$. The exact solution is given by $u(x,y) = xy$.

The results are discussed through the Figure 3.2 and Tables 3.1 to 3.5. Since the analytic solution is known for all \bar{q} , errors have been obtained for several fractional values of q_1 and q_2 and found that RBF approximations (MQ, GA and PS) very accurate with small set of nodes (11×11). Further, the proposed scheme yields convergent and accurate solutions even for small values of \bar{q} , say $(0.1,0.1)$. It can also be seen that as $\bar{q} \rightarrow (0,0)$, number of iterations for successive iteration increases. This must be expected in view of the fact that according to the definition of fractional derivatives, $\frac{1}{\Gamma q_1 \Gamma q_2} \rightarrow 0$ as $\bar{q} \rightarrow (0,0)$. Also nonuniform distribution, where nodes near boundary are finer, gives a solution with more accuracy and suppresses the error near the boundary (refer Figure 3.2 and Table 3.1).

Tables 3.2 to 3.5 present the order of convergence of the RBF collocation as $\Delta x, \Delta y \rightarrow 0$ for various fractional orders \bar{q} . For MQ and GA, the rate have been calculated for fixed ε , while β is kept constant for polyharmonic splines (PS). Both MQ and GA give an exponential convergence rate, where as PS solutions do not improve as nodal points get refined. However, it is observed from these tables that as $\bar{q} \rightarrow (0,0)$, solutions become more inaccurate in some cases or method diverges. This is caused by the severe ill-conditioning of the resulting linear systems as $\Delta x, \Delta y \rightarrow 0$. Also it is to be noted that ε chosen to evaluate the order of convergence are not optimal values, due to ill-conditioning issue for smaller ε (optimal ε 's are close to zero) with larger number of nodes n . CPU time is also presented in 3.5. Time increases as \bar{q} -values becomes fractional, which requires the calculation of fractional derivative terms in the coefficient matrix. Further, number of iterations increases as $\bar{q} \rightarrow (0,0)$.

Example 3.5.2.

$${}^c D_0^{\bar{q}} u = 0.1[u^3 + u + \cos y e^{0.1x} - g(x,y)^3 - g(x,y)], (x,y) \in [0,0.5] \times [0,0.5],$$

subject to the initial conditions $u(x,0) = 1 + x^4$ and $u(0,y) = 1 + y + \sin y, 0 \leq x, y \leq 0.5$. Here $g(x,y) = \sin y e^{0.1x} + y + x^4 + 1$. The exact solution, when $\bar{q} = (1,1)$, is given by $u(x,y) = g(x,y), \forall (x,y) \in [0,0.5] \times [0,0.5]$.

The results for this example are presented in Tables 3.6 to 3.8 and Figures 3.3 to 3.5. Since analytic solution is known only for integer order problem ($q_1 = q_2 = 1$), this case has been chosen to analyse the method in detail. Figure 3.3 gives surface plots for exact and numerical solution as well as the corresponding error graphs. The solutions using uniform and nonuniform nodes do not show any visible difference with respect to the corresponding analytic solution plots. However, it can be observed through the error plots that nonuniform solution is more accurate with error being subsided throughout the domain. In Figures 3.4-3.5, the solutions are depicted at various cross-sections of x and y . Each subplot shows how solutions are changing by varying q_2 by keeping q_1 constant. When $q_1 \geq 0.5$, the proposed scheme captures solutions for q_2 as low as 0.1, whereas when $q_1 < 0.5$ (for eg: $q_1 = 0.3$) the accurate solution is obtained only till $q_2 = 0.2$.

As in Example 3.5.1, in an effort to understand each radial basis function, an exhaustive comparison among MQ, GA and PS have been done and presented in Tables 3.6-3.8. Table 3.6 compares solutions obtained using proposed schemes with that given in (Cheung, 1977). Further, the errors are presented in Tables 3.7 for both uniform and nonuniform distribution of nodes. For these calculations, the shape parameter ' ε ' has been chosen optimally (solution may further improve by reducing ε , however system becomes highly ill-conditioned). It is observed that MQ is marginally better in accuracy than GA, but PS is less accurate. However, it is surprised to observe that the accuracy of PS has been greatly improved by appending a polynomial of degree 2. This characteristic is not observed in the case of MQ and GA. Table 3.8 provides numerical rate of convergence (obtained by keeping ε and β fixed) for each RBF. An exponential rate of convergence is observed in case of MQ, as predicted in RBF interpolation. Exponential rate is expected even in case of GA, however the solution is sensitive to ε and number of points in the domain. PS is shown to have a fixed algebraic order of convergence, which clearly is proportionate to $\frac{\beta}{2}$.

Example 3.5.3. Consider the nonlinear fractional Darboux problem:

$${}^c D_0^{\bar{q}} u = e^{2u}, (x, y) \in [0, 1] \times [0, 1]$$

The exact solution for $\bar{q} = (1, 1)$ is $u(x, y) = \frac{x+y}{2} - \log(e^x + e^y)$ Day (1966); Jain and Sharma (1968). Initial conditions can be obtained using the exact solution.

From Table 3.9, where MQ, GA and PS solutions are compared point wise with cubature method (Jain and Sharma, 1968), it can be observed that PS appended by polynomials gives a superior solution using 21×21 uniform set of nodes. For MQ and GA solutions are improved by using nonuniform nodes, however optimal accuracy is not achieved for larger set of nodes due to ill-conditioning. Results in Table 3.10 show that by appending a polynomial to PS, accuracy has been improved substantially both in uniform and nonuniform cases. The order of convergence of each RBF is presented in Table 3.11 and it is found that convergence behaviour is similar to that of Example 2. Figure 3.6 describes the solutions and corresponding error graphs. Nonuniform nodal distribution where nodes near boundary are finer gives a solution with more accuracy and further the errors are suppressed uniformly throughout the domain. Figures 3.7-3.8 describes solutions at various cross-sections for different values of \bar{q} . For $0.3 \leq q_1, q_2 \leq 1$, solutions are smooth and shows a gradual change, however for $0 \leq q_1, q_2 < 0.3$ obtaining accurate solution and convergence of successive approximation is observed to be hard. This issue needs further attention.

Further, Table 3.12 describes the dependence of the scheme on the shape parameter ε in the case of MQ and GA. Smaller values of ε could not be explored due to ill-conditioning of the corresponding linear system. Since for many problems optimal accuracy can be obtained as $\varepsilon \rightarrow 0$, solution for those values are not explored in the case of larger set of nodes. Further, as observed in earlier tables, Gaussian basis function is more sensitive to the shape parameter when compared to multiquadric.

3.5.1 Implementation of Rippa's optimisation algorithm

The results presented in earlier subsections have considered optimal ε , which is obtained by trial and error. Rippa (1999) has proposed a modification to "Leave-one-out cross validation" (LOOCV) algorithm to obtain the optimum value for ε for RBF interpolation. This was later extended to various RBF based schemes, namely RBF pseudo spectral methods (Fasshauer and Zhang, 2007), asymmetric collocation (Roque and Ferreira, 2010), and employed in finding the satisfactory source locations by Chen

et al. (2016). The present scheme has been modified to implement LOOCV strategy to obtain the optimal values of ε for all three examples and the results are presented in Figures 3.9-3.11 and Table 3.13.

Figures 3.9-3.11 illustrates how the algorithm chooses optimal ε at each iteration (for the linear problem) and how it converges to a value closer to ε_{opt} for all three examples. It is found that in most cases it converges to a value closer to ε_{opt} , however in a few cases the sequence $\{\varepsilon_{opt}^{iter}\}$ converge to a different ε_{opt} . Here, $\{\varepsilon_{opt}^{iter}\}$ represent the optimum ε at each successive iteration. It is also observed that as q_1 and q_2 decrease, oscillation of the sequence $\{\varepsilon_{opt}^{iter}\}$ is severe. Accuracy (Table 3.13) can also be compared with that in the Tables 3.1, 3.7 and 3.10. CPU time also increases drastically as the number of iterations increases because LOOCV optimises ε for each successive iteration. It is to be noted that we have considered the search interval which includes our ε_{opt} , however, LOOCV algorithm provides locally optimal values even for other stable intervals. As observed in earlier literature (Rippa, 1999; Roque and Ferreira, 2010), it is important to choose appropriate interval, which can be challenging for large scale problems.

3.5.2 Effect of variable shape parameters

As an alternative way of improving accuracy, stability and convergence (for nonlinear problems), variable shape parameter strategy (Kansa, 1990; Sarra and Sturgill, 2009; Golbabai et al., 2015) has also been employed. Various choices (formula) on variable shape parameters are discussed in (Golbabai et al., 2015), such as i) increasing and decreasing linear, ii) exponential, iii) random and iv) trigonometric parameters. After experimenting numerically with these shape parameter distribution formulae in the fractional Darboux problem, it is found that the trigonometric shape parameter defined as $\varepsilon(j) = \varepsilon_{min} + (\varepsilon_{max} - \varepsilon_{min}) \sin(j)$, $j = 1, \dots, n$ provides better solution (when compared to others) with less number of nodal points.

Results obtained are discussed in Table 3.14. Comparing this with Tables 3.1, 3.7 and 3.10, for Examples 3.5.1, 3.5.2 and 3.5.3 respectively, it is seen that the accuracy is improved at least one order, if variable shape parameters are chosen over constant ones. In addition, as mentioned in earlier discussions GA is very sensitive to ε and a minor change in the choice of interval leads to divergence. For large values of n , say 60×60 , where the method diverged due to ill-conditionness, it is observed that some of the variable shape parameter strategies yield converged solutions. For instance, when $(q_1, q_2) = (0.5, 0.5)$, using linearly distributed $\varepsilon(j)$ we have obtained converged solutions with errors $2.39E - 05$ (MQ) and $9.69E - 06$ (GA) in the ε -intervals (7.5, 8.5) and (9, 10), respectively.

3.6 CONCLUSIONS

The present chapter has considered an RBF collocation method for fractional Darboux problem. The proposed scheme linearises the nonlinear problem using successive approximation and then approximate using the proposed radial functions based scheme. The convergence of the successive approximation for Darboux equation has been proved. Discretisation has been done using RBF collocation and Gauss-Jacobi quadrature. Through the examples, we have made an attempt to study several issues pertaining to RBF approximations to fractional Darboux problem: accuracy, convergence and dependency of the method on shape parameters in radial functions. From the comparison with exact solutions or solutions in the literature, we can conclude numerical solution obtained using the proposed RBF scheme gives excellent accuracy using less number of nodal points. However, the well known instability issue due to ill-conditioning for all RBFs are observed in these schemes too. To circumvent this, a brief study by employing variable shape parameters (for MQ and GA) has also been made. This helps in improving the accuracy and stabilising the system, however, a more detailed analysis is required to generalise the conclusions. This can be done as a separate study. Further, LOOCV algorithm to evaluate the optimal ε has been implemented and results are compared to the ε_{opt} obtained using trial and error. As mentioned in earlier literature, the choice of stable interval is very important and challenging issue in LOOCV as well as variable shape parameter distribution.

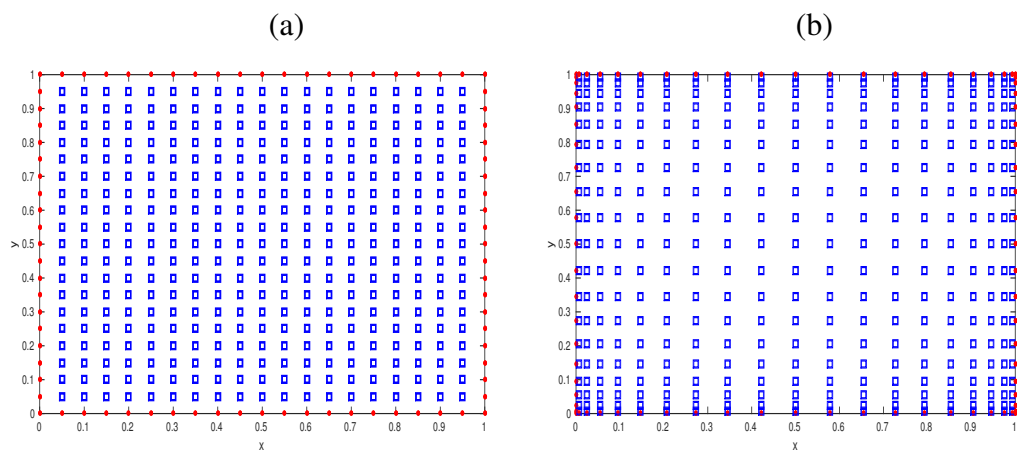


Figure 3.1 Schematic of nodal distributions. (a) uniform, (b) nonuniform

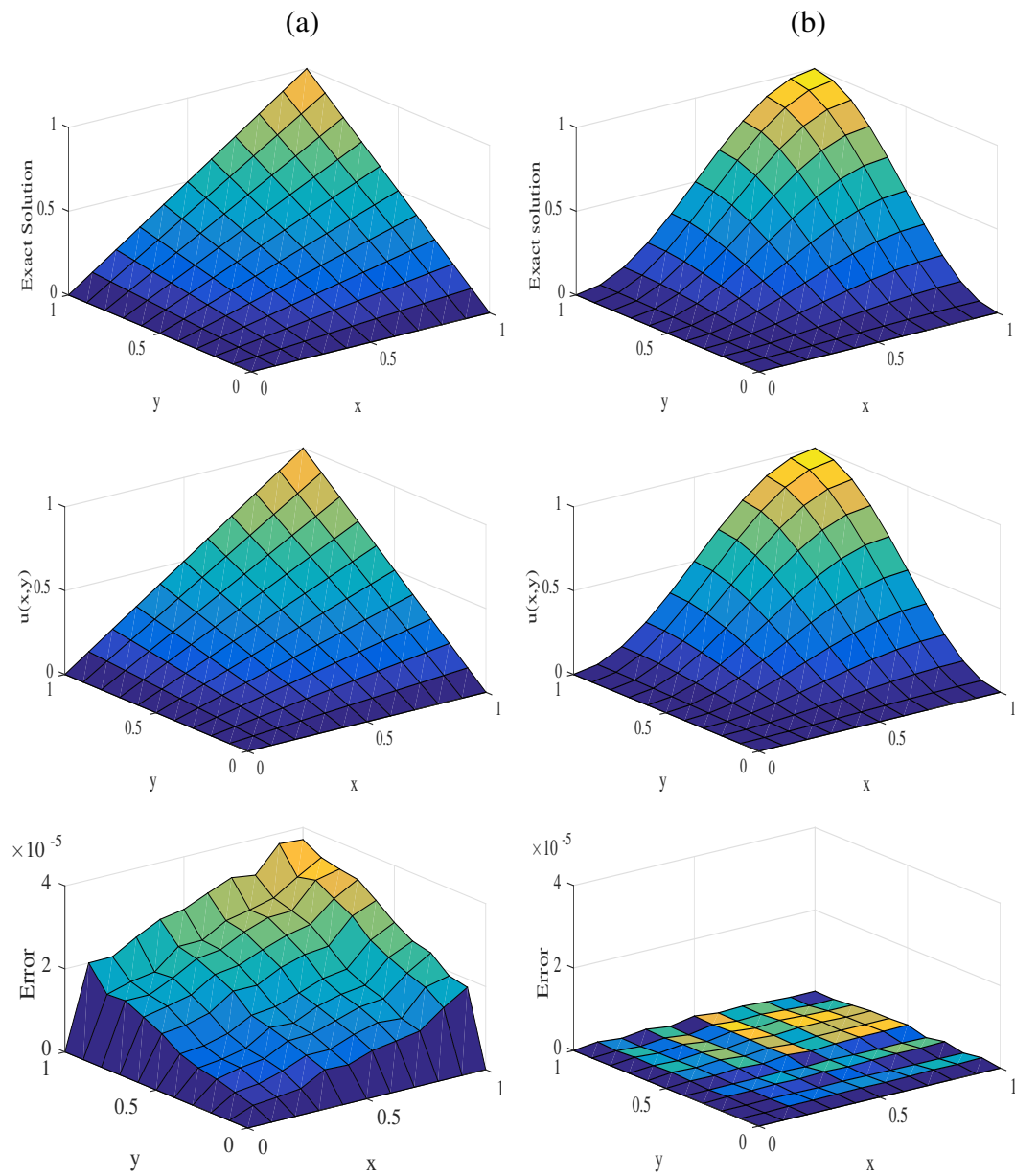


Figure 3.2 Surface plots of Example 3.5.1 with (a) uniform (b) nonuniform node distributions. Row 1-3: Exact Solutions, RBF solutions, Error plots.

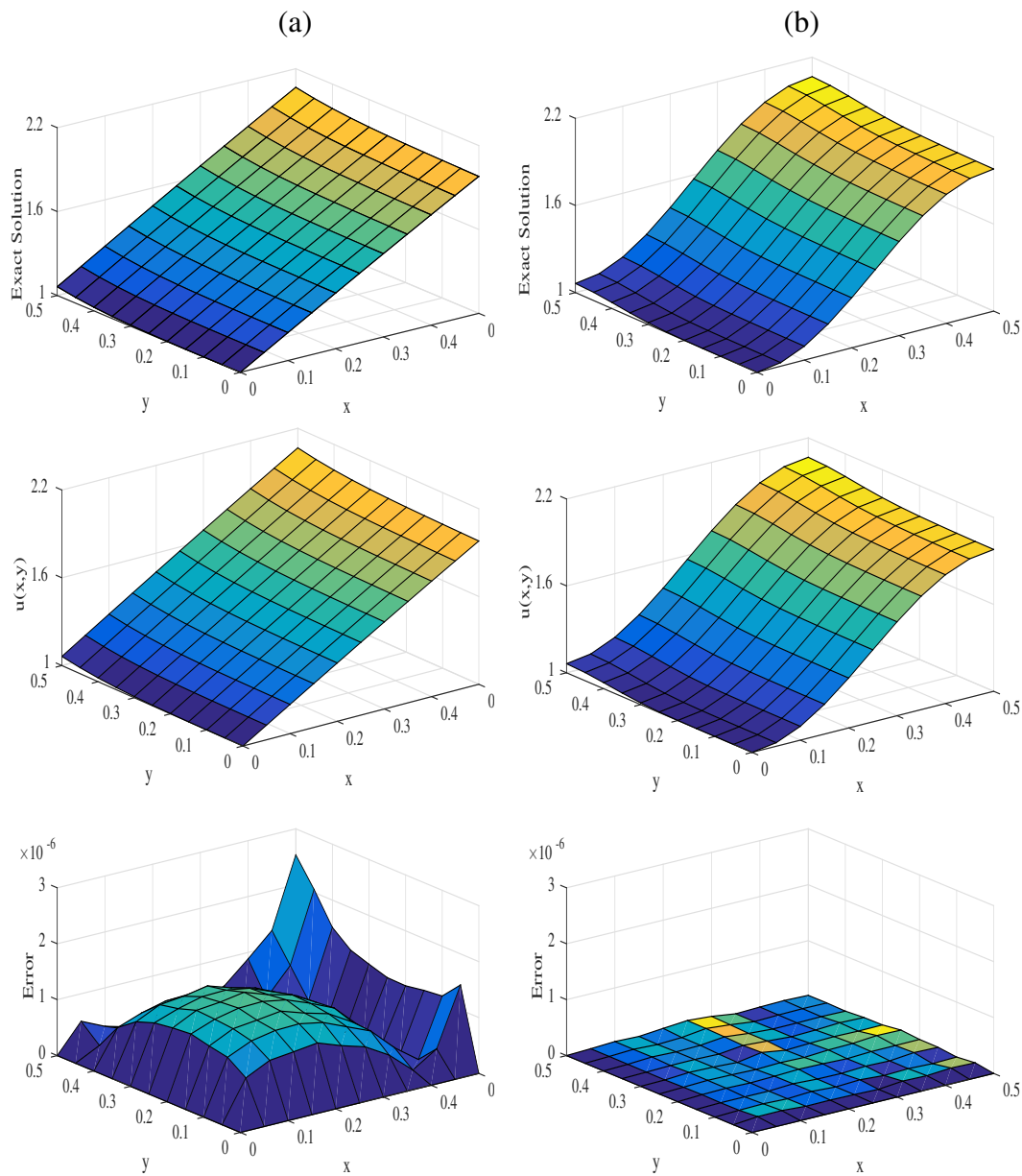


Figure 3.3 Surface plots of Example 3.5.2 with (a) uniform (b) nonuniform node distributions. Row 1-3: Exact Solutions, RBF solutions, Error plots.

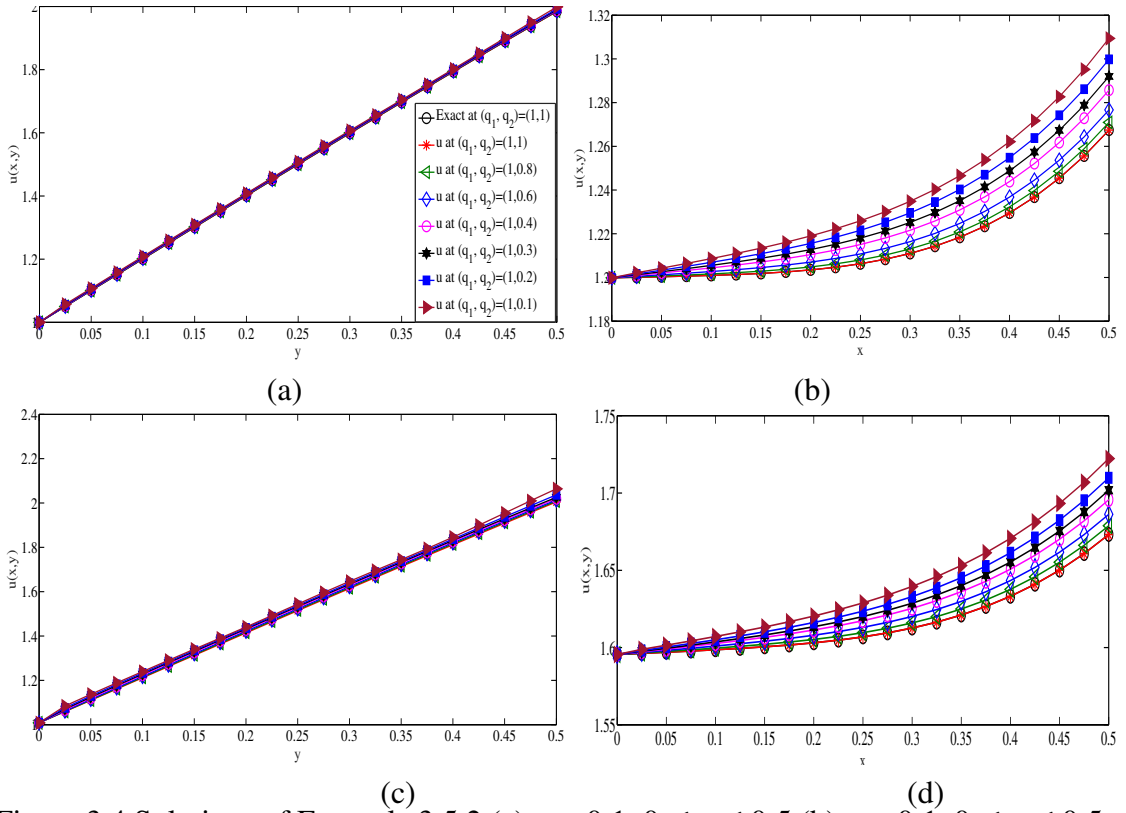


Figure 3.4 Solutions of Example 3.5.2 (a) $x = 0.1$, $0 \leq y \leq 0.5$ (b) $y = 0.1$, $0 \leq x \leq 0.5$ (c) $x = 0.3$, $0 \leq y \leq 0.5$ (d) $y = 0.3$, $0 \leq x \leq 0.5$, for $q_1 = 1$ and various values of q_2 .

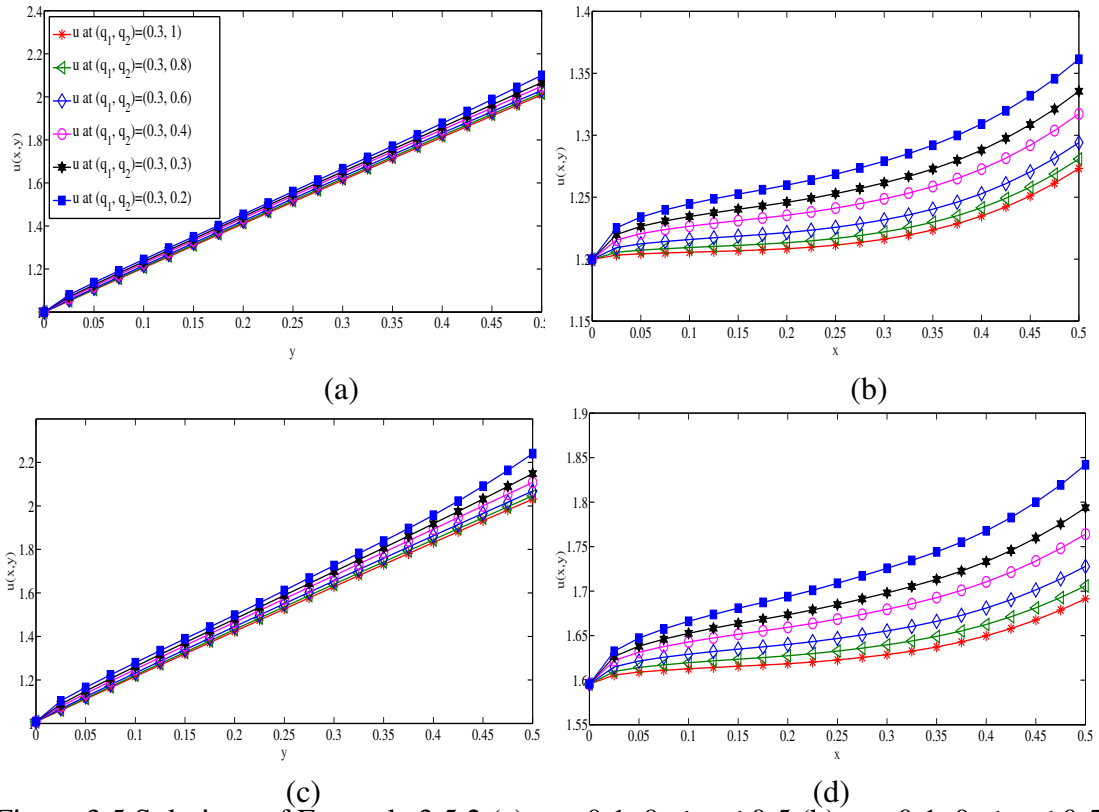


Figure 3.5 Solutions of Example 3.5.2 (a) $x = 0.1$, $0 \leq y \leq 0.5$ (b) $y = 0.1$, $0 \leq x \leq 0.5$ (c) $x = 0.3$, $0 \leq y \leq 0.5$ (d) $y = 0.3$, $0 \leq x \leq 0.5$, for $q_1 = 0.3$ and various values of q_2 .

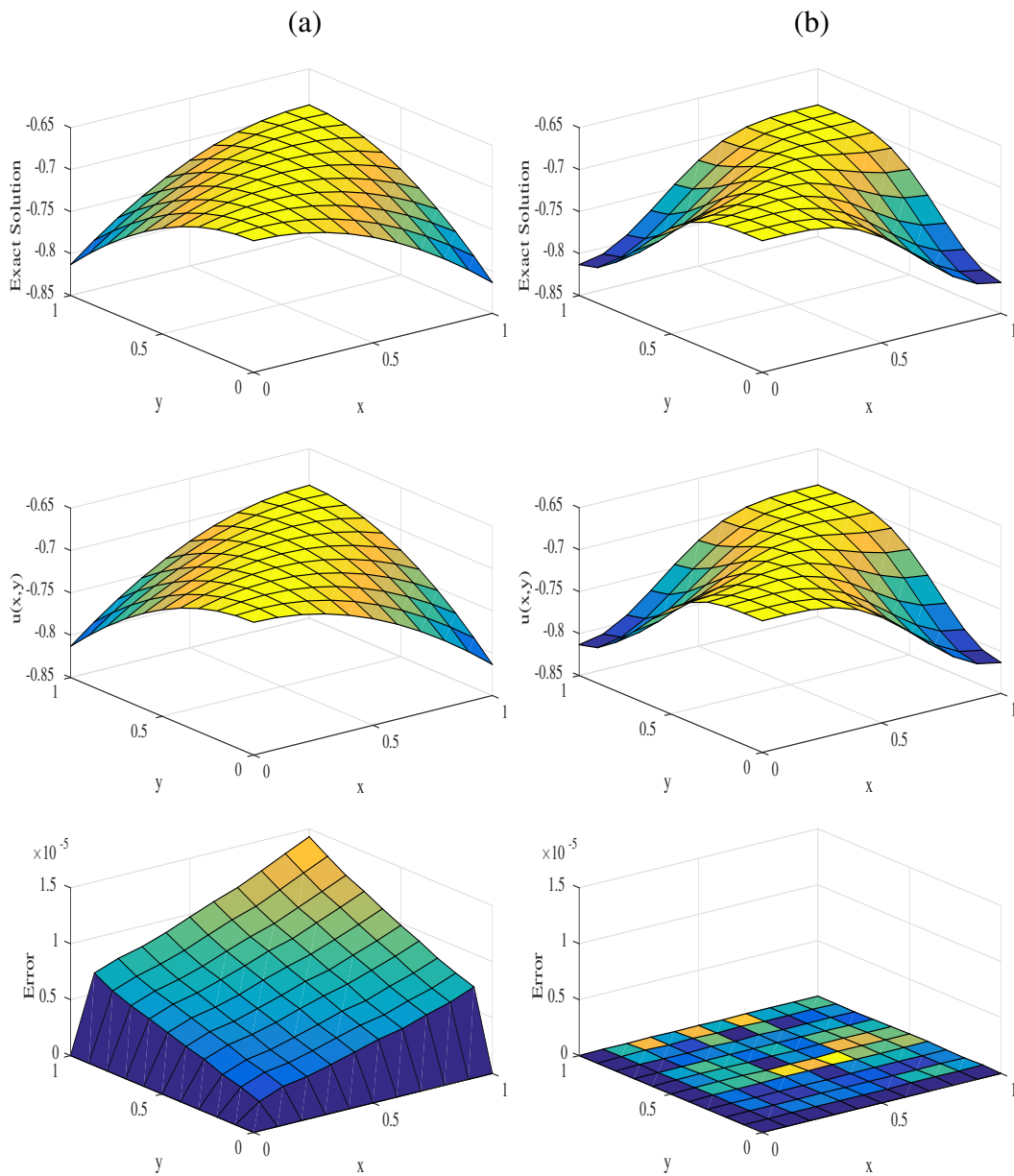
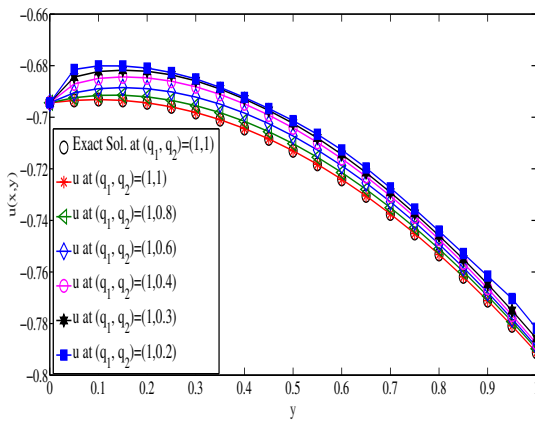
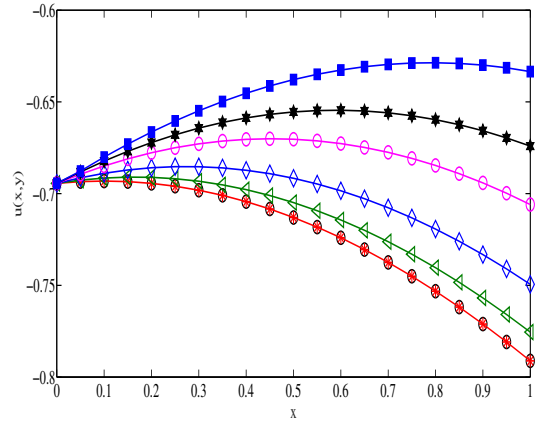


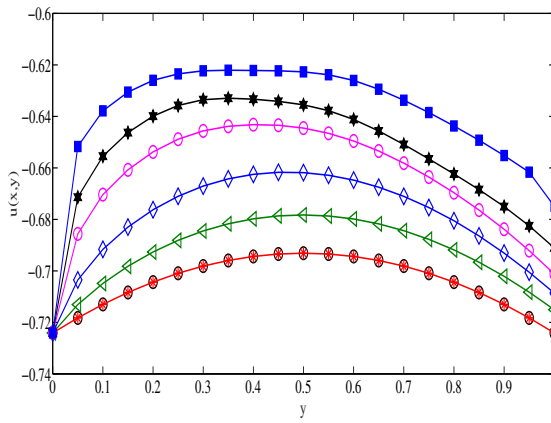
Figure 3.6 Surface plots of Example 3.5.3 with (a) uniform (b) nonuniform node distributions. Row 1-3: Exact Solutions, RBF solutions, Error plots.



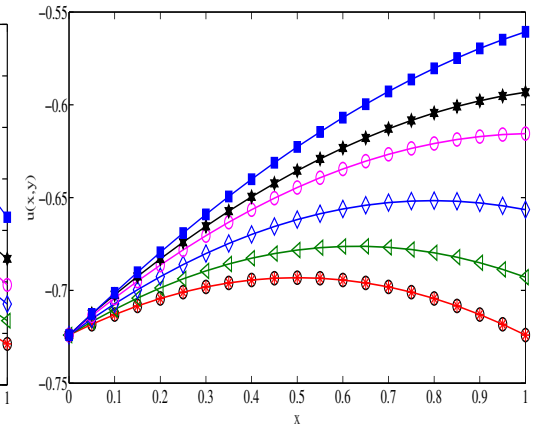
(a)



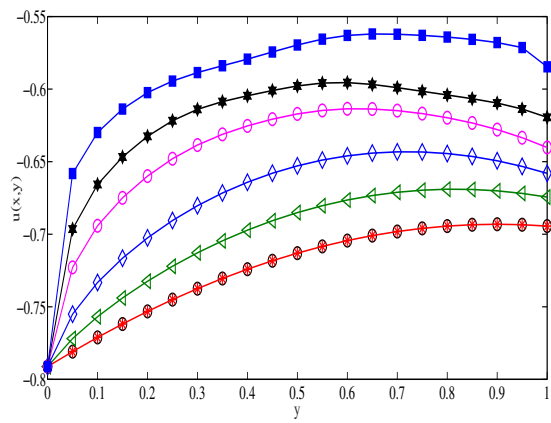
(b)



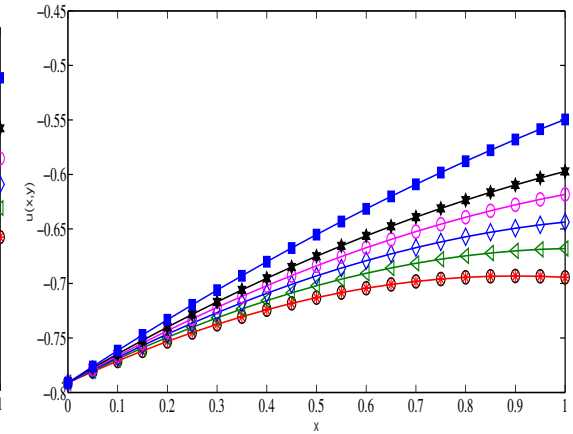
(c)



(d)

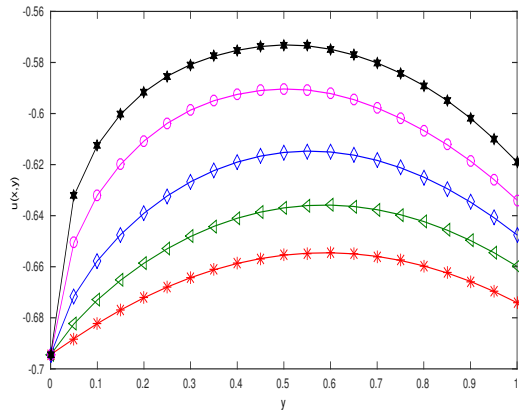


(e)

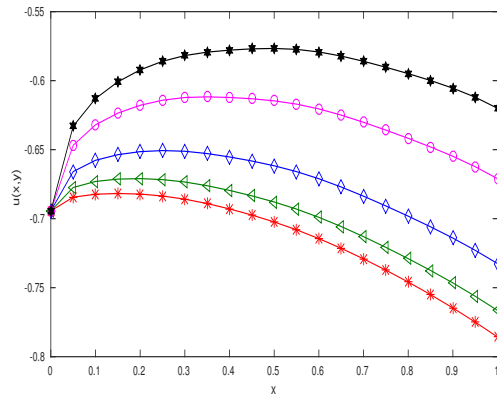


(f)

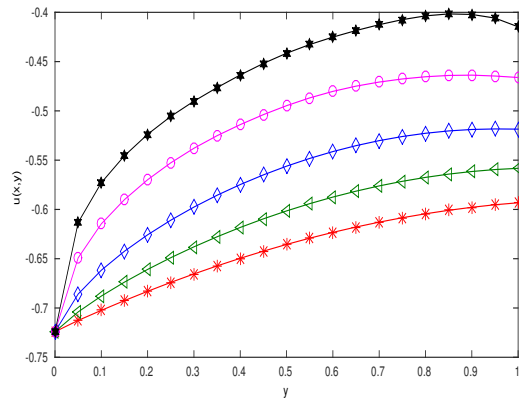
Figure 3.7 Solutions of Example 3.5.3 (a) $x = 0.1, 0 \leq y \leq 1$ (b) $y = 0.1, 0 \leq x \leq 1$ (c) $x = 0.5, 0 \leq y \leq 1$ (d) $y = 0.5, 0 \leq x \leq 1$ (e) $x = 0.9, 0 \leq y \leq 1$ (f) $y = 0.9, 0 \leq x \leq 1$, for $q_1 = 1$ and various values of q_2 .



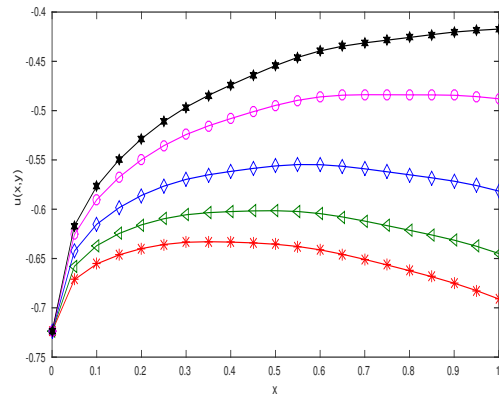
(a)



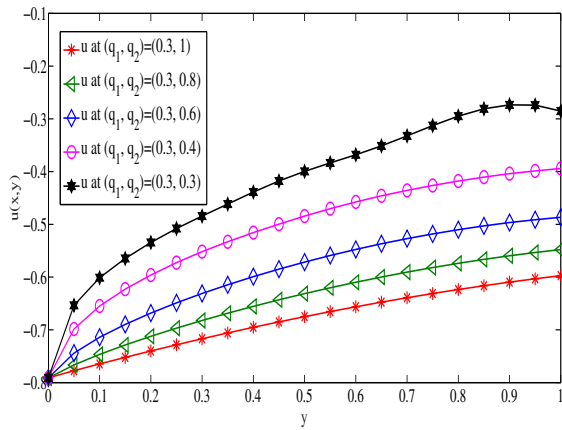
(b)



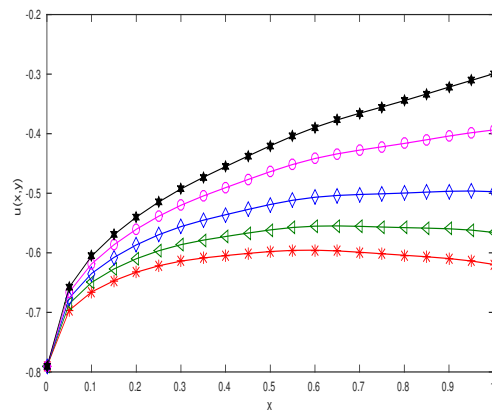
(c)



(d)



(e)



(f)

Figure 3.8 Solutions of Example 3.5.3 (a) $x = 0.1, 0 \leq y \leq 1$ (b) $y = 0.1, 0 \leq x \leq 1$ (c) $x = 0.5, 0 \leq y \leq 1$ (d) $y = 0.5, 0 \leq x \leq 1$ (e) $x = 0.9, 0 \leq y \leq 1$ (f) $y = 0.9, 0 \leq x \leq 1$, for $q_1 = 0.3$ and various values of q_2 .

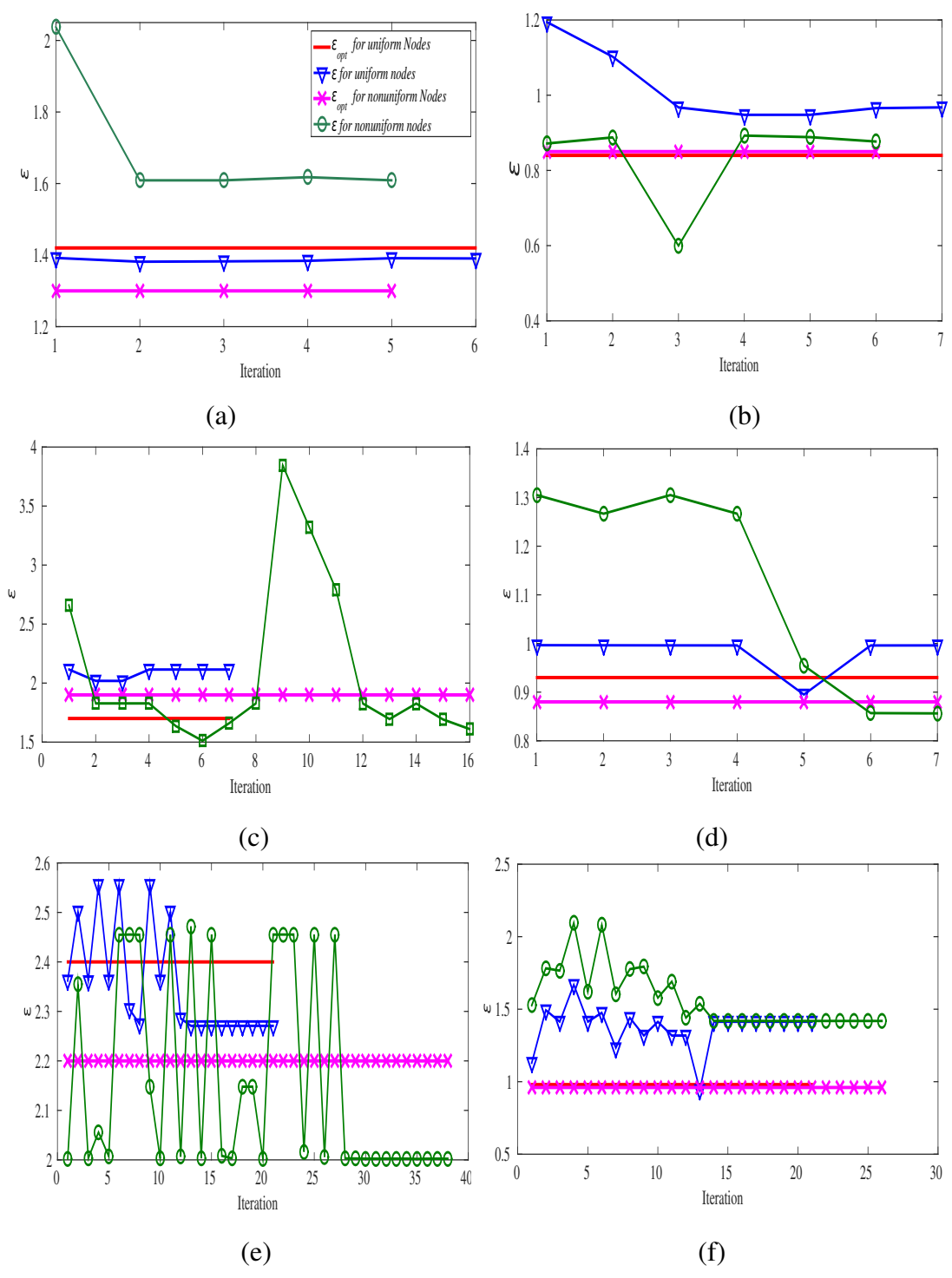
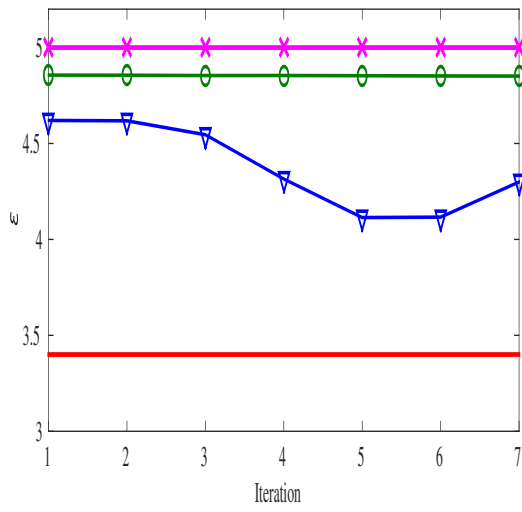
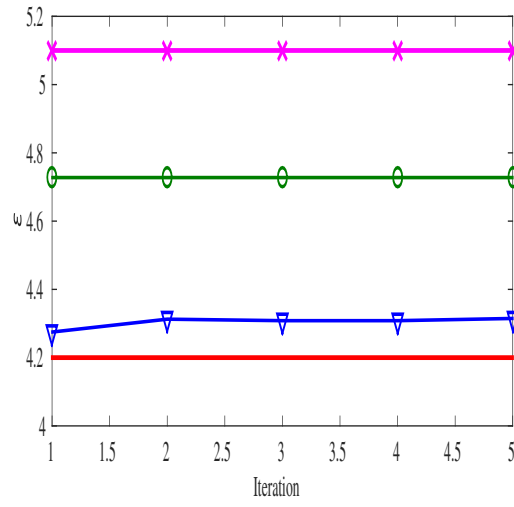


Figure 3.9 Example 3.5.1: Convergence of ε using Rippa's algorithm-iteration Vs ε_{opt} for GA (left) and MQ (right): (a) & (b) $(q_1, q_2) = (1, 1)$, (c) & (d) $(q_1, q_2) = (0.9, 0.1)$, (e) & (f) $(q_1, q_2) = (0.1, 0.1)$

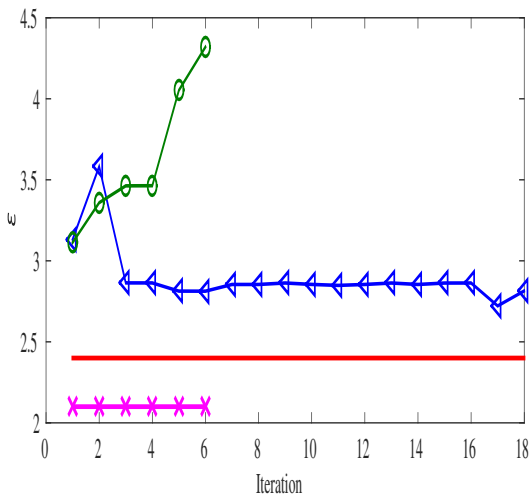


(a)

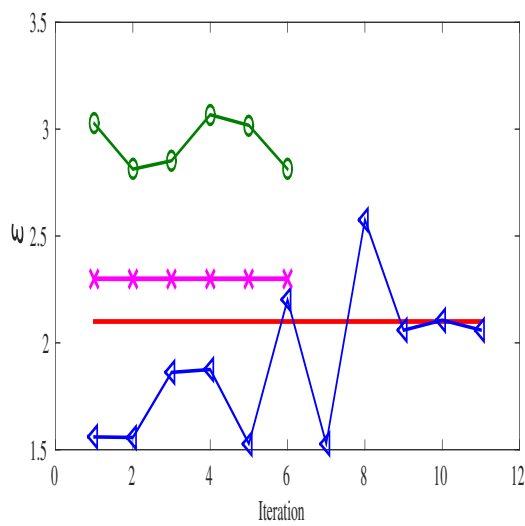


(b)

Figure 3.10 Example 3.5.2: Convergence of ε using Rippa's algorithm - iteration Vs ε_{opt} for GA and MQ: $(q_1, q_2) = (1, 1)$.



(a)



(b)

Figure 3.11 Example 3.5.3: Convergence of ε using Rippa's algorithm - iteration Vs ε_{opt} for GA and MQ: $(q_1, q_2) = (1, 1)$.

Table 3.1 Comparison of errors for Example 3.5.1 using MQ, GA, PS ($\beta = 8$) and PS+polynomial ($\beta = 8$) for various q_1 and q_2 (11×11).

q_1	q_2	RBF	Nodes	RBF parameter	Iter	RMS error	L_∞ error	CPU Time(s)
1	1	MQ	Nonuniform	$\varepsilon=0.85$	5	5.81E-07	1.33E-06	0.0799
			Uniform	$\varepsilon=0.84$	5	1.76E-05	3.75E-05	0.0804
		GA	Nonuniform	$\varepsilon=1.3$	7	6.29E-07	1.74E-06	0.1034
			Uniform	$\varepsilon=1.42$	7	1.11E-05	2.71E-05	0.0997
		PS	Nonuniform	$\beta=8$	6	1.15E-04	4.54E-04	0.0939
			Uniform	$\beta=8$	6	2.30E-03	3.20E-03	0.0851
		PS+poly.	Nonuniform	$\beta=8$	6	1.52E-09	5.88E-09	0.1289
			Uniform	$\beta=8$	6	1.35E-08	2.74E-08	0.1094
1	0.5	MQ	Nonuniform	$\varepsilon=0.8439$	7	4.0E-07	1.26E-06	0.5671
			Uniform	$\varepsilon=0.91$	7	1.84E-05	3.87E-05	0.5654
		GA	Nonuniform	$\varepsilon=1.6$	7	1.67E-06	6.02E-06	0.5913
			Uniform	$\varepsilon=1.8$	7	1.10E-04	2.07E-04	0.5707
		PS	Nonuniform	$\beta=8$	7	4.61E-05	1.92E-04	0.6613
			Uniform	$\beta=8$	7	1.88E-03	2.69E-03	0.5983
		PS+poly.	Nonuniform	$\beta=8$	7	4.09E-09	2.22E-08	0.6888
			Uniform	$\beta=8$	7	2.66E-08	6.16E-08	0.6994
0.9	0.1	MQ	Nonuniform	$\varepsilon=0.88$	8	1.31E-06	4.03E-06	1.5044
			Uniform	$\varepsilon=0.93$	8	1.67E-05	3.42E-05	1.5141
		GA	Nonuniform	$\varepsilon=1.9$	8	1.44E-05	4.30E-05	1.3960
			Uniform	$\varepsilon=1.7$	8	4.44E-05	8.46E-05	1.4187
		PS	Nonuniform	$\beta=8$	8	6.40E-05	1.84E-04	1.9368
			Uniform	$\beta=8$	9	2.20E-03	3.34E-03	1.8948
		PS+poly.	Nonuniform	$\beta=8$	8	2.18E-07	9.92E-07	2.4228
			Uniform	$\beta=8$	8	2.98E-07	9.45E-07	2.5054
0.1	0.1	MQ	Nonuniform	$\varepsilon=0.96$	27	2.63E-06	9.48E-06	1.6999
			Uniform	$\varepsilon=0.98$	26	5.10E-06	1.52E-05	1.6382
		GA	Nonuniform	$\varepsilon=2.2$	26	7.36E-05	2.62E-04	1.6178
			Uniform	$\varepsilon=2.4$	20	1.36E-04	4.77E-04	1.5129
		PS	Nonuniform	$\beta=8$	24	4.31E-04	1.49E-03	2.0816
			Uniform	$\beta=8$	72	6.64E-03	3.55E-02	2.4545
		PS+poly.	Nonuniform	$\beta=8$	26	1.05E-06	4.78E-06	4.2242
			Uniform	$\beta=8$	20	7.08E-06	3.22E-05	3.7953

Table 3.2 Rate of convergence of Example 3.5.1 for $\bar{q} = (1, 1)$.

RBF parameter	$\Delta x = \Delta y$	RMS error	Rate of convergence	L_∞ error	Rate of convergence
MQ					
$\varepsilon=7$	1/10	4.91E-02	-	9.31E-02	-
	1/20	9.58E-03	2.3576	1.67E-02	2.4789
	1/40	4.55E-04	4.3961	7.90E-04	4.4019
	1/60	4.31E-05	5.8125	1.12E-04	4.8180
$\varepsilon=8$	1/10	5.34E-02	-	1.03E-01	-
	1/20	1.23E-02	2.1182	2.17E-02	2.2469
	1/40	8.17E-04	3.9122	1.41E-03	3.9439
	1/60	6.33E-05	6.3082	1.13E-04	6.2248
$\varepsilon=9$	1/10	5.66E-02	-	1.11E-01	-
	1/20	1.48E-02	1.9352	2.64E-02	2.0719
	1/40	1.28E-03	3.5314	2.21E-03	3.5784
	1/60	1.28E-04	5.6789	2.25E-04	5.6346
GA					
$\varepsilon=7$	1/10	1.97E-01	-	4.31E-01	-
	1/20	1.53E-02	3.6866	2.92E-02	3.8836
	1/40	1.37E-04	6.8032	2.59E-04	6.8169
	1/60	4.12E-06	8.6422	1.44E-05	7.1266
$\varepsilon=8$	1/10	2.31E-01	-	5.29E-01	-
	1/20	3.35E-02	2.7857	6.52E-02	3.0203
	1/40	1.80E-04	7.5400	5.39E-04	6.9184
	1/60	2.26E-05	5.1176	4.50E-05	6.1240
$\varepsilon=9$	1/10	2.55E-01	-	6.08E-01	-
	1/20	5.76E-02	2.1464	1.15E-01	2.4024
	1/40	8.64E-05	9.3808	2.53E-04	8.8283
	1/60	2.72E-05	2.8505	5.72E-05	3.6670
PS+polynomial					
$\beta=2$	1/10	8.76E-07	-	1.98E-06	-
	1/20	1.12E-07	2.9652	2.92E-07	2.7601
	1/40	2.24E-08	2.3258	6.75E-08	2.1154
	1/60	9.99E-09	1.9889	3.20E-08	1.8365
$\beta=4$	1/10	3.63E-08	-	1.04E-07	-
	1/20	8.79E-08	-1.2759	2.20E-07	-1.0809
	1/40	1.59E-08	2.4668	4.19E-08	2.3925
	1/60	5.29E-09	2.7142	1.75E-08	2.1533
$\beta=8$	1/10	1.35E-08	-	2.74E-08	-
	1/20	1.68E-09	3.0064	4.03E-09	2.7653
	1/40	1.44E-09	0.2224	5.00E-09	-0.3111
	1/60	1.47E-09	-0.0509	4.93E-09	0.0348

Table 3.3 Rate of convergence of Example 3.5.1 for $\bar{q} = (0.7, 0.7)$.

RBF parameter	$\Delta x = \Delta y$	RMS error	Rate of convergence	L_∞ error	Rate of convergence
MQ					
$\varepsilon=7$	1/10	5.24E-03		1.26E-02	
	1/20	8.36E-04	2.6480	2.67E-03	2.2358
	1/40	4.25E-05	4.2973	2.81E-04	3.2478
	1/60	3.12E-06	6.4419	3.70E-05	4.9968
$\varepsilon=8$	1/10	5.57E-03		1.41E-02	
	1/20	1.06E-03	2.3895	3.47E-03	2.0283
	1/40	7.50E-05	3.8247	5.13E-04	2.7565
	1/60	7.38E-06	5.7201	8.94E-05	4.3111
$\varepsilon=9$	1/10	5.80E-03		1.55E-02	
	1/20	1.28E-03	2.1822	4.24E-03	1.8696
	1/40	1.16E-04	3.4569	8.20E-04	2.3703
	1/60	1.44E-05	5.1516	1.78E-04	3.7726
GA					
$\varepsilon=8$	1/10	3.10E-02		1.07E-01	
	1/20	3.17E-03	3.2862	9.18E-03	3.5409
	1/40	6.99E-06	8.8270	2.87E-05	8.3220
	1/60	1.17E-06	4.4058	3.65E-06	5.0886
$\varepsilon=9$	1/10	3.30E-02		1.26E-01	
	1/20	4.53E-03	2.8664	1.38E-02	3.1834
	1/40	1.88E-05	7.9151	8.92E-05	7.2752
	1/60	5.59E-06	2.9878	4.42E-05	1.7331
$\varepsilon=10$	1/10	3.34E-02		1.35E-01	
	1/20	5.51E-03	2.6018	1.76E-02	2.9414
	1/40	1.30E-04	5.4051	3.82E-04	5.5264
	1/60	5.03E-06	8.0213	2.54E-05	6.6830
PS+polynomial					
$\beta=2$	1/10	2.04E-08		5.23E-08	
	1/20	1.78E-08	0.1970	4.44E-08	0.2358
	1/40	1.79E-08	-0.0076	4.35E-08	0.0274
	1/60	diverging			
$\beta=4$	1/10	6.51E-09		1.83E-08	
	1/20	1.84E-08	-1.4943	4.45E-08	-1.2774
	1/40	1.91E-08	-0.0573	4.58E-08	-0.0420
	1/60	diverging			
$\beta=8$	1/10	5.35E-09		1.75E-08	
	1/20	1.89E-08	-1.8192	4.55E-08	-1.3783
	1/40	1.92E-08	-0.0232	4.60E-08	-0.0139
	1/60	1.92E-08	-0.0021	4.59E-08	0.0020

Table 3.4 Rate of convergence of Example 3.5.1 for $\bar{q} = (0.5, 0.5)$.

RBF parameter	$\Delta x = \Delta y$	RMS error	Rate of convergence	L_∞ error	Rate of convergence
MQ					
$\varepsilon=7$	1/10	2.90E-03		8.60E-03	
	1/20	9.27E-04	1.6448	4.50E-03	0.9344
	1/40	5.16E-05	4.1682	5.77E-04	2.9638
	1/60	Diverging			
$\varepsilon=8$	1/10	3.18E-03		9.41E-03	
	1/20	1.22E-03	1.3858	6.06E-03	0.6364
	1/40	9.00E-05	3.7571	9.85E-04	2.6210
	1/60	Not converging			
$\varepsilon=9$	1/10	3.38E-03		1.02E-02	
	1/20	1.49E-03	1.1779	7.66E-03	0.4159
	1/40	1.38E-04	3.4375	1.47E-03	2.3775
	1/60	Not converging			
GA					
$\varepsilon=8$	1/10	2.06E-02		8.41E-02	
	1/20	2.69E-03	2.9375	1.75E-02	2.2656
	1/40	Diverging			
	1/60	Diverging			
$\varepsilon=9$	1/10	1.83E-02		7.77E-02	
	1/20	4.47E-03	2.0348	3.14E-02	1.3051
	1/40	2.74E-05	7.3481	4.48E-04	6.1335
	1/60	Diverging			
$\varepsilon=10$	1/10	1.48E-02		6.51E-02	
	1/20	6.47E-03	1.1944	4.85E-02	0.4250
	1/40	9.75E-05	6.0518	1.04E-03	5.5479
	1/60	1.53E-05	4.5594	2.62E-04	3.3906
PS+polynomial					
$\beta=2$	1/10	2.27E-07		4.98E-07	
	1/20	1.82E-07	0.3177	3.84E-07	0.3751
	1/40	diverging			
	1/60	Diverging			
$\beta=4$	1/10	1.82E-07		4.00E-07	
	1/20	1.82E-07	0.0002	3.83E-07	0.0622
	1/40	1.81E-07	0.0048	3.79E-07	0.0150
	1/60	Diverging			
$\beta=8$	1/10	1.56E-07		3.47E-07	
	1/20	1.81E-07	-0.2145	3.81E-07	-0.1355
	1/40	1.81E-07	0.0004	3.78E-07	0.0105
	1/60	Diverging			

Table 3.5 Rate of convergence of Example 3.5.1 for $\bar{q} = (0.3, 0.3)$.

RBF parameter	$\Delta x = \Delta y$	RMS error	Rate of convergence	L_∞ error	Rate of convergence
MQ					
$\varepsilon=7$	1/10	2.87E-03		1.40E-02	
	1/20	1.35E-03	1.0842	4.40E-03	1.6679
	1/40	1.08E-04	3.6449	1.70E-03	1.3732
	1/60	Diverging			
$\varepsilon=8$	1/10	3.10E-03		1.65E-02	
	1/20	1.76E-03	0.8188	5.83E-03	1.4986
	1/40	2.22E-04	2.9825	3.81E-03	0.6154
	1/60	Diverging			
$\varepsilon=9$	1/10	3.42E-03		1.96E-02	
	1/20	2.11E-03	0.6968	7.14E-03	1.4540
	1/40	4.41E-04	2.2596	7.55E-03	-0.0791
	1/60	Diverging			
GA					
$\varepsilon=8$	1/10	2.62E-02		1.20E-01	
	1/20	3.80E-03	2.7855	2.60E-02	2.2065
	1/40	Diverging			
	1/60	Diverging			
$\varepsilon=9$	1/10	2.25E-02		0.1196	
	1/20	6.80E-03	1.7263	0.0475	1.3322
	1/40	Diverging			
	1/60	Diverging			
$\varepsilon=10$	1/10	2.07E-02		1.20E-01	
	1/20	1.04E-02	0.9953	7.35E-02	0.7036
	1/40	1.95E-04	5.7320	1.52E-03	5.5971
	1/60	Diverging			
PS+polynomial					
$\beta=2$	1/10	1.51E-06		5.92E-06	
	1/20	Diverging			
	1/40	Diverging			
	1/60	Diverging			
$\beta=4$	1/10	1.55E-05		8.83E-05	
	1/20	3.82E-06	2.0206	2.56E-05	1.7863
	1/40	Diverging			
	1/60	Diverging			
$\beta=8$	1/10	1.54E-06		3.01E-06	
	1/20	1.66E-06	-0.1083	3.08E-06	-0.0332
	1/40	Diverging			
	1/60	Diverging			

Table 3.6 Comparison of errors for Example 3.5.2 using MQ, GA, PS ($\beta=12$), PS+polynomial ($\beta=12$), CS1 (Cheung, 1977) and CS2 (Cheung, 1977) with uniform collocation nodes (25×25) ($q_1 = q_2 = 1$).

x	y	MQ	GA	PS	PS+poly	CS1 (Cheung, 1977)	CS2 (Cheung, 1977)
0	0	5.05E-09	3.30E-08	-3.77E-06	1.39E-11	3.51E-08	-1.16E-10
0.125	0	-1.80E-08	1.23E-07	-6.35E-06	-4.30E-10	1.63E-05	-1.63E-05
0.375	0	-3.76E-08	-1.27E-08	-2.64E-06	-1.42E-09	-1.63E-05	-1.63E-05
0.5	0	-4.60E-08	1.01E-07	-3.33E-06	-2.39E-09	-1.05E-07	8.73E-11
0	0.25	-1.36E-08	2.29E-07	5.33E-07	-1.42E-10	3.51E-08	-5.82E-11
0.375	0.25	-1.60E-06	-8.64E-07	9.53E-06	-7.40E-08	-1.63E-05	-1.63E-05
0.5	0.25	3.54E-07	-8.30E-07	7.27E-06	-8.78E-08	-1.11E-07	-2.59E-09
0	0.4583	-2.75E-08	-3.31E-07	-2.66E-06	-1.78E-09	3.17E-07	5.81E-08
0.3333	0.4583	-1.21E-06	-1.32E-06	9.09E-06	-5.96E-08	2.55E-07	6.60E-08
0.25	0.5	-8.43E-07	-1.17E-07	1.27E-05	5.33E-09	3.43E-08	-2.01E-09
0.375	0.5	-5.82E-07	-5.32E-07	1.02E-05	1.38E-09	-1.64E-05	-1.63E-05
0.5	0.5	1.29E-06	-5.97E-07	9.16E-06	-4.15E-09	-1.58E-07	-3.78E-09

Table 3.7 Comparison of errors for Example 3.5.2 (21×21) using MQ, GA, PS ($\beta=12$), PS+polynomial ($\beta=12$) ($q_1 = q_2 = 1$).

RBF	Nodes	RBF parameter	Iter	RMS error	L_∞ error	CPU Time(s)
MQ	Nonuniform	$\epsilon=5.1$	6	2.73E-07	1.07E-06	0.3658
	Uniform	$\epsilon=4.2$	6	8.37E-07	2.67E-06	0.3636
GA	Nonuniform	$\epsilon=5$	6	4.05E-07	1.17E-06	0.3958
	Uniform	$\epsilon=3.4$	6	5.39E-07	1.46E-06	0.3800
PS	Nonuniform	$\beta=12$	10	1.73E-05	4.57E-05	1.0252
	Uniform	$\beta=12$	6	3.42E-06	9.23E-06	0.6487
PS+poly	Nonuniform	$\beta=12$	6	1.77E-07	4.04E-07	0.6790
	Uniform	$\beta=12$	6	2.14E-07	3.04E-07	0.7248

Table 3.8 Rate of convergence of Example 3.5.2.

RBF parameter	$\Delta x = \Delta y$	RMS error	Rate of convergence	L_∞ error	Rate of convergence
MQ					
$\varepsilon=12$	1/10	2.19E-03	-	5.35E-03	-
	1/20	2.09E-04	3.3894	3.83E-04	3.8041
	1/40	1.16E-05	4.1713	1.53E-05	4.6457
	1/60	8.05E-07	6.5799	2.68E-06	4.2964
$\varepsilon=13$	1/10	2.80E-03	-	6.55E-03	-
	1/20	2.39E-04	3.5503	4.61E-04	3.8287
	1/40	1.75E-05	3.7716	2.36E-05	4.2879
	1/60	1.18E-06	6.6508	1.70E-06	6.4879
$\varepsilon=14$	1/10	3.46E-03	-	7.79E-03	-
	1/20	2.67E-04	3.6959	5.46E-04	3.8347
	1/40	2.48E-05	3.4284	3.40E-05	4.0053
	1/60	3.45E-06	4.8647	4.25E-06	5.1285
GA					
$\varepsilon=11$	1/10	1.59E-02	-	3.88E-02	-
	1/20	6.70E-05	7.8906	1.60E-04	7.9218
	1/40	2.97E-05	1.1737	8.01E-05	0.9982
	1/60	1.25E-05	2.1344	2.98E-05	2.4386
$\varepsilon=12$	1/10	2.39E-02	-	5.88E-02	-
	1/20	2.36E-04	6.6621	4.93E-04	6.8981
	1/40	1.81E-05	3.7047	6.29E-05	2.9705
	1/60	2.09E-05	-0.3547	6.19E-05	0.0395
$\varepsilon=13$	1/10	3.42E-02	-	8.38E-02	-
	1/20	4.86E-04	6.1369	1.05E-03	6.3185
	1/40	9.89E-05	2.2969	3.45E-04	1.6057
	1/60	2.10E-05	3.8218	7.03E-05	3.9233
PS+polynomial					
$\beta=2$	1/10	2.69E-04	-	9.86E-04	-
	1/20	1.08E-04	1.3167	3.64E-04	1.4372
	1/40	4.64E-05	1.2154	1.29E-04	1.4922
	1/60	2.80E-05	1.2499	6.99E-05	1.5177
$\beta=4$	1/10	8.74E-05	-	2.36E-04	-
	1/20	2.35E-05	1.8950	5.47E-05	2.1092
	1/40	5.38E-06	2.1270	1.12E-05	2.2880
	1/60	2.15E-06	2.2621	4.26E-06	2.3840
$\beta=8$	1/10	2.87E-05	-	4.72E-05	-
	1/20	1.26E-06	4.5096	1.92E-06	4.6196
	1/40	5.67E-08	4.4739	8.11E-08	4.5653
	1/60	8.64E-09	4.6400	1.87E-08	3.6185

Table 3.9 Comparison of solutions of Example 3.5.3 using MQ, GA, PS ($\beta=12$) and PS+polynomial ($\beta=12$) with uniform collocation points (21×21) and Cubature method (Jain and Sharma, 1968) with exact solutions ($q_1 = q_2 = 1$).

x	y	Exact Solution	MQ	GA	PS	PS+poly	Cubature Method
0.1	0.1	-0.693147181	-0.693153933	-0.6931458817	-0.693144727	-0.693147187	-0.693147270
0.1	0.3	-0.698138869	-0.698147191	-0.6981378975	-0.698139315	-0.698138876	-0.698139080
0.1	0.5	-0.713015252	-0.713024502	-0.7130156081	-0.713016549	-0.713015259	-0.713015310
0.2	0.1	-0.694396660	-0.694404385	-0.6943978272	-0.694396194	-0.694396667	-0.694396730
0.2	0.3	-0.694396660	-0.694406065	-0.6943955400	-0.694399321	-0.694396667	-0.694397230
0.2	0.5	-0.704355244	-0.704365650	-0.7043554561	-0.704358797	-0.704355252	-0.704355920
0.3	0.1	-0.698138869	-0.698147141	-0.6981373212	-0.698139341	-0.698138876	-0.698139080
0.3	0.3	-0.693147181	-0.693157212	-0.6931433514	-0.693150842	-0.693147188	-0.693148270
0.3	0.5	-0.698138869	-0.698149999	-0.6981363771	-0.698143466	-0.698138877	-0.698140480
0.4	0.1	-0.704355244	-0.704364021	-0.7043552334	-0.704356052	-0.704355251	-0.704355420
0.4	0.3	-0.694396660	-0.694407277	-0.6943943100	-0.694400702	-0.694396668	-0.694398130
0.4	0.5	-0.694396660	-0.694408473	-0.6943956401	-0.694401686	-0.694396668	-0.694399030

Table 3.10 Comparison of errors in the solutions of Example 3.5.3 (21×21) using MQ, GA, PS ($\beta=12$), PS+polynomial ($\beta=12$) ($q_1 = q_2 = 1$).

RBF	Nodes	RBF parameter	Iter	RMS error	L_∞ error	CPU Time(s)
MQ	Nonuniform	$\epsilon=2.3$	7	1.67E-07	4.93E-07	0.4612
	Uniform	$\epsilon=2.1$	7	1.29E-05	2.34E-05	0.4850
GA	Nonuniform	$\epsilon=2.1$	7	1.77E-07	5.92E-07	0.4171
	Uniform	$\epsilon=2.4$	7	2.89E-07	5.95E-07	0.4106
PS	Nonuniform	$\beta=12$	16	3.91E-05	1.44E-04	1.5081
	Uniform	$\beta=12$	7	4.02E-06	7.92E-06	0.6886
PS+poly	Nonuniform	$\beta=12$	8	7.97E-10	2.26E-09	0.8637
	Uniform	$\beta=12$	8	7.93E-09	1.30E-08	0.8712

Table 3.11 Rate of convergence of Example 3.5.3.

RBF parameter	$\Delta x = \Delta y$	RMS error	Rate of convergence	L_∞ error	Rate of convergence
MQ					
$\varepsilon=8$	1/10	1.03E-02	-	2.18E-02	-
	1/20	2.63E-03	1.9695	4.99E-03	2.1272
	1/40	1.86E-04	3.8217	3.40E-04	3.8754
	1/60	1.47E-05	6.2592	2.74E-05	6.2111
$\varepsilon=9$	1/10	1.06E-02	-	2.32E-02	-
	1/20	3.11E-03	1.7691	6.02E-03	1.9463
	1/40	2.90E-04	3.4228	5.30E-04	3.5057
	1/60	2.96E-05	5.6284	5.46E-05	5.6055
$\varepsilon=10$	1/10	1.08E-02	-	2.43E-02	-
	1/20	3.52E-03	1.6174	6.96E-03	1.8038
	1/40	4.10E-04	3.1019	7.52E-04	3.2103
	1/60	5.14E-05	5.1213	9.45E-05	5.1155
GA					
$\varepsilon=7$	1/10	3.81E-02	-	7.91E-02	-
	1/20	3.43E-03	3.4735	6.92E-03	3.5148
	1/40	3.46E-04	3.3094	6.91E-04	3.3240
	1/60	4.34E-06	10.7989	1.34E-05	9.7244
$\varepsilon=8$	1/10	4.06E-02	-	8.90E-02	-
	1/20	7.40E-03	2.4559	1.48E-02	2.5882
	1/40	1.83E-04	5.3376	3.18E-04	5.5404
	1/60	5.11E-06	8.8251	1.28E-05	7.9233
$\varepsilon=9$	1/10	4.15E-02	-	9.29E-02	-
	1/20	1.25E-02	1.7312	2.53E-02	1.8765
	1/40	2.84E-04	5.4599	5.88E-04	5.4272
	1/60	7.76E-05	3.1998	1.51E-04	3.3528
PS+polynomial					
$\beta=2$	1/10	6.53E-04	-	1.10E-03	-
	1/20	2.30E-04	1.5067	3.80E-04	1.5332
	1/40	8.05E-05	1.5125	1.36E-04	1.4824
	1/60	4.34E-05	1.5218	7.41E-05	1.4987
$\beta=4$	1/10	2.01E-04	-	3.26E-04	-
	1/20	3.85E-05	2.3843	6.33E-05	2.3646
	1/40	7.08E-06	2.4430	1.18E-05	2.4234
	1/60	2.60E-06	2.4707	4.37E-06	2.4499
$\beta=8$	1/10	3.40E-06	-	5.03E-06	-
	1/20	1.39E-07	4.6124	1.88E-07	4.7418
	1/40	6.47E-09	4.4252	3.77E-08	2.3181
	1/60	3.92E-09	1.2358	4.45E-08	-0.4090

Table 3.12 Comparison of range for ' ε ' using MQ, GA with initial approximation $u \equiv 0$

Examples	q_1	q_2		MQ	GA
Example 3.5.1	1	1	n=5×5	≥ 0.16	(0.23, 5.8)
			n=9×9	≥ 0.64	(1, 12.2)
			n=17×17	≥ 1.7	(3.5, 24.8)
			n=33×33	≥ 3.5	(7.4, 50)
		n=65×65	≥ 6.8	≥ 3.8	
	0.9	1	n=5×5	≥ 0.16	(0.23, 6)
		n=9×9	≥ 0.64	(1.19, 12.2)	
		n=17×17	≥ 1.5	(1.6, 27.9)	
		n=33×33	≥ 3.3	(3.4, 60)	
		n=65×65	≥ 6.6	No convergence	
	0.5	1	n=5×5	≥ 0.17	(0.25, 6.2)
		n=9×9	≥ 0.64	(1.2, 13.1)	
		n=17×17	≥ 1.7	(4.1, 31)	
		n=33×33	≥ 3.5	(6.1, 49)	
		n=65×65	No convergence		
	0.2	1	n=5×5	(0.19, 91)	(0.25, 5.5)
		n=9×9	(0.68, 105)	(2.7, 11.7)	
		n=17×17	(1.8, 100)	(3, 24)	
		n=33×33	(3.6, 22)	(7.8, 30)	
		n=65×65	No convergence		
Example 3.5.2	1	1	n=5×5	≥ 0.3	(0.45, 15.3)
		n=9×9	≥ 1.25	(1.69, 31.5)	
		n=17×17	≥ 3	(3.4, 63)	
		n=33×33	≥ 6.1	(4, 128)	
		n=65×65	≥ 11	No convergence	
Example 3.5.3	1	1	n=5×5	≥ 0.15	(0.25, 5.7)
		n=9×9	≥ 0.68	(1.5, 11.7)	
		n=17×17	≥ 1.7	(3.5, 23.9)	
		n=33×33	≥ 3.5	(4.2, 48)	
		n=65×65	≥ 7.3	≥ 4.4	

Table 3.13 Comparison of errors using MQ, GA for various q_1 and q_2 with LOOCV algorithm.

q_1	q_2	RBF	Nodes	RBF (ϵ) parameter	Iter	RMS error	L_∞ error	CPU Time(s)
Example 3.5.1 (11×11)								
1	1	MQ	Nonuniform	0.8768	7	5.22E-07	1.23E-06	1.6991
			Uniform	0.9676	8	7.95E-05	1.41E-04	2.1372
		GA	Nonuniform	1.6090	6	1.34E-06	3.35E-06	1.3322
			Uniform	1.3906	7	2.12E-05	3.92E-05	1.3470
0.9	0.1	MQ	Nonuniform	0.8563	8	1.14E-06	3.57E-06	32.3969
			Uniform	0.9960	8	2.91E-05	5.74E-05	31.8009
		GA	Nonuniform	1.6102	17	2.73E-06	8.39E-06	62.8451
			Uniform	2.1147	8	2.60E-04	4.92E-04	30.2693
0.1	0.1	MQ	Nonuniform	1.4188	26	5.07E-05	1.97E-04	107.3408
			Uniform	1.4133	22	5.61E-05	1.74E-04	97.3608
		GA	Nonuniform	2.0023	39	2.97E-05	1.08E-04	152.9792
			Uniform	2.2708	22	8.88E-05	3.12E-04	84.0719
Example 3.5.2 (21×21)								
1	1	MQ	Nonuniform	4.7276	6	2.43E-07	8.08E-07	23.3952
			Uniform	4.3148	6	2.07E-06	2.98E-06	22.6957
		GA	Nonuniform	4.8513	8	9.83E-07	3.08E-06	32.5213
			Uniform	4.2994	8	5.56E-07	1.73E-06	31.3391
Example 3.5.3 (21×21)								
1	1	MQ	Nonuniform	2.8132	7	6.97E-07	2.17E-06	23.9788
			Uniform	2.0600	12	9.16E-06	1.76E-05	47.2570
		GA	Nonuniform	4.3197	7	2.00E-07	5.75E-07	26.2423
			Uniform	2.8144	19	1.50E-06	3.01E-06	68.3558

Table 3.14 Comparison of errors using MQ, GA for various q_1 and q_2 with trigonometric variable shape parameter.

q_1	q_2	RBF	Nodes	interval ϵ	Iter	RMS error	L_∞ error	CPU Time(s)
Example 3.5.1 (11×11)								
1	1	MQ	Nonuniform	(1.2, 2.2)	6	1.49E-09	3.88E-09	0.1324
			Uniform	(1.2, 2.2)	6	5.88E-08	1.25E-07	0.0869
		GA	Nonuniform	(1.4, 2.4)	6	1.55E-09	5.29E-09	0.0804
			Uniform	(1.6, 2.6)	6	8.75E-08	2.15E-07	0.0854
0.9	0.1	MQ	Nonuniform	(1.4, 2.4)	9	1.17E-07	2.91E-07	1.5331
			Uniform	(1.3, 2.3)	10	1.09E-06	2.82E-06	1.5952
		GA	Nonuniform	(1.7, 2.7)	8	1.19E-06	4.14E-06	1.4096
			Uniform	(1.7, 2.7)	10	1.38E-06	2.25E-06	1.4458
0.1	0.1	MQ	Nonuniform	(1.3, 2.3)	52	8.01E-07	3.22E-06	2.4104
			Uniform	(1.4, 2.4)	27	6.33E-07	3.16E-06	1.4681
		GA	Nonuniform				Diverging	
			Uniform	(2.7, 3.7)	67	6.18E-04	2.30E-03	1.6899
Example 3.5.2 (21×21)								
1	1	MQ	Nonuniform	(3.5, 4.5)	6	2.47E-08	1.26E-07	0.7470
			Uniform	(4.3, 5.3)	6	3.84E-06	8.18E-06	0.7674
		GA	Nonuniform	(3.5, 4.5)	6	2.97E-09	1.30E-08	0.7194
			Uniform	(3.5, 4.5)	6	4.73E-09	1.55E-08	0.7065
Example 3.5.3 (21×21)								
1	1	MQ	Nonuniform	(2.5, 3.5)	7	1.14E-08	4.57E-08	0.9089
			Uniform	(2.5, 3.5)	7	7.45E-07	1.78E-06	0.9123
		GA	Nonuniform	(2.5, 3.5)	7	1.03E-08	4.64E-08	0.7743
			Uniform	(2, 3)	23	1.01E-07	1.65E-07	2.6565

CHAPTER 4

ON STABILISATION OF RADIAL BASIS FUNCTIONS BASED SCHEMES FOR FRACTIONAL DERIVATIVES

4.1 INTRODUCTION

From the time radial basis functions were constructed and identified to be a powerful tool to approximate functions from scattered data in higher dimensions, RBF practitioners had to fight with the curse of instability due to high ill-conditioning of the corresponding linear system. This system become unstable whenever the shape parameter $\varepsilon \rightarrow 0$ (flatter radial functions) and/or data or nodal points become closer. However for many application problems, accurate solutions are obtained for smaller ε values. Also to capture high gradient solutions as well to improve the solutions near boundaries, it is important to cluster more nodal points in those subregions of the problem domain.

In the initial developments of radial basis functions based methods, Robert Schaback (1995) proved the “uncertainty principle” stating that both the error and condition number of the coefficient matrix cannot be small simultaneously for interpolation problems. Also many numerical and theoretical studies (Carlson and Foley, 1991; Rippa, 1999; Roque and Ferreira, 2010; Sanyasiraju and Satyanarayana, 2013) suggests that optimal ε falls in to the category of ‘very small’ value, which prohibits RBF schemes obtaining accurate and stable solutions due to high ill-conditioning. The efforts for stable computation of RBF solutions were seen initially from Beatson et al. (1999) by rewriting the basis for the RBF interpolation. Following this some pre-conditioning strategies were proposed by Ling and Kansa (2005) by

constructing approximate cardinal basis functions, but with moderate success.

It is understood from the literature that a great deal of progress on ‘stable computation’ of solutions using radial functions are made during last decade. In 2004, Fornberg and Wright developed an algorithm based on contour integration in complex ε -plane for stable evaluation of RBF interpolants. Even though this was restricted for small number of data, this has clearly shown the possibility of obtaining radial function approximations in a stable manner. Based on rewriting the RBF basis in terms of spherical harmonics (on sphere) or Chebyshev expansions and then using appropriate QR factorisation for any domain in 1-3 dimensions, Fornberg and his co-workers have proposed RBF-QR algorithm. In this algorithm restrictions on the number of nodes are loosened to do computations for moderately large set of nodes (Fornberg and Piret, 2007; Fornberg et al., 2011). Some of the other important contributions towards developing robust and stable RBF solution evaluation methods are from Fasshauer and McCourt (2012), Cheung et al. (2015), Gonzalez-Rodriguez et al. (2015) and Wright and Fornberg (2017). As an application of RBF-QR algorithms to fractional model problems, we can refer the works of Piret and Hanert (2013) on fractional diffusion model in one dimension and Antunes and Ferreira (2015) on fractional Sturm-Liouville eigenvalue problems in one dimension. In their later work, Antunes and Ferreira developed a new method augmenting RBF basis with fractional polynomials and then obtained solutions incorporating RBF-QR method (Antunes and Ferreira, 2015).

Tikhonov regularisation method is one of the successful regularisation method usually considered to solve ill-posed problems. An ill-conditioned linear system can be treated as a discretised ill-posed problem. Unlike RBF interpolation which produces a symmetric matrix that can be regularised by Lavrentiev regularisation (Sarra, 2014), some of the RBF collocation methods for differential equations lead to an asymmetric collocation matrix. In such situation, Tikhonov regularisation is more suitable in getting stable solutions. There are only a few efforts in the literature that incorporates Tikhonov regularisation (TR) along with RBF discretisation (Lin et al., 2012; Arghand and Amirfakhrian, 2015; Zhang and Li, 2016) and they focus on classical PDE models.

In the current work, we have proposed two efficient stabilisation schemes based on 1) Tikhonov regularisation and 2) RBF-QR to approximate fractional derivatives. As mentioned, there are very limited work considering Tikhonov regularisation in RBF discretisation. Thus algorithm 1, henceforth called RBF-TR is developed to

regularise the linear system obtained by discretising fractional order differential equations, where the optimal regularisation parameter is computed using generalised cross validation (GCV) method. In order to simplify the computations, singular value decomposition method is implemented. On the other hand RBF-QR focuses on replacing extremely unstable radial basis functions basis with a more stable one such that it generates the same space. The importance of the present work is that RBF-QR method is made applicable to any choice of radial functions. The originally proposed RBF-QR algorithm for non-spherical domains was limited to Gaussian RBF due to the complexity involved in obtaining the coefficient matrix by changing the basis using hypergeometric series expansion and truncating appropriately. Hence in the current work, the hypergeometric series approximation is replaced with Chebyshev-Gauss quadrature rule, which consequently makes RBF-QR method flexible enough to include more class of radial functions.

In the following section, formulation of both the algorithms are discussed in detail. Then these methods are illustrated using well known fractional model problems such as fractional diffusion, Bagley-Torvik equation and system of fractional ODEs.

4.2 METHODOLOGY

4.2.1 A direct RBF collocation space fractional diffusion model

To demonstrate the implementation of RBF-QR and RBF-TR methods, we derive direct collocation for fractional diffusion model as given below.

$$\begin{aligned} \frac{\partial u(x,t)}{\partial t} &= d(x) \frac{\partial^q u(x,t)}{\partial x^q} + f(x,t), \quad x \in [a,b] \\ IC : u(x,0) &= u_0(x) \quad BC : u(a,t) = 0, u(b,t) = u_b(t) \end{aligned} \quad (4.2.1)$$

Expressing $u(x,t)$ in terms of RBFs as;

$$u(x,t) \approx \sum_{j=1}^n \lambda_j(t) \phi(|x - x_j|), \quad (4.2.2)$$

$x \in [a,b]$ and $t > 0$, where $x_j, j = 1, 2, \dots, n$, are collocation points in $[a,b]$. Discretised form of (4.2.1) after substituting (4.2.2) at each of these collocation points, we get

$$\begin{aligned} \sum_{j=1}^n \phi_{ij} \frac{d\lambda_j(t)}{dt} &= \sum_{j=1}^n d(x_i) \left(\frac{\partial^q \phi}{\partial x^q} \right)_{ij} \lambda_j(t) + f(x_i), \quad i = 1, 2, \dots, n \\ \sum_{j=1}^n \phi_{1j} \lambda_j(t) &= 0; \quad \sum_{j=1}^n \phi_{nj} \lambda_j(t) = u_b \end{aligned} \quad (4.2.3)$$

Considering Crank-Nicolson scheme to advance in time,

$$\begin{aligned} \sum_{j=1}^n \left(\phi_{ij} - \frac{d(x_i)\Delta t}{2} \left(\frac{\partial^q \phi}{\partial x^q} \right)_{ij} \right) \lambda_j^s &= \sum_{j=1}^n \left(\phi_{ij} + \frac{d(x_i)\Delta t}{2} \left(\frac{\partial^q \phi}{\partial x^q} \right)_{ij} \right) \lambda_j^{s-1} + \left(\frac{\Delta t}{2} (f_i^s + f_i^{s-1}) \right) \\ \sum_{j=1}^n \phi_{1j} \lambda_j^s &= 0, \quad \sum_{j=1}^n \phi_{nj} \lambda_j^s = u_b \end{aligned}$$

where $i = 1, 2, \dots, n$ and $s = 2, 3, \dots$, which leads to a system,

$$A\bar{\lambda}^s = B\bar{\lambda}^{s-1} + F \quad (4.2.4)$$

where

$$A_{ij} = \begin{cases} \phi_{ij}, & \text{if } x_i = a \text{ or } x_i = b \\ \phi_{ij} - \frac{d(x_i)\Delta t}{2} \left(\frac{\partial^q \phi}{\partial x^q} \right)_{ij}, & \text{if } x_i \in (a, b) \end{cases}$$

$$B_{ij} = \begin{cases} 0, & \text{if } x_i = a \text{ or } x_i = b \\ \phi_{ij} + \frac{d(x_i)\Delta t}{2} \left(\frac{\partial^q \phi}{\partial x^q} \right)_{ij}, & \text{if } x_i \in (a, b) \end{cases}$$

and

$$F_i = \begin{cases} 0 & \text{if } x_i = a \\ \frac{\Delta t}{2} (f_i^s + f_i^{s-1}), & \text{if } x_i \in (a, b) \\ u_b & \text{if } x_i = b \end{cases}$$

However, we require $\bar{\lambda}^1$ which is evaluated, using initial condition, by solving the system,

$$A\bar{\lambda}^1 = F \quad (4.2.5)$$

where $A_{ij} = \phi_{ij}$ and $F_i = u_0(x_i)$, $i, j = 1, 2, \dots, n$.

The fractional derivatives present in equations are evaluated by Gauss-Jacobi quadrature rule as discussed in Chapter 2. The coefficient matrix A is dense and becomes increasingly ill-conditioned as $\varepsilon \rightarrow 0$ or nodal points becomes closer to each

other which results in unreliable solution. So, in order to overcome this ill-conditioning issues, the present chapter illustrates the extension of two stabilisation schemes RBF-TR and RBF-QR.

4.2.2 RBF-QR method

RBF-QR method by Fornberg et al. (2011) relies on representing the ill-conditioned RBF bases in terms of a well-conditioned one that spans exactly the same space. Then the coefficient matrix thus obtained is factorised into the product $Q \times R$, where Q is a unitary matrix and R is an upper triangular matrix. In their work, RBF basis is transformed in the following way.

$$\phi(|x - x_j|) = \sum_{k=0}^{\infty} c_k(x_j) \tilde{T}_k(x) = \sum_{k=0}^{\infty} c_k(x_j) T_k(2x - 1) \quad (4.2.6)$$

where \tilde{T} denotes the shifted Chebyshev polynomials to generalise the domain from $[-1, 1]$ to $[a, b] = [0, 1]$ using the transformation $x = \frac{a+b}{2} + \frac{b-a}{2}\xi = \frac{1}{2} + \frac{1}{2}\xi$ and c_1, c_2, \dots are the coefficients to be evaluated using the orthogonality property of Chebyshev's polynomials,

$$\int_{-1}^1 \frac{T_k(\xi) T_i(\xi)}{\sqrt{(1-\xi^2)}} d\xi = \begin{cases} 0 & k \neq i \\ \pi, & k = i = 0 \\ \frac{\pi}{2}, & k = i \geq 1 \end{cases}, \quad (4.2.7)$$

Considering the transformation $x = \frac{1}{2}\xi + \frac{1}{2}$, integrate (4.2.6) after multiplying by $\frac{T_i(\xi)}{\sqrt{(1-\xi^2)}}$ to obtain c_k 's for each x_j , $j = 1, 2, \dots, n$.

$$c_i(x_j) = \hat{b} \int_{-1}^1 \frac{\phi(|0.5\xi + 0.5 - x_j|) T_i(\xi)}{\sqrt{(1-\xi^2)}} d\xi \quad (4.2.8)$$

where $\hat{b} = \frac{1}{\pi}$, $i = 0$ and $\hat{b} = \frac{2}{\pi}$, $i \geq 1$.

In their formulation for general domains, Fornberg and collaborators have considered only Gaussian radial function. The splitting of $e^{-\varepsilon^2(|x-x_j|)^2}$ as $e^{-\varepsilon^2 x^2} e^{-\varepsilon^2 x_j^2} e^{\varepsilon^2 2xx_j}$ have made them to propose the following representation, which in turn provides the coefficients in terms of hypergeometric series.

$$e^{-\varepsilon^2(|x-x_j|)^2} = \sum_{k=0}^{\infty} c_k(x_j) e^{-\varepsilon^2 x^2} T_k(x); \quad c_k(x_j) = d_k \tilde{b}_k e^{-\varepsilon^2 x_j^2} x_j^k {}_0F_1([], k+1, \varepsilon^4 x_j^2)$$

where $d_k = \frac{2\varepsilon^{2k}}{k!}$, $\tilde{b}_0 = 1/2$ and $\tilde{b}_k = 1$, $k > 0$. With appropriate modification the formula is translated to general domain $[a, b]$. Based on this RBF-QR process, many classical differential models are solved (Ilati and Dehghan (2015); Dehghan and Najafi (2016), to name a few). Very few attempts (Piret and Hanert, 2013; Antunes and Ferreira, 2015) are reported in the context of solving fractional model problems. However, it is observed from RBF literature that other commonly considered radial functions are multiquadrics and inverse multiquadrics. Thus its important to generalise the algorithm to include more class of functions. Hence, in this work, we propose to obtain the coefficients $c_k(x_j)$'s in (4.2.8) using Chebyshev-Gauss quadrature rule. Throughout the chapter RBF-QR algorithm with Chebyshev-Gauss quadrature is referred as RBF-QR-CH.

4.2.2.1 RBF-QR using Chebyshev-Gauss quadrature rule

Choosing $F(\xi) = \phi(0.5\xi + 0.5 - x_j)T_i(\xi)$, Chebyshev-Gauss quadrature can be considered to evaluate the integral $\int_{-1}^1 W(\xi)F(\xi)d\xi$, with weight function $W(\xi) = \frac{1}{\sqrt{1-\xi^2}}$. The approximation then becomes,

$$\int_{-1}^1 \frac{F(\xi)}{\sqrt{1-\xi^2}}d\xi \approx \sum_{l=1}^{n_c} W_l F(\xi_l) \quad (4.2.9)$$

where n_c is the number of Chebyshev quadrature points obtained from the zeros of Chebyshev polynomials $\xi_l = \cos\left(\frac{2l-1}{2n_c}\pi\right)$ with $W_l = \frac{\pi}{n_c}$ being the corresponding weights. Thus,

$$\int_{-1}^1 \frac{F(\xi)}{\sqrt{1-\xi^2}}d\xi \approx \frac{\pi}{n_c} \sum_{l=1}^{n_c} F\left(\cos\left(\frac{2l-1}{2n_c}\pi\right)\right) \quad (4.2.10)$$

which leads to

$$c_i(x_j) = \begin{cases} \frac{1}{n_c} \sum_{l=1}^{n_c} \phi(0.5\xi_l + 0.5 - x_j)T_i(\xi_l), & i = 0 \\ \frac{2}{n_c} \sum_{l=1}^{n_c} \phi(0.5\xi_l + 0.5 - x_j)T_i(\xi_l), & i \geq 1 \end{cases} \quad (4.2.11)$$

for $i = 0, 1, \dots, j = 1, 2, \dots, n$. Truncating the series (4.2.6) for computations considering sufficiently large p ($p > n$) terms, radial function basis is expressed as,

$$\begin{pmatrix} \phi(|x-x_1|) \\ \phi(|x-x_2|) \\ \vdots \\ \phi(|x-x_n|) \end{pmatrix} = \underbrace{\begin{pmatrix} c_0(x_1) & c_1(x_1) & \cdots & c_p(x_1) \\ c_0(x_2) & c_1(x_2) & \cdots & c_p(x_2) \\ \vdots & \ddots & & \vdots \\ c_0(x_n) & c_1(x_n) & \cdots & c_p(x_n) \end{pmatrix}}_C \begin{pmatrix} \tilde{T}_0(x) \\ \tilde{T}_1(x) \\ \vdots \\ \tilde{T}_p(x) \end{pmatrix} \quad (4.2.12)$$

Thus at each node x_i , $i = 1, 2, \dots, n$, Eqn.(4.2.12) gives an expression as in the following:

$$\underbrace{\begin{pmatrix} \phi(|x_1-x_1|) & \phi(|x_2-x_1|) & \cdots & \phi(|x_n-x_1|) \\ \phi(|x_1-x_2|) & \phi(|x_2-x_2|) & \cdots & \phi(|x_n-x_2|) \\ \vdots & \vdots & \ddots & \vdots \\ \phi(|x_1-x_n|) & \phi(|x_2-x_n|) & \cdots & \phi(|x_n-x_n|) \end{pmatrix}}_\Phi = C \underbrace{\begin{pmatrix} \tilde{T}_0(x_1) & \tilde{T}_0(x_2) & \cdots & \tilde{T}_0(x_n) \\ \tilde{T}_1(x_1) & \tilde{T}_1(x_2) & \cdots & \tilde{T}_1(x_n) \\ \vdots & \vdots & \ddots & \vdots \\ \tilde{T}_p(x_1) & \tilde{T}_p(x_2) & \cdots & \tilde{T}_p(x_n) \end{pmatrix}}_E \quad (4.2.13)$$

Then factorizing C into Q and R , where Q is an unitary matrix and R is an upper triangular matrix, (4.2.13) becomes

$$\Phi_{n \times n} = \underbrace{\begin{pmatrix} Q_{n \times n} & R_{n \times (p+1)} \end{pmatrix}}_C E_{(p+1) \times n} = Q [R_1 \ R_2] E = Q R_1 [I \ R_1^{-1} R_2] E \quad (4.2.14)$$

where R_1 contains first n columns of matrix R and R_2 contains the remaining $(p+1-n)$ columns of R . To simplify further, pre-multiply (4.2.14) by $R_1^{-1} Q^T$. This finally leads to a basis which is a linearly independent combinations of RBFs which keeps the approximation space intact.

$$\Psi(x) = R_1^{-1} Q^T \Phi(x) = [I \ R_1^{-1} R_2] E \quad (4.2.15)$$

Hence the interpolation matrix is rewritten in terms of the following new basis,

$$[\Psi(x_1), \Psi(x_2), \dots, \Psi(x_n)]^T = (R_1^{-1} Q^T \Phi)^T = E^T [I \ R_1^{-1} R_2]^T \quad (4.2.16)$$

4.2.2.2 Fractional RBF-QR-CH basis:

Since the fractional operators possess linearity property, when ${}^c D_a^q$ acts on both sides (4.2.6) term by term, yields,

$${}^c D_a^q \phi(|x - x_j|) = \sum_{k=0}^{\infty} c_k(x_j) {}^c D_a^q \tilde{T}_k(x) \quad (4.2.17)$$

Thus at each node $x_i, i = 1, 2, \dots, n$, the fractional derivative of RBFs can be approximated as follows:

$$\underbrace{\begin{pmatrix} {}^c D_a^q \phi(|x_1 - x_1|) & {}^c D_a^q \phi(|x_2 - x_1|) & \cdots & {}^c D_a^q \phi(|x_n - x_1|) \\ {}^c D_a^q \phi(|x_1 - x_2|) & {}^c D_a^q \phi(|x_2 - x_2|) & \cdots & {}^c D_a^q \phi(|x_n - x_2|) \\ \vdots & \vdots & \ddots & \vdots \\ {}^c D_a^q \phi(|x_1 - x_n|) & {}^c D_a^q \phi(|x_2 - x_n|) & \cdots & {}^c D_a^q \phi(|x_n - x_n|) \end{pmatrix}}_{\tilde{\Phi}} = C \underbrace{\begin{pmatrix} {}^c D_a^q \tilde{T}_0(x_1) & {}^c D_a^q \tilde{T}_0(x_2) & \cdots & {}^c D_a^q \tilde{T}_0(x_n) \\ {}^c D_a^q \tilde{T}_1(x_1) & {}^c D_a^q \tilde{T}_1(x_2) & \cdots & {}^c D_a^q \tilde{T}_1(x_n) \\ \vdots & \vdots & \ddots & \vdots \\ {}^c D_a^q \tilde{T}_p(x_1) & {}^c D_a^q \tilde{T}_p(x_2) & \cdots & {}^c D_a^q \tilde{T}_p(x_n) \end{pmatrix}}_{\tilde{E}} \quad (4.2.18)$$

Considering QR factorisation of $\tilde{\Phi}$ and further simplifications lead to the representation

$\tilde{\Phi} = Q R_1 [I \ R_1^{-1} R_2] \tilde{E}$. Then the matrix corresponding to the one in (4.2.16) takes the form

$$[{}^c D_a^q \Psi(x_1), {}^c D_a^q \Psi(x_2), \dots, {}^c D_a^q \Psi(x_n)]^T = (R_1^{-1} Q^T \tilde{\Phi})^T = \tilde{E}^T [I \ R_1^{-1} R_2]^T \quad (4.2.19)$$

where ${}^c D_a^q \Psi(x_j) = [{}^c D_a^q \Psi(x_{j1}), {}^c D_a^q \Psi(x_{j2}), \dots, {}^c D_a^q \Psi(x_{jn})]^T$, $j = 1, 2, \dots, n$. The evaluation of ${}^c D_a^q \tilde{T}_i(x)$, $i = 0, 1, \dots, p$ may be done analytically for small 'p', however becomes tedious even for moderately large number. Hence Gauss-Jacobi quadrature rule (refer Chapter 2) that can be generalised for any 'p' is considered in our computations.

4.2.2.3 RBF-QR-CH algorithm of fractional diffusion problem

This section provides an algorithm for direct RBF collocation described in subsection 4.2.1, with

1. Input x_i 's, ϕ , n , $p > n$.
2. Compute $C_{n \times (p+1)}$ (refer (4.2.11)).
3. Factorise $C = QR$, then write $R = [R_1 \ R_2]$ as in (4.2.14).
4. For $t=0$,
 - (a) Compute $A = \tilde{E}^T [I \ R_1^{-1} R_2]^T$, where $\tilde{E}_{ij} = \tilde{T}_{i-1}(x_j)$, $i = 1, 2, \dots, (p+1)$, $j = 1, 2, \dots, n$.
 - (b) Evaluate $\tilde{\lambda}^1 = A^{-1} F$, where $F_i = u_0(x_i)$, $i = 1, 2, \dots, n$.
5. For $t > 0$,

(a) Compute $A = \widehat{E}^T [I \ R_1^{-1} R_2]^T$, where

$$\widehat{E}_{ij} = \begin{cases} \widetilde{T}_{i-1}(x_j), & \text{if } x_j = a \text{ or } b \\ \widetilde{T}_{i-1}(x_j) - \frac{d(x_j)\Delta t}{2} {}^c D_a^q \widetilde{T}_{i-1}(x_j), & \text{if } x_j \in (a, b) \end{cases}$$

(b) Evaluate $\bar{\lambda}^s = A^{-1}(B\bar{\lambda}^{s-1} + F)$ with F as in (4.2.4).

$$6. u_i(t_s) = \sum_{j=1}^n \lambda_j^s \Psi_{ij}, \quad i = 1, 2, \dots, n.$$

4.2.3 Tikhonov Regularisation

In general, regularisation process replaces ill-posed problem with a nearby well-posed model by considering certain additional informations. Literature survey suggests the interests in the field in developing theory on important regularisation methods such as Lavrentiev and Tikhonov regularisation methods and their applications to inverse problems, image processing, statistics problems and many more (Neumaier, 1998).

While considering RBF interpolation problems, where resulting linear system is symmetric, Lavrentiev regularisation is applicable. However, many RBF based schemes produce asymmetric systems, wherein Tikhonov regularisation is suitable. In the following, we briefly describe the technique and their extension to Kansa's method on one dimensional fractional diffusion model (4.2.1).

Let $A \in \mathbb{C}^{m \times n}$, $F \in \mathbb{C}^m$. The minimum-norm least-squares solution of the system $A\bar{\lambda} = F$ is $\bar{\lambda} = A^\dagger F$, where A^\dagger is the pseudoinverse or generalised inverse of the matrix A (Ben-Israel and Greville, 2003). It is precisely the solution of two stage minimisation problem:

- Stage 1: Solve $\text{Min } \|A\bar{\lambda} - F\|$.
- Stage 2: Obtain $\text{Min } \|\bar{\lambda}\|$ from all solutions of Stage 1.

Thus if A is a well-conditioned matrix, then the solution is expressed as $\bar{\lambda} = (A^*A)^{-1}A^*F = A^\dagger F$, provided A has full column rank. Here, A^* is the Hermitian matrix.

However, for an ill-conditioned matrix, the condition number of symmetric and positive definite matrix A^*A , can be reduced by adding a small constant to every diagonal element. Then the corresponding solution becomes $\bar{\lambda} = (A^*A + \mu^2 I)^{-1}A^*F$, a formula proposed by Tikhonov (1963). Thus above two stage minimisation problem becomes

$$\text{Min } f_{\mu^2}(\bar{\lambda}) \tag{4.2.20}$$

where $f_{\mu^2}(\bar{\lambda}) = \|A\bar{\lambda} - F\|^2 + \mu^2\|\bar{\lambda}\|^2$ depends on a nonzero real parameter μ^2 , known as regularisation parameter. Following theorem proves the existence of the solution of (4.2.20).

Theorem 4.2.1. (Ben-Israel and Greville, 2003) *The function $f_{\mu^2}(\bar{\lambda})$ has a unique minimiser $\bar{\lambda}_{\mu^2}$ given by, $\bar{\lambda}_{\mu^2} = (A^*A + \mu^2I)^{-1}A^*F$ whose norm $\|\bar{\lambda}_{\mu^2}\|$ is a monotone decreasing function of μ^2 .*

It is clear that $f_{\mu^2}(\bar{\lambda}_{\mu^2}) \rightarrow A^\dagger F$ as $\mu \rightarrow 0$. Thus, in Tikhonov regularisation the linear system $A\bar{\lambda} = F$ is replaced by a the regularised system

$$(A^*A + \mu^2I)\bar{\lambda} = A^*F$$

The efficiency of the regularisation methods mainly depends on the effective evaluation of the regularisation parameter μ . Well known methods like L-curve, generalised cross validation (GCV) (Hansen and O'Leary, 1993) are some of the important algorithms helpful in finding optimal value of μ .

4.2.3.1 RBF-TR for fractional diffusion problem

Thus according to Tikhonov regularisation, the system $A\bar{\lambda}^s = B\bar{\lambda}^{s-1} + F$ where A is a real matrix obtained by RBF (refer Eqn.(4.2.4)), is replaced with regularised system $(A^T A + \mu^2 I)\bar{\lambda}^s = A^T (B\bar{\lambda}^{s-1} + F)$, with A , B and F defined as in Subsection 4.2.1. This leads to the solution,

$$\bar{\lambda}^s = (A^T A + \mu^2 I)^{-1} A^T (B\bar{\lambda}^{s-1} + F) \quad (4.2.21)$$

For further simplification, let us consider the singular value decomposition (SVD) of matrix $A = USV^T$ where U and V are unitary (here, orthogonal) matrices and $S = \text{diag}(\sigma_1, \sigma_2, \dots, \sigma_n)$ where σ_i 's are singular values of the matrix A . Thus the SVD along with the properties of orthogonal matrices, reduces Eqn. (4.2.21) to

$$\bar{\lambda}^s = V \left[(S^2 + \mu^2 I)^{-1} S \right] \left[U^T (B\bar{\lambda}^{s-1} + F) \right] \quad (4.2.22)$$

where optimal μ^2 has been evaluated using generalised cross validation (GCV) method which mainly dealt by minimising the function

$$G(\mu) = \frac{\|A\bar{\lambda} - (B\bar{\lambda}^{s-1} + F)\|^2}{(\text{trace}(I - AA^T))^2} \quad (4.2.23)$$

where $A^I = (A^T A + \mu^2 I)^{-1} A^T$.

4.3 NUMERICAL ILLUSTRATIONS

In this section, the efficiency of the presented methods is illustrated by considering various types of linear fractional order differential equations for both uniform and nonuniform nodal distributions. Nonuniform nodes are Chebyshev-Gauss-Lobatto points defined by $\left[\frac{1 - \cos(i\pi/n)}{2} \right]$, $i = 0, 1, 2, \dots, n$. Results by the proposed RBF-TR (MQ-TR) and RBF-QR-CH (MQ, GA, IMQ, Sech) methods are compared with the RBF-QR by Fornberg and collaborators, henceforth referred in the thesis as GA-QR. Also these solutions are compared to MQ-direct and solutions obtained using other existing methods. The shape parameters are chosen as $\varepsilon = 2E - 08$ for RBF-QR and RBF-QR-CH and $\varepsilon_j = \varepsilon_{min} + 0.2 * \sin(j)$, $\varepsilon_{min} = 2E - 06$ ($j = 1, 2, \dots, n$), for RBF-TR, unless specified otherwise. For known exact solutions, accuracy is compared in terms of L_∞ errors.

Example 4.3.1. Consider the space fractional diffusion problem (Pang et al., 2015),

$$\frac{\partial u(x,t)}{\partial t} = \frac{\Gamma(2.2)}{6} x^{2.8} \frac{\partial^{1.8} u(x,t)}{\partial x^{1.8}} - x^3 (1+x) e^{-t}, \quad 0 < x < 1, \quad 0 < t < T. \quad (4.3.1)$$

subject to the IC : $u(x,0) = x^3$ and BCs : $u(0,t) = 0$ and $u(1,t) = e^{-t}$, $t > 0$. The analytical solution $u(x,t) = x^3 e^{-t}$.

The results are illustrated through Figure 4.1 and 4.2 as well as Table 4.1 to 4.3. Figure 4.1 provides visual appearance of MQ-QR-CH solution in comparison with exact solution $t = 20$. L_∞ errors for various ‘ ε ’ are plotted in Figure 4.2 for both MQ-QR-CH (Row 1) and MQ-TR (Row 2). The results show that irrespective of the nodal distributions, MQ-TR solution improve as n increases. However, for uniform nodes MQ-QR-CH solution start diverging from exact solution for $n \geq 18$. In the case of nonuniform nodes, solution accuracy remains better with increase in number of nodes for both the algorithms. This is similar to the behaviour reported by Piret and Hanert (2013) for a fractional diffusion model using GA-QR. Using the proposed RBF-QR-CH algorithm, other radial functions GA, IMQ, sech also have shown similar characteristics.

Table 4.1 presents L_∞ error and convergence rate for all the proposed algorithms and MQ-direct (Pang et al., 2015). From Table 4.2, we can see analogous features by all radial functions using RBF-QR-CH algorithm, which is also observed in Figure 4.2. Table 4.3 provides a pointwise comparison of solutions of MQ-direct, MQ-TR, GA-QR and RBF-QR-CH (using all infinitely smooth radial functions) at $t = 1$ and $t = 10$. In spite of using smaller Δt , MQ-direct solution accuracy is considerably less in comparison with stabilised RBF methods.

Example 4.3.2. Consider another space fractional diffusion problem (Sweilam et al., 2015),

$$\frac{\partial u(x,t)}{\partial t} = \Gamma(1.2)x^{1.8} \frac{\partial^{1.8} u(x,t)}{\partial x^{1.8}} + 3x^2(2x-1)e^{-t}, \quad 0 < x < 1, \quad t > 0 \quad (4.3.2)$$

subject to the IC : $u(x,0) = x^2(1-x)$ and BCs : $u(0,t) = u(1,t) = 0, \quad t > 0$. The analytical solution $u(x,t) = x^2(1-x)e^{-t}$.

The results (Figure 4.3 and Table 4.4, 4.5) shows a similar pattern obtained for Example 4.3.1. Table 4.5 compares proposed algorithms with MQ-direct and a method based on second kind shifted Chebyshev polynomials (SKSCP) by Sweilam et al. (2015). RBF-QR-CH (using MQ, IMQ, GA and Sech), RBF-TR solutions are as accurate as GA-QR (Fornberg et al. (2011), Piret and Hanert (2013)) and provides significantly higher accuracy when compared with MQ-direct and the solutions of Sweilam et al. (2015).

Example 4.3.3. To validate the proposed methods, we choose Bagley-Torvik equation (Rehman and Khan, 2012),

$$au''(x) + b^c D^{3/2}u(x) + cu(x) = g(x), \quad x \in [0, 1] \quad (4.3.3)$$

with boundary conditions $u(0) = 0, u(1) = 0$ when $a = 1, b = \frac{8}{17}$ and $c = \frac{13}{51}$, the exact solution $u(x) = x^5 - \frac{29}{10}x^4 + \frac{76}{25}x^3 - \frac{339}{250}x^2 + \frac{27}{125}x$. Here $g(x) = \frac{x^{-1/2}}{89250\sqrt{\pi}}(48P(x) + 7\sqrt{\pi x}Q(x))$ with $P(x) = 16000x^4 - 32480x^3 + 21280x^2 - 4746x$ and $Q(x) = 3250x^5 - 9425x^4 + 264880x^3 - 448107x^2 + 233262x - 34578$.

Figure 4.4 shows the manner in which both the stabilisation methods using MQ radial function respond to increase in number of nodes. Even though MQ-QR-CH solution accuracy is close to 10^{-15} for small $n < 20$, accuracy starts deteriorating as n increases. This scenario is observed for uniform distribution. But solution

obtained using Chebyshev-Gauss-Lobatto points retains the accuracy with increase in n . From Tables 4.6 and 4.7, it is clear that RBF-QR-CH and RBF-QR (using Gaussian) produce significantly improved solution when compared to MQ-direct, MQ-TR and Haar wavelet method by Rehman and Khan (2012).

Example 4.3.4. Consider a system of fractional BVP as follows,

$$\begin{aligned} u''(x) - v'(x) + {}^c D_0^{0.4} v(x) + v(x) &= f_1(x) \\ v''(x) - u'(x) + {}^c D_0^{0.6} u(x) + u(x) &= f_2(x) \end{aligned} \quad (4.3.4)$$

along with the boundary conditions $u(0) = u(1) = 0$, $v(0) = v(1) = 0$, where $f_1(x) = 11x^2 + 3x - 1 - \frac{2x^{1.6}}{\Gamma(2.6)} + \frac{x^{0.6}}{\Gamma(1.6)}$ and $f_2(x) = x^4 - 4x^3 - x - 1 + \frac{24x^{3.4}}{\Gamma(4.4)} - \frac{x^{0.4}}{\Gamma(1.4)}$. The exact solution for u and v are $u(x) = x(x^3 - 1)$, $v(x) = x(1 - x)$.

From Tables 4.8 and 4.9, we can see that the accuracy using RBF-QR-CH (MQ, GA, IMQ, Sech) and GA-QR are significantly higher when compared with that of MQ-TR and sinc-collocation method (SCM) by Hatipoglu et al. (2017). However, as observed in earlier examples both RBF-QR-CH and RBF-QR (GA-QR) are sensitive to increase in nodal points n . Table 4.10 provides pointwise error comparison of all the schemes, while Figure 4.5 depicts the exact and MQ-QR-CH solutions for both u and v .

4.4 CONCLUSIONS

In this chapter, we have extended Tikhonov regularisation and RBF-QR algorithms to RBF collocation method formulated for fractional order differential equations. Other main contribution is towards generalising RBF-QR algorithm for any infinitely smooth radial functions, referred as RBF-QR-CH algorithm in the thesis. By solving fractional diffusion model, Bagley-Torvik equation and a system of fractional ODEs, all the proposed methods are tested for accuracy and effect on increase in number of nodes and shape parameter. Comparisons among them as well as with other schemes in the literature proves how efficient these algorithms are. While RBF-QR-CH algorithm helps in stable computation of the solution for very small ε values, RBF-TR is suitable for moderately small ε 's. In spite of their efficiency in obtaining accurate solutions for very small ε 's, both RBF-QR-CH and RBF-QR are sensitive to the nodal distributions.

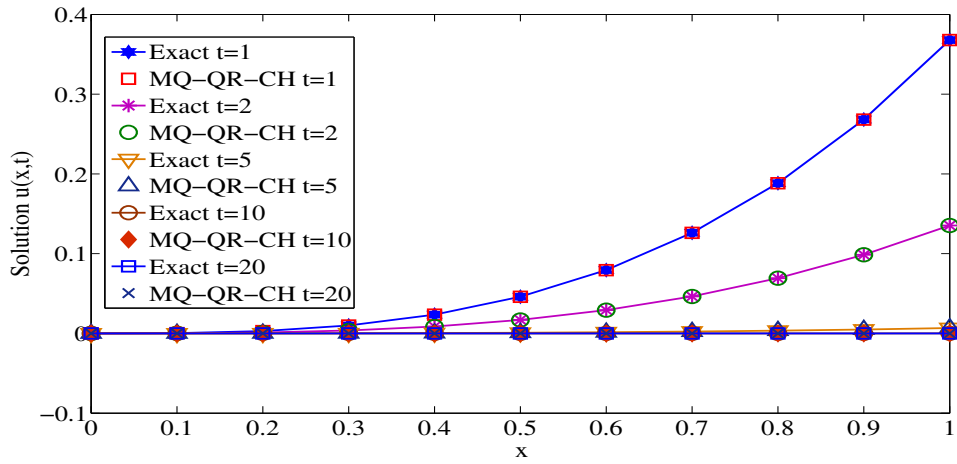


Figure 4.1 Solutions using MQ-QR-CH method for Example 4.3.1.

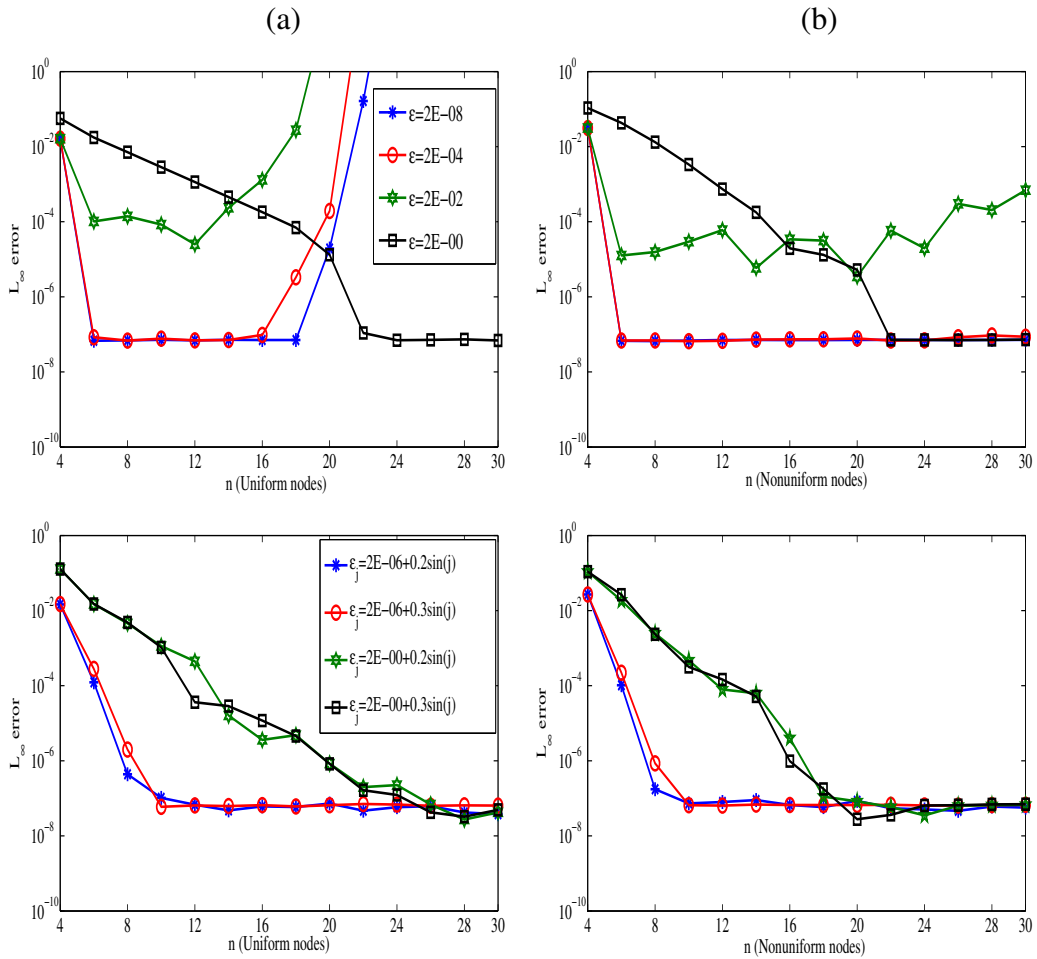


Figure 4.2 Example 4.3.1: n Vs L_∞ error for different ϵ (a) uniform and (b) nonuniform nodes. Row 1: MQ-QR-CH; Row 2: MQ-TR ($\Delta t = 0.0025$).

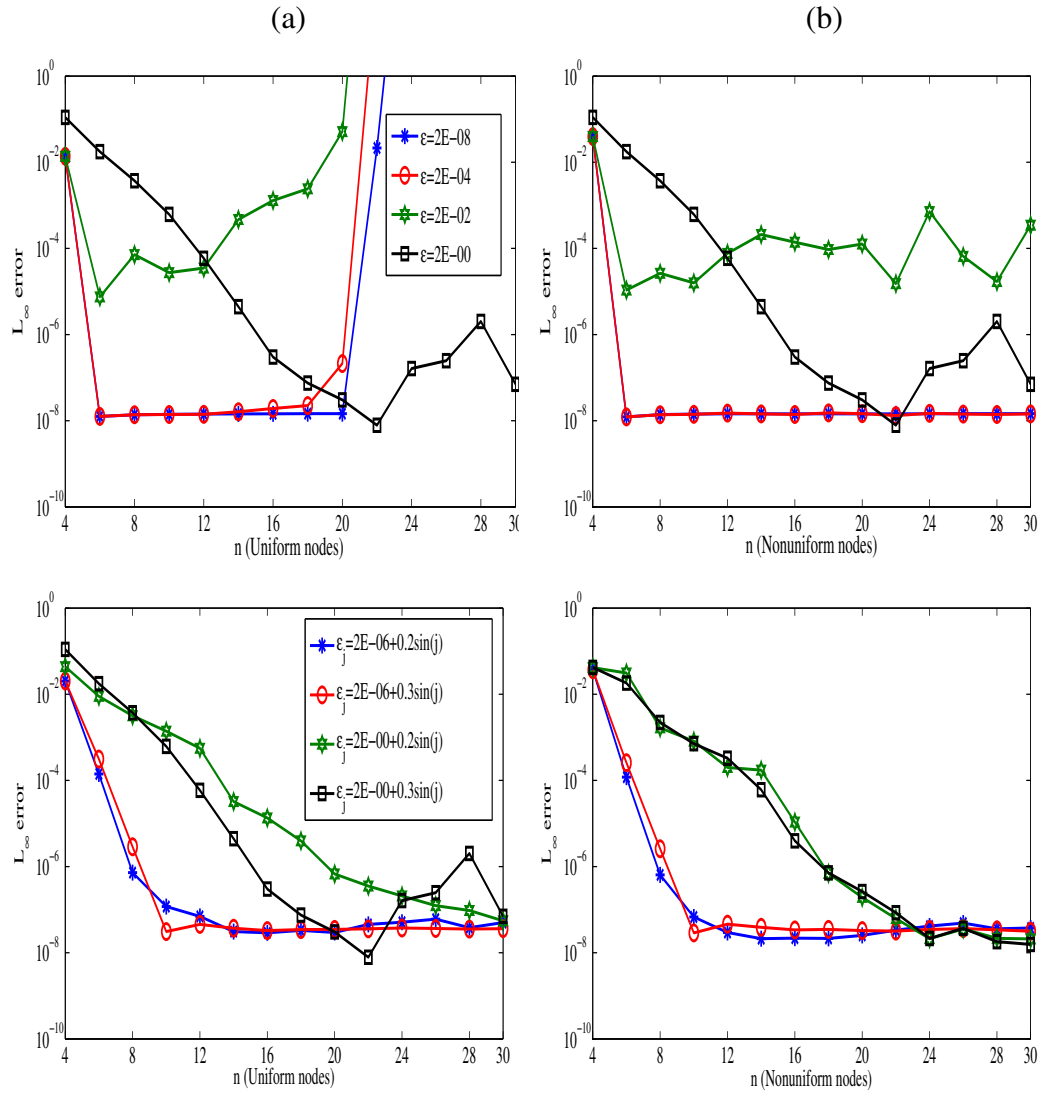


Figure 4.3 Example 4.3.2: n Vs L_∞ error for different ϵ (a) uniform and (b) nonuniform nodes. Row 1: MQ-QR-CH; Row 2: MQ-TR ($\Delta t = 0.0025$).

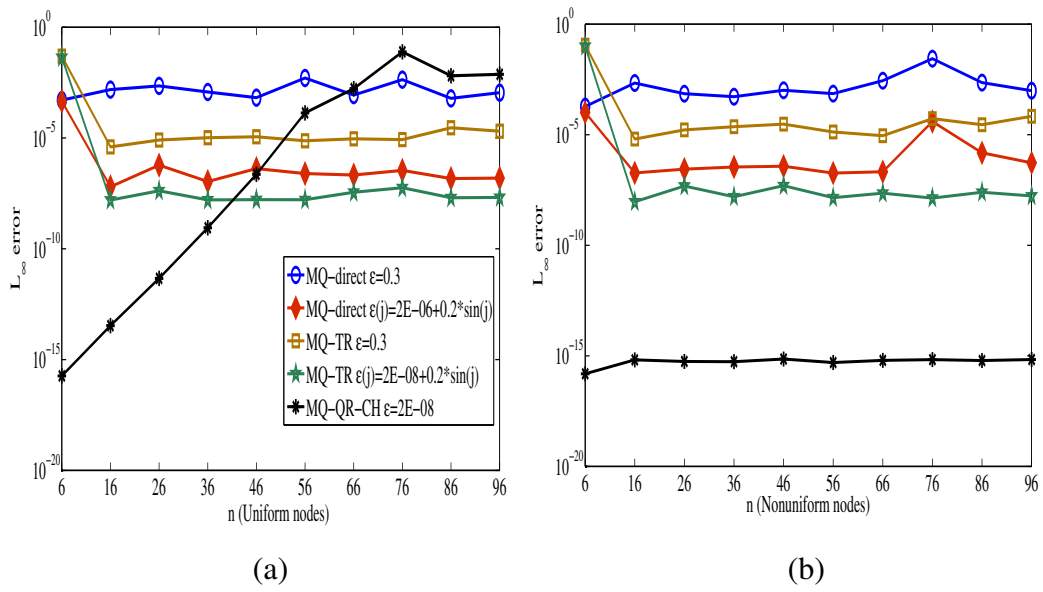


Figure 4.4 Comparison of L_∞ error for Example 4.3.3 .

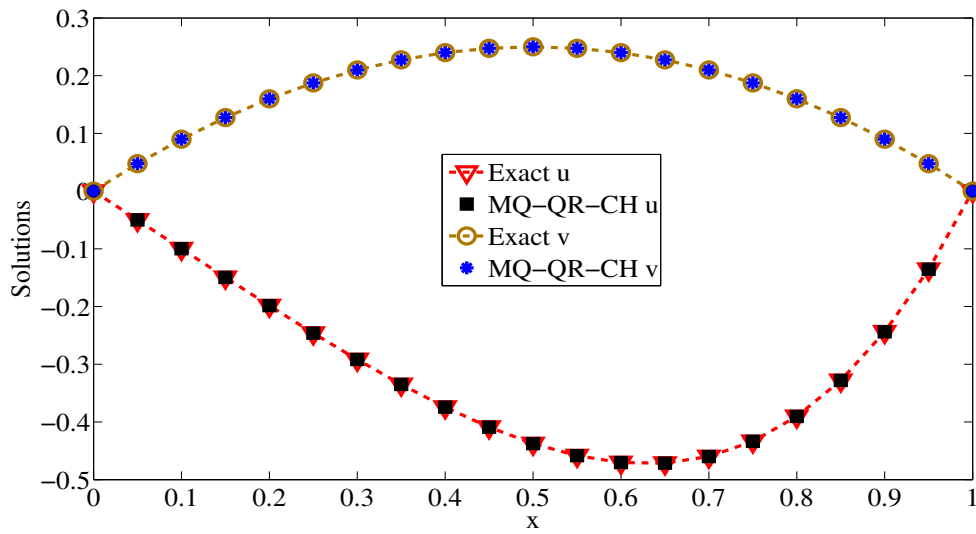


Figure 4.5 Solutions using MQ-QR-CH method for Example 4.3.4.

Table 4.1 L_∞ error and rate of convergence for Example 4.3.1 ($\Delta x = \Delta t$)

Δx	MQ-TR		MQ-QR-CH		IMQ-QR-CH		Sech-QR-CH	
	L_∞ error	ROC	L_∞ error	ROC	L_∞ error	ROC	L_∞ error	ROC
1/ 10	1.1485E-04		1.1326E-04		1.1326E-04		1.1326E-04	
1/ 15	5.0642E-05	2.02	5.0323E-05	2.00	5.0323E-05	2.00	5.0323E-05	2.00
1/ 20	2.8557E-05	1.99	2.8417E-05	1.99	2.8417E-05	1.99	2.8417E-05	1.99
1/ 25	1.8289E-05	2.00	1.8266E-05	1.98	1.8266E-05	1.98	1.8266E-05	1.98
	GA-QR-CH		GA-QR		MQ-direct ($\varepsilon = n^{0.5}/2$) (Pang et al., 2015)			
1/ 10	1.1326E-04		1.1229E-04		5.29135E-4			
1/ 15	5.0323E-05	2.00	5.0570E-05	1.97	1.38298E-4	3.83		
1/ 20	2.8417E-05	1.99	2.8344E-05	2.01	6.20013E-5	2.25		
1/ 25	1.8266E-05	1.98	1.8239E-05	1.98	3.42345E-5	1.82		

Table 4.2 L_∞ error for Example 4.3.1 ($\Delta t = 0.0025$)

n	MQ-TR	MQ-QR-CH	IMQ-QR-CH	Sech-QR-CH	GA-QR-CH	GA-QR
Uniform nodes						
6	1.23E-04	6.7831E-08	6.7831E-08	6.78E-08	6.78E-08	6.64E-08
11	4.29E-08	7.0683E-08	7.0683E-08	7.07E-08	7.07E-08	7.01E-08
21	5.84E-08	1.2417E-03	1.2417E-03	1.24E-03	1.24E-03	4.91E+00
26	6.19E-08	3.7180E+09	3.7180E+09	3.62E+09	3.62E+09	4.49E+14
31	6.79E-08	9.2062E+26	9.2062E+26	9.21E+26	9.21E+26	8.09E+33
Nonuniform nodes						
6	1.03E-04	6.7462E-08	6.7462E-08	6.75E-08	6.75E-08	7.08E-08
11	6.46E-08	7.0467E-08	7.0467E-08	7.05E-08	7.05E-08	7.05E-08
21	8.23E-08	7.0471E-08	7.0471E-08	7.05E-08	7.05E-08	7.05E-08
26	4.69E-08	7.0749E-08	7.0749E-08	7.07E-08	7.07E-08	7.07E-08
31	6.92E-08	7.1061E-08	7.1061E-08	7.11E-08	7.11E-08	7.11E-08

Table 4.3 Absolute error for Example 4.3.1 ($\Delta x = 0.1, \Delta t = 0.0025$)

x	MQ-direct Pang et al. (2015)	MQ-TR	MQ-QR-CH	IMQ-QR-CH	Sech-QR-CH	GA-QR-CH	GA-QR
$T=1$							
0	2.84E-14	1.82E-11	4.73E-15	4.73E-15	4.73E-15	4.73E-15	4.95E-18
0.1	3.59E-08	3.95E-08	3.49E-10	3.49E-10	3.49E-10	3.49E-10	3.50E-10
0.5	8.33E-05	4.08E-08	4.80E-08	4.80E-08	4.80E-08	4.80E-08	4.81E-08
0.9	3.60E-04	4.29E-08	3.45E-08	3.45E-08	3.45E-08	3.45E-08	3.65E-08
1	1.73E-14	2.16E-11	4.27E-15	4.27E-15	4.27E-15	4.27E-15	5.55E-17
$T=10$							
0	1.11E-16	1.71E-13	5.31E-16	5.31E-16	5.31E-16	5.31E-16	5.18E-22
0.1	2.71E-06	1.96E-08	1.73E-09	1.73E-09	1.73E-09	1.73E-09	1.73E-09
0.5	2.37E-05	3.00E-08	1.11E-08	1.11E-08	1.11E-08	1.11E-08	1.08E-08
0.9	4.84E-06	9.69E-09	3.33E-09	3.33E-09	3.33E-09	3.33E-09	2.50E-09
1	1.47E-16	4.67E-13	4.96E-16	4.96E-16	4.96E-16	4.96E-16	1.36E-20

Table 4.4 L_∞ error for Example 4.3.2 ($\Delta t = 0.0025$)

n	MQ-TR	MQ-QR-CH	IMQ-QR-CH	Sech-QR-CH	GA-QR-CH	GA-QR
Uniform nodes						
6	1.41E-04	1.29E-08	1.29E-08	1.26E-08	1.26E-08	1.32E-08
11	3.05E-08	1.43E-08	1.43E-08	1.43E-08	1.43E-08	1.44E-08
21	3.55E-08	1.67E-06	1.67E-06	1.67E-06	1.67E-06	4.49E+01
31	3.65E-08	7.16E+17	7.16E+17	7.16E+17	1.01E+18	8.04E+21
Nonuniform nodes						
6	1.19E-04	1.28E-08	1.23E-08	1.23E-08	1.23E-08	1.36E-08
11	1.22E-08	1.40E-08	1.40E-08	1.40E-08	1.40E-08	1.41E-08
21	2.34E-08	1.46E-08	1.46E-08	1.46E-08	1.46E-08	1.46E-08
31	3.22E-08	1.45E-08	1.45E-08	1.45E-08	1.45E-08	1.45E-08

Table 4.5 Absolute error for Example 4.3.2 ($\Delta x = 0.1, \Delta t = 0.0025$)

x	MQ-direct	MQ-TR	MQ-QR-CH	IMQ-QR-CH	Sech-QR-CH	GA-QR-CH	GA-QR	SKSCP (Sweilam et al.) (2015)
$T = 1$								
0	7.11E-15	3.64E-11	8.61E-16	8.72E-16	8.72E-16	8.72E-16	1.62E-18	0.00E+00
0.2	1.90E-04	2.49E-09	1.01E-08	1.01E-08	1.01E-08	1.01E-08	1.01E-08	8.51E-06
0.4	3.23E-04	1.46E-08	1.43E-08	1.43E-08	1.43E-08	1.43E-08	1.44E-08	9.18E-06
0.6	3.57E-04	2.37E-08	1.21E-08	1.21E-08	1.21E-08	1.21E-08	1.21E-08	5.60E-06
0.8	3.23E-04	2.58E-08	6.48E-09	6.48E-09	6.48E-09	6.48E-09	6.40E-09	1.34E-06
1	7.11E-15	5.46E-11	5.75E-16	5.71E-16	5.71E-16	5.71E-16	8.65E-20	0.00E+00
$T = 10$								
0	8.67E-19	2.22E-15	4.15E-19	4.14E-19	4.14E-19	4.14E-19	1.87E-22	0.00E+00
0.2	4.35E-08	2.21E-12	1.55E-12	1.55E-12	1.55E-12	1.55E-12	1.51E-12	2.34E-08
0.4	3.82E-08	3.81E-12	1.03E-12	1.03E-12	1.03E-12	1.03E-12	9.78E-13	4.78E-09
0.6	3.33E-08	3.98E-12	4.84E-13	4.84E-13	4.84E-13	4.84E-13	4.52E-13	7.39E-09
0.8	3.11E-08	3.53E-12	7.82E-14	7.82E-14	7.82E-14	7.82E-14	1.01E-13	2.84E-08
1	8.67E-19	2.66E-15	2.74E-19	2.74E-19	2.74E-19	2.74E-19	2.40E-22	0.00E+00

Table 4.6 Comparison of L_∞ error for Example 4.3.3

n	MQ-TR	MQ-QR-CH	IMQ-QR-CH	Sech-QR-CH	GA-QR-CH	GA-QR
Uniform nodes						
6	4.32E-02	1.83E-16	1.80E-16	1.90E-16	1.86E-16	1.85E-16
11	1.03E-07	3.20E-16	3.41E-16	3.30E-16	3.44E-16	1.88E-16
21	1.49E-08	3.31E-14	3.87E-14	3.45E-14	3.41E-14	3.82E-14
31	3.56E-08	2.72E-11	2.86E-11	2.51E-11	3.34E-11	1.53E-12
41	2.33E-08	4.40E-09	4.90E-09	5.85E-09	4.04E-09	1.34E-09
Nonuniform nodes						
6	9.94E-02	1.54E-16	1.59E-16	1.60E-16	1.59E-16	1.61E-16
11	4.30E-08	2.71E-16	2.68E-16	2.77E-16	2.59E-16	2.72E-16
21	6.52E-08	3.17E-16	3.44E-16	3.33E-16	3.68E-16	2.59E-16
31	4.34E-08	6.51E-16	6.45E-16	6.56E-16	6.43E-16	6.52E-16
41	2.21E-08	5.32E-16	5.67E-16	5.43E-16	5.87E-16	5.35E-16

Table 4.7 Absolute error for Example 4.3.3 (n=11)

x	MQ-direct ($\epsilon = 0.1$)	MQ-TR	MQ-QR-CH	IMQ-QR-CH	Sech-QR-CH	GA-QR-CH	GA-QR	HWM (Rehman and Khan) (2012)
0.1	6.70E-10	5.15E-08	1.73E-17	2.26E-17	1.73E-17	1.39E-17	8.67E-18	3.90E-06
0.2	2.00E-10	8.50E-08	1.91E-17	1.56E-17	1.91E-17	1.56E-17	4.51E-17	4.17E-06
0.3	8.96E-09	8.84E-08	1.56E-17	1.08E-17	1.56E-17	8.67E-19	6.03E-17	3.94E-06
0.4	3.56E-08	9.13E-08	3.06E-17	2.44E-17	3.06E-17	9.27E-18	9.37E-17	3.37E-06
0.5	2.72E-08	7.53E-08	8.67E-18	1.65E-17	8.67E-18	3.19E-17	7.50E-17	2.61E-06
0.6	2.86E-08	1.03E-07	1.74E-17	9.23E-18	1.74E-17	4.57E-18	1.26E-16	1.79E-06
0.7	2.68E-09	8.78E-08	3.24E-16	3.33E-16	3.24E-16	3.40E-16	1.88E-16	1.04E-06
0.8	1.88E-09	8.98E-08	3.13E-16	3.22E-16	3.13E-16	3.21E-16	1.50E-16	4.92E-07
0.9	2.81E-09	7.92E-08	2.50E-16	2.60E-16	2.50E-16	2.47E-16	5.41E-17	2.61E-07

Table 4.8 L_∞ error for Example 4.3.4

n	MQ-TR		MQ-QR-CH		MQ-direct			SCM Hatipoglu et al. (2017)	
	$L_\infty error_u$	$L_\infty error_v$	$L_\infty error_u$	$L_\infty error_v$	ϵ	$L_\infty error_u$	$L_\infty error_v$	$L_\infty error_u$	$L_\infty error_v$
Uniform nodes									
6	4.97E+00	3.22E+00	8.88E-16	4.16E-16	0.03	9.38E-02	9.82E-01	9.64E-03	3.15E-03
11	2.05E-04	1.09E-03	3.66E-15	1.50E-15	0.1	2.74E-01	2.57E-01	9.84E-04	4.18E-04
21	1.36E-06	8.36E-06	2.87E-13	1.42E-13	0.3	1.02E-02	1.03E-01	5.08E-05	8.19E-05
31	2.14E-07	1.70E-06	4.82E-11	2.43E-11	0.5	7.31E-03	4.35E-02	-	-
41	5.81E-07	5.15E-06	1.52E-09	3.80E-09	0.5	7.03E-03	4.13E-03	-	-
Nonuniform nodes									
6	1.59E+00	6.88E-01	8.56E-16	1.11E-16	0.03	2.20E-02	4.59E-01	-	-
11	1.61E-06	1.38E-05	1.67E-16	1.11E-16	0.1	1.10E-03	1.97E-02	-	-
21	1.22E-07	1.14E-06	3.84E-16	8.33E-17	0.3	5.57E-03	4.24E-03	-	-
31	4.27E-08	4.59E-07	8.41E-16	8.33E-17	0.5	4.42E-04	1.34E-03	-	-
41	4.29E-08	4.43E-07	2.39E-15	2.22E-16	0.7	9.92E-05	1.72E-04	-	-

Table 4.9 L_∞ error for Example 4.3.4.

n	IMQ-QR-CH		Sech-QR-CH		GA-QR-CH		GA-QR	
	$L_\infty error_u$	$L_\infty error_v$	$L_\infty error_u$	$L_\infty error_v$	$L_\infty error_u$	$L_\infty error_v$	$L_\infty error_u$	$L_\infty error_v$
Uniform nodes								
6	6.66E-16	5.55E-16	7.22E-16	5.00E-16	6.38E-16	5.00E-16	1.11E-16	5.55E-17
11	2.84E-15	1.67E-15	2.65E-15	1.58E-15	2.89E-15	1.40E-15	8.33E-17	1.11E-16
21	2.58E-13	1.46E-13	2.62E-13	1.37E-13	2.85E-13	1.28E-13	1.97E-14	7.41E-15
31	5.71E-11	2.85E-11	4.10E-11	2.25E-11	5.92E-11	2.76E-11	8.35E-12	5.62E-12
41	9.05E-09	1.97E-09	9.45E-09	3.51E-09	3.59E-09	1.06E-09	5.65E-09	3.63E-09
Nonuniform nodes								
6	8.33E-16	8.33E-17	2.22E-16	8.33E-17	7.23E-16	8.33E-17	5.55E-17	1.25E-16
11	1.41E-15	1.39E-16	5.00E-16	1.11E-16	1.46E-15	1.39E-16	6.90E-16	9.71E-17
21	1.37E-15	1.39E-16	6.11E-16	1.11E-16	1.24E-15	1.11E-16	1.37E-15	1.67E-16
31	2.29E-15	1.39E-16	5.69E-16	8.33E-17	7.93E-16	1.11E-16	1.73E-15	1.11E-16
41	2.55E-15	1.11E-16	1.66E-15	2.22E-16	8.88E-16	1.39E-16	2.14E-15	1.39E-16

Table 4.10 Absolute error for Example 4.3.4.

x	MQ-TR (n=41)		MQ-QR-CH (n=11)		IMQ-QR-CH (n=11)		Sech-QR-CH (n=11)	
	$Error_u$	$Error_v$	$Error_u$	$Error_v$	$Error_u$	$Error_v$	$Error_u$	$Error_v$
0	3.26E-09	0	7.97E-17	6.39E-18	1.82E-16	1.22E-17	2.20E-16	3.87E-18
0.1	9.25E-08	1.58E-07	2.94E-15	1.42E-15	2.84E-15	1.50E-15	2.65E-15	1.42E-15
0.4	3.24E-07	6.20E-07	2.94E-15	9.44E-16	2.33E-15	1.14E-15	1.94E-15	1.03E-15
0.5	4.02E-07	7.76E-07	3.00E-15	9.44E-16	2.28E-15	1.11E-15	1.94E-15	1.05E-15
0.9	7.61E-07	1.44E-06	3.66E-15	1.50E-15	2.33E-15	1.67E-15	2.00E-15	1.58E-15
1	8.82E-07	1.62E-06	1.02E-15	3.01E-17	5.89E-16	1.43E-17	1.02E-15	2.21E-17
x	GA-QR-CH (n=11)		GA-QR (n=11)		SCM Hatipoglu et al. (2017) (n=41)			
	$Error_u$	$Error_v$	$Error_u$	$Error_v$	$Error_u$	$Error_v$		
0	7.55E-17	1.02E-17	7.69E-18	5.58E-19	0	0		
0.1	2.87E-15	1.29E-15	1.39E-17	6.94E-17	7.02E-07	1.27E-05		
0.4	2.55E-15	8.88E-16	0.00E+00	2.78E-17	3.71E-06	1.28E-05		
0.5	2.61E-15	8.33E-16	0.00E+00	0.00E+00	3.62E-06	1.14E-05		
0.9	2.83E-15	1.40E-15	0.00E+00	5.55E-17	1.24E-06	8.14E-06		
1	1.20E-16	1.08E-17	5.20E-18	5.48E-18	0	0		

CHAPTER 5

CONCLUSIONS

In the present thesis, we have attempted to extend two radial basis functions based global schemes to a class of fractional nonlinear ordinary differential equations. Referred as direct RBF collocation and integrated RBF collocation (DRBF and IRBF), they are formulated to solve both initial and boundary value problems. Later, direct RBF collocation is extended to fractional Darboux problem, which involves mixed fractional partial derivatives. The main numerical challenge in solving fractional order models using radial functions are obtaining fractional derivatives, which involves integral of radial functions. For polynomial basis, corresponding fractional derivatives in closed form can be readily obtained. To avoid representing the fractional derivatives of RBFs in terms of complex infinite series form, we have chosen to numerically evaluate them using Gauss-Jacobi quadrature method. Desired accuracy is obtained by choosing approximately 6 to 8 quadrature points in one direction.

Since the fractional models considered are of nonlinear in nature, any approximation methods involves linearisation. The linearisation may be done to the continuous nonlinear differential equation model or to the corresponding discretised difference equation model. In this work, we have linearised the given nonlinear fractional differential equations, either via generalised monotone quasilinearisation or successive approximation. Using these proposed iterative processes, the existence and uniqueness of the solution for the problems as well as the convergence of the sequence of solutions of the linear models to the corresponding solution of the nonlinear problems are proved. The monotone nature of the convergence of generalised quasilinearisation is observed in the numerical solutions obtained for the examples. Many model problems are solved using the proposed DRBF and IRBF methods and then compared with solutions obtained using other numerical/semi-analytical methods in the literature.

In spite of high accuracy and order of convergence, radial functions based schemes often suffer instability due to ill-conditioning of the discretised system. i.e., RBFs are sensitive to both shape parameter and closeness of the nodal points in the domain. This disadvantage is observed even while approximating fractional order derivatives. Hence an effort is made to extend Tikhonov regularisation and RBF-QR algorithms in the stable computation of fractional derivatives and then to solve fractional differential equations using RBF based schemes. Further, RBF-QR algorithm is generalised to include more class of radial functions (RBF-QR-CH), wherein the algorithm was earlier restricted to Gaussian RBF.

Some of the observations based on the above mentioned works are:

- Being global methods, RBF based collocation schemes (DRBF and IRBF) produce very accurate results for considerably small nodal distributions.
- While both DRBF and IRBF yield very accurate solutions with small set of nodes for problems with derivative order q close to corresponding order of the classical problem ($q = 1$ or 2 for the examples considered), DRBF demands increase in quadrature points for accurate solutions. However, IRBF scheme is robust in terms of rate of convergence, required number of quadrature points for the effective implementation of Gauss-Jacobi rule and the convergence of quasilinearisation even for smaller q values.
- For all the examples considered, the conditions are verified to confirm that the iterative techniques are convergent. The conditions given in the main theorem can be easily verified. Monotone nature of the proposed quasilinearisation is observed in all the examples chosen.
- Another interesting observation is that appending polynomial to polyharmonic splines has significantly improved the accuracy of the solutions. This characteristics is recently analysed in detail by Flyer et al. (2016).
- Implementation of variable shape parameters in DRBF scheme for fractional Darboux model has helped in stabilising the scheme moderately.
- Leave-one-out cross validation (LOOCV) algorithm is effectively implemented and verified that optimal shape parameter ϵ_{opt} values obtained using LOOCV matches closely with that is estimated through trial and error approach.
- An extension of RBF-QR algorithm by Fornberg et al. (2011) to fractional model

problems are proposed. Further, the algorithm is generalised/extended to include more class of radial functions.

- An extension of Tikhonov regularisation to RBF collocation system obtained by discretising fractional order differential equations is made. Singular value decomposition and generalised cross validation are implemented to make the regularisation computationally robust.

5.1 SCOPE FOR THE FUTUTE RESEARCH

The interest towards fractional order models in applications have increased in the last two decades (See Chapter 1). This necessitate the need for the development of robust numerical methods to solve practical problems. The work done in this thesis is a step forward in this direction. During the present study and implementation of the proposed radial functions based schemes to various fractional order differential equations, we have observed a few issues that may be addressed to widen the applicability of RBF based schemes. Some of them are,

- It may be noted that integrated RBF (IRBF) scheme is formulated only for fractional ordinary differential equations. Effective formulation of the scheme to higher dimensional problems is an interesting and challenging problem.
- Present work does not completely exploit the naturally gridfree nature of radial functions. However, the optimal nodal distribution is problem dependent. Hence, solving application problems that involves fractional derivatives that demands flexible nodal distribution can be an important contribution to scientific community.
- Possible extension of RBF-QR-CH algorithm to higher dimension is an interesting work that needs further exploration. The works done on RBF-QR by Fornberg and co-authors with respect to Gaussian radial function can give an insight into these possibilities.

REFERENCES

- Abbas, S., Benchohra, M., and N'Guérékata, G. M. (2012). *Topics in fractional differential equations*, volume 27 of *Developments in Mathematics*. Springer, New York.
- Agarwal, R. P., Benchohra, M., and Hamani, S. (2010). A survey on existence results for boundary value problems of nonlinear fractional differential equations and inclusions. *Acta Appl. Math.*, 109(3):973–1033.
- Agrawal, O. P. (2002). Solution for a fractional diffusion-wave equation defined in a bounded domain. *Nonlinear Dynam.*, 29(1-4):145–155.
- Al-Bassam, M. A. (1965). Some existence theorems on differential equations of generalized order. *J. Reine Angew. Math.*, 218:70–78.
- Antunes, P. R. S. and Ferreira, R. A. C. (2015). An augmented-RBF method for solving fractional Sturm-Liouville eigenvalue problems. *SIAM J. Sci. Comput.*, 37(1):A515–A535.
- Area, I., Losada, J., and Nieto, J. J. (2016). A note on the fractional logistic equation. *Phys. A*, 444:182 – 187.
- Arghand, M. and Amirfakhrian, M. (2015). A meshless method based on the fundamental solution and radial basis function for solving an inverse heat conduction problem. *Adv. Math. Phys.*, pages Art. ID 256726, 8.
- Aslefallah, M. and Shivanian, E. (2015). Nonlinear fractional integro-differential reaction-diffusion equation via radial basis functions. *Eur. Phys. J. Plus*, 130(3):47.
- Ateş, I. and Zegeling, P. A. (2017). A homotopy perturbation method for fractional-order advection-diffusion-reaction boundary-value problems. *Appl. Math. Model.*, 47:425–441.

- Bagley, R. L. and Torvik, P. (1983). A theoretical basis for the application of fractional calculus to viscoelasticity. *J. Rheol.*, 27(3):201–210.
- Beatson, R. K., Cherrie, J. B., and Mouat, C. T. (1999). Fast fitting of radial basis functions: Methods based on preconditioned GMRES iteration. *Adv. Comput. Math.*, 11(2-3):253–270.
- Ben-Israel, A. and Greville, T. N. (2003). *Generalized Inverses: Theory and Applications*, volume 15. Springer Science & Business Media.
- Blair, G. S. and Reiner, M. (1951). The rheological law underlying the Nutting equation. *Appl. sci. Res.*, 2(1):225.
- Blank, L. (1996). Numerical treatment of differential equations of fractional order. *Numerical Analysis Report 287, Manchester Centre for Computational Mathematics, Manchester.*
- Brunner, H., Ling, L., and Yamamoto, M. (2010). Numerical simulations of 2D fractional subdiffusion problems. *J. Comput. Phys.*, 229(18):6613–6622.
- Buhmann, M. D. (2003). *Radial basis functions: Theory and Implementations*, volume 12 of *Cambridge Monographs on Applied and Computational Mathematics*. Cambridge University Press, Cambridge.
- Butera, S. and Di Paola, M. (2015). Mellin transform approach for the solution of coupled systems of fractional differential equations. *Commun. Nonlinear Sci. Numer. Simul.*, 20(1):32–38.
- Cang, J., Tan, Y., Xu, H., and Liao, S.-J. (2009). Series solutions of non-linear Riccati differential equations with fractional order. *Chaos Solitons Fractals*, 40(1):1–9.
- Caputo, M. and Mainardi, F. (1971). A new dissipation model based on memory mechanism. *Pure Appl. Geophys.*, 91(1):134–147.
- Carlson, R. E. and Foley, T. A. (1991). The parameter R^2 in multiquadric interpolation. *Comput. Math. Appl.*, 21(9):29–42.
- Chandhini, G. and Sanyasiraju, Y. V. S. S. (2007). Local RBF-FD solutions for steady convection-diffusion problems. *Internat. J. Numer. Methods Engrg.*, 72(3):352–378.
- Chen, C. S., Karageorghis, A., and Li, Y. (2016). On choosing the location of the sources in the MFS. *Numer. Algorithms*, 72(1):107–130.

- Chen, W., Fu, Z. J., and Chen, C. S. (2014). *Recent advances in radial basis function collocation methods*. Springer Briefs in Applied Sciences and Technology. Springer, Heidelberg.
- Chen, W., Sun, H., Zhang, X., and Korošak, D. (2010a). Anomalous diffusion modeling by fractal and fractional derivatives. *Comput. Math. Appl.*, 59(5):1754–1758.
- Chen, W., Ye, L., and Sun, H. (2010b). Fractional diffusion equations by the Kansa method. *Comput. Math. Appl.*, 59(5):1614–1620.
- Cheung, K. C., Ling, L., and Ruuth, S. J. (2015). A localized meshless method for diffusion on folded surfaces. *J. Comput. Phys.*, 297:194–206.
- Cheung, T. Y. (1977). Three nonlinear initial value problems of the hyperbolic type. *SIAM J. Numer. Anal.*, 14(3):484–491.
- Ciuchi, F., Mazzulla, A., Scaramuzza, N., Lenzi, E., and Evangelista, L. (2012). Fractional diffusion equation and the electrical impedance: Experimental evidence in liquid-crystalline cells. *J. Phys. Chem. C*, 116(15):8773–8777.
- Człapiński, T. (1999). Difference methods for the Darboux problem for functional partial differential equations. *Ann. Polon. Math.*, 71(2):171–193.
- Day, J. T. (1966). A Runge-Kutta method for the numerical solution of the Goursat problem in hyperbolic partial differential equations. *Comput. J.*, 9(1):81–83.
- Dehghan, M., Abbaszadeh, M., and Mohebbi, A. (2015). An implicit RBF meshless approach for solving the time fractional nonlinear sine-Gordon and Klein-Gordon equations. *Eng. Anal. Bound. Elem.*, 50:412–434.
- Dehghan, M., Abbaszadeh, M., and Mohebbi, A. (2016). Analysis of a meshless method for the time fractional diffusion-wave equation. *Numer. Algorithms*, 73(2):445–476.
- Dehghan, M. and Najafi, M. (2016). Numerical solution of a non-classical two-phase Stefan problem via radial basis function (RBF) collocation methods. *Eng. Anal. Bound. Elem.*, 72:111–127.
- Delbosco, D. and Rodino, L. (1996). Existence and uniqueness for non-linear fractional differential equations. *J. Math. Anal. Appl.*, 204:609–625.
- Deng, W. (2008). Finite element method for the space and time fractional Fokker-Planck equation. *SIAM J. Numer. Anal.*, 47(1):204–226.

- Denton, Z., Ng, P., and Vatsala, A. (2011). Quasilinearization method via lower and upper solutions for Riemann-Liouville fractional differential equation. *Nonlinear Dyn. Syst. Theory*, 11(3):239–252.
- Devi, J. V., McRae, F. A., and Drici, Z. (2010). Generalized quasilinearization for fractional differential equations. *Comput. Math. Appl.*, 59(3):1057–1062.
- Diethelm, K. (2010). *The analysis of fractional differential equations*. CRC Press.
- Diethelm, K. and Freed, A. D. (1999). *On the solution of nonlinear fractional-order differential equations used in the modeling of viscoplasticity*. Springer.
- Duchon, J. (1977). Splines minimizing rotation-invariant semi-norms in Sobolev spaces. pages 85–100. Lecture Notes in Math., Vol. 571.
- Ertürk, V. S. and Momani, S. (2008). Solving systems of fractional differential equations using differential transform method. *J. Comput. Appl. Math.*, 215(1):142–151.
- Ervin, V. J., Heuer, N., and Roop, J. P. (2007). Numerical approximation of a time dependent, nonlinear, space-fractional diffusion equation. *SIAM J. Numer. Anal.*, 45(2):572–591.
- Evans, D. J. and Sanugi, B. B. (1988). Numerical solution of the Goursat problem by a nonlinear trapezoidal formula. *Appl. Math. Lett.*, 1(3):221–223.
- Faber, T., Jaishankar, A., and McKinley, G. (2017). Describing the firmness, springiness and rubberiness of food gels using fractional calculus. Part I: Theoretical framework. *Food Hydrocolloids*, 62:311 – 324.
- Fakhr Kazemi, B. and Ghoreishi, F. (2013). Error estimate in fractional differential equations using multiquadratic radial basis functions. *J. Comput. Appl. Math.*, 245:133–147.
- Fasshauer, G. E. and McCourt, M. J. (2012). Stable evaluation of Gaussian radial basis function interpolants. *SIAM J. Sci. Comput.*, 34(2):A737–A762.
- Fasshauer, G. E. and Zhang, J. G. (2007). On choosing “optimal” shape parameters for RBF approximation. *Numer. Algorithms*, 45(1-4):345–368.
- Fasshauer, G. F. (2007). *Meshfree approximation methods with MATLAB*, volume 6 of *Interdisciplinary Mathematical Sciences*. World Scientific.

- Fellah, M., Fellah, Z. E. A., and Depollier, C. (2006). Transient wave propagation in inhomogeneous porous materials: Application of fractional derivatives. *Signal Process.*, 86(10):2658–2667.
- Flyer, N., Fornberg, B., Bayona, V., and Barnett, G. A. (2016). On the role of polynomials in RBF-FD approximations: I. Interpolation and accuracy. *J. Comput. Phys.*, 321:21–38.
- Fornberg, B. and Flyer, N. (2015). *A primer on radial basis functions with applications to the geosciences*, volume 87 of *CBMS-NSF Regional Conference Series in Applied Mathematics*. Society for Industrial and Applied Mathematics (SIAM), Philadelphia, PA.
- Fornberg, B., Larsson, E., and Flyer, N. (2011). Stable computations with Gaussian radial basis functions. *SIAM J. Sci. Comput.*, 33(2):869–892.
- Fornberg, B. and Piret, C. (2007). A stable algorithm for flat radial basis functions on a sphere. *SIAM J. Sci. Comput.*, 30(1):60–80.
- Fornberg, B. and Wright, G. (2004). Stable computation of multiquadric interpolants for all values of the shape parameter. *Comput. Math. Appl.*, 48(5-6):853–867.
- Franke, R. (1982). Scattered data interpolation: Tests of some methods. *Math. Comp.*, 38(157):181–200.
- Galeone, L. and Garrappa, R. (2008). Fractional Adams-Moulton methods. *Math. Comput. Simulation*, 79(4):1358–1367.
- Ghehsareh, H. R., Heydari Bateni, S., and Zaghian, A. (2015). A meshfree method based on the radial basis functions for solution of two-dimensional fractional evolution equation. *Eng. Anal. Bound. Elem.*, 61:52–60.
- Golbabai, A., Mohebianfar, E., and Rabiei, H. (2015). On the new variable shape parameter strategies for radial basis functions. *Comp. Appl. Math.*, (34):691–704.
- Gonzalez-Rodriguez, P., Bayona, V., Moscoso, M., and Kindelan, M. (2015). Laurent series based RBF-FD method to avoid ill-conditioning. *Eng. Anal. Bound. Elem.*, 52:24–31.
- Gou, K. and Sun, B. (2011). Numerical solution of the Goursat problem on a triangular domain with mixed boundary conditions. *Appl. Math. Comput.*, 217(21):8765–8777.

- Gourlay, A. R. (1970). A note on trapezoidal methods for the solution of initial value problems. *Math. Comp.*, 24:629–633.
- Hale, N. and Townsend, A. (2013). Fast and accurate computation of Gauss-Legendre and Gauss-Jacobi quadrature nodes and weights. *SIAM J. Sci. Comput.*, 35(2):A652–A674.
- Hamarsheh, M., Ismail, A. M., et al. (2017). Analytical approximation for fractional order logistic equation. *Int. J. Pure Appl. Math.*, 115(2):225–245.
- Hanert, E. and Piret, C. (2014). A Chebyshev pseudospectral method to solve the space-time tempered fractional diffusion equation. *SIAM J. Sci. Comput.*, 36(4):A1797–A1812.
- Hansen, P. C. and O’Leary, D. P. (1993). The use of the L -curve in the regularization of discrete ill-posed problems. *SIAM J. Sci. Comput.*, 14(6):1487–1503.
- Hardy, R. L. (1971). Multiquadric equations of topography and other irregular surfaces. *J. Geophys. Res.*, 76(8):1905–1915.
- Hatipoglu, V. F., Alkan, S., and Secer, A. (2017). An efficient scheme for solving a system of fractional differential equations with boundary conditions. *Adv. Difference Equ.*, pages 2017:204, 13.
- He, J.-H. (1998). Approximate analytical solution for seepage flow with fractional derivatives in porous media. *Comput. Methods Appl. Mech. Engrg.*, 167(1-2):57–68.
- Hosseini, V. R., Chen, W., and Avazzadeh, Z. (2014). Numerical solution of fractional telegraph equation by using radial basis functions. *Eng. Anal. Bound. Elem.*, 38:31–39.
- Ilati, M. and Dehghan, M. (2015). The use of radial basis functions (RBFs) collocation and RBF-QR methods for solving the coupled nonlinear sine-Gordon equations. *Eng. Anal. Bound. Elem.*, 52:99–109.
- Jafari, H. and Daftardar-Gejji, V. (2006). Solving a system of nonlinear fractional differential equations using Adomian decomposition. *J. Comput. Appl. Math.*, 196(2):644–651.
- Jain, M. K. and Sharma, K. D. (1968). Cubature method for the numerical solution of the characteristic initial value problem $u_{xy} = f(x, y, u, u_x, u_y)$. *J. Austral. Math. Soc.*, 8:355–368.

- Jaishankar, A. and McKinley, G. H. (2012). Power-law rheology in the bulk and at the interface: quasi-properties and fractional constitutive equations. *Proc. R. Soc. Lond. Ser. A Math. Phys. Eng. Sci.*, 469(2149):20120284, 18.
- Jang, B. (2014). Efficient analytic method for solving nonlinear fractional differential equations. *Appl. Math. Modelling*, 38(5):1775 – 1787.
- Kansa, E. J. (1990). Multiquadrics - a scattered data approximation scheme with applications to computational fluid-dynamics - II. Solutions to parabolic, hyperbolic and elliptic partial differential equations. *Comput. Math. Appl.*, 19(8):147–161.
- Khader, M. M. (2011). On the numerical solutions for the fractional diffusion equation. *Commun. Nonlinear Sci. Numer. Simul.*, 16(6):2535–2542.
- Kilbas, A. A., Marichev, O. I., and Samko, S. G. (1993). *Fractional Integral and Derivatives (Theory and Applications)*. Gordon and Breach Science.
- Lakshmikantham, V., Carl, S., and Heikkilä, S. (2009). Fixed point theorems in ordered Banach spaces via quasilinearization. *Nonlinear Anal.*, 71(7-8):3448–3458.
- Li, C., Yi, Q., and Chen, A. (2016). Finite difference methods with non-uniform meshes for nonlinear fractional differential equations. *J. Comput. Phys.*, 316:614–631.
- Li, C., Zhao, Z., and Chen, Y. (2011). Numerical approximation of nonlinear fractional differential equations with subdiffusion and superdiffusion. *Comput. Math. Appl.*, 62(3):855–875.
- Lin, J., Chen, W., and Sze, K. (2012). A new radial basis function for Helmholtz problems. *Eng. Anal. Bound. Elem.*, 36(12):1923–1930.
- Lin, Z., Liu, F., Wang, D., and Gu, Y. (2018). Reproducing kernel particle method for two-dimensional time-space fractional diffusion equations in irregular domains. *Eng. Anal. Bound. Elem.*, 97:131–143.
- Ling, L. and Kansa, E. J. (2005). A least-squares preconditioner for radial basis functions collocation methods. *Adv. Comput. Math.*, 23(1-2):31–54.
- Liu, F., Zhuang, P., Turner, I., Burrage, K., and Anh, V. (2014a). A new fractional finite volume method for solving the fractional diffusion equation. *Appl. Math. Model.*, 38(15-16):3871–3878.

- Liu, Q., Gu, Y. T., Zhuang, P., Liu, F., and Nie, Y. F. (2011). An implicit RBF meshless approach for time fractional diffusion equations. *Comput. Mech.*, 48(1):1–12.
- Liu, Q., Liu, F., Gu, Y. T., Zhuang, P., Chen, J., and Turner, I. (2015). A meshless method based on point interpolation method (PIM) for the space fractional diffusion equation. *Appl. Math. Comput.*, 256:930–938.
- Liu, Q., Liu, F., Turner, I., Anh, V., and Gu, Y. (2014b). A RBF meshless approach for modeling a fractal mobile/immobile transport model. *Appl. Math. Comput.*, 226:336–347.
- Lubich, C. (1986). Discretized fractional calculus. *SIAM J. Math. Anal.*, 17(3):704–719.
- Magin, R. L. (2006). *Fractional calculus in bioengineering*. Begell House Redding.
- Mai-Duy, N. and Tran-Cong, T. (2001). Numerical solution of differential equations using multiquadric radial basis function networks. *Neural Networks*, 14(2):185–199.
- Mainardi, F., Luchko, Y., and Pagnini, P. (2001). The fundamental solution of the space-time fractional diffusion equation. *Frac. Calculus Appl. Anal*, 4:153–192.
- Mao, Z. and Karniadakis, G. E. (2017). Fractional Burgers equation with nonlinear non-locality: spectral vanishing viscosity and local discontinuous Galerkin methods. *J. Comput. Phys.*, 336:143–163.
- Meerschaert, M. M. and Tadjeran, C. (2004). Finite difference approximations for fractional advection-dispersion flow equations. *J. Comput. Appl. Math.*, 172(1):65–77.
- Micchelli, C. A. (1986). Interpolation of scattered data: Distance matrices and conditionally positive definite functions. *Constr. Approx.*, 2(1):11–22.
- Miller, K. and Samko, S. (2001). Completely monotonic functions. *Integr. Trans. and Spec. Funct.*, 12:389–402.
- Miller, K. S. and Ross, B. (1993). *An Introduction to the Fractional Calculus and Fractional Differential Equations*. Wiley.
- Mohammadi, F. and Cattani, C. (2018). A generalized fractional-order Legendre wavelet Tau method for solving fractional differential equations. *J. Comput. Appl. Math.*, 339:306–316.

- Mohammadi, M. and Schaback, R. On the fractional derivatives of radial basis functions.
- Mohebbi, A., Abbaszadeh, M., and Dehghan, M. (2013). The use of a meshless technique based on collocation and radial basis functions for solving the time fractional nonlinear Schrödinger equation arising in quantum mechanics. *Eng. Anal. Bound. Elem.*, 37(2):475–485.
- Mustapha, K. and McLean, W. (2013). Superconvergence of a discontinuous Galerkin method for fractional diffusion and wave equations. *SIAM J. Numer. Anal.*, 51(1):491–515.
- Neumaier, A. (1998). Solving ill-conditioned and singular linear systems: A tutorial on regularization. *SIAM Rev.*, 40(3):636–666.
- Nutting, P. (1921). A new general law of deformation. *J. Franklin Inst.*, 191(3):679–685.
- Odibat, Z. and Momani, S. (2008). Modified homotopy perturbation method: Application to quadratic Riccati differential equation of fractional order. *Chaos Solitons Fractals*, 36(1):167–174.
- Oldham, K. B. (1972). Signal-independent electroanalytical method. *Anal. Chem.*, 44(1):196–198.
- Oldham, K. B. and Spanier, J. (1974). *The fractional calculus : Theory and Applications of Differentiation and Integration to Arbitrary Order*. Mathematics in science and engineering. Academic Press, New York.
- Pang, G., Chen, W., and Fu, Z. (2015). Space-fractional advection-dispersion equations by the Kansa method. *J. Comput. Phys.*, 293:280 – 296.
- Piret, C. and Hanert, E. (2013). A radial basis functions method for fractional diffusion equations. *J. Comput. Phys.*, 238:71–81.
- Podlubny, I. (1998). *Fractional differential equations: An introduction to fractional derivatives, fractional differential equations, to methods of their solution and some of their applications*, volume 198. Academic press.
- Qu, H. and Liu, X. (2015). A numerical method for solving fractional differential equations by using neural network. *Adv. Math. Phys.*, pages Art. ID 439526, 1–12.

- Rehman, M. u. and Khan, R. A. (2012). A numerical method for solving boundary value problems for fractional differential equations. *Appl. Math. Model.*, 36(3):894–907.
- Rippa, S. (1999). An algorithm for selecting a good value for the parameter c in radial basis function interpolation. *Adv. Comput. Math.*, 11(2-3):193–210.
- Roque, C. M. C. and Ferreira, A. J. M. (2010). Numerical experiments on optimal shape parameters for radial basis functions. *Numer. Methods Partial Differential Equations*, 26(3):675–689.
- Roy, R., Vijesh, V. A., and Chandhini, G. (2018). Iterative methods for a fractional order volterra population model. *J. Integral Equations Applications*.
- Saeed, U. and ur Rehman, M. (2013). Haar wavelet-quasilinearization technique for fractional nonlinear differential equations. *Appl. Math. Comput.*, 220:630–648.
- Saichev, A. I. and Zaslavsky, G. M. (1997). Fractional kinetic equations: Solutions and Applications. *Chaos*, 7(4):753–764.
- Sanyasiraju, Y. and Satyanarayana, C. (2013). On optimization of the RBF shape parameter in a grid-free local scheme for convection dominated problems over non-uniform centers. *Appl. Math. Modelling*, 37(12-13):7245–7272.
- Sarra, S. A. (2014). Regularized symmetric positive definite matrix factorizations for linear systems arising from RBF interpolation and differentiation. *Eng. Anal. Bound. Elem.*, 44:76–86.
- Sarra, S. A. and Sturgill, D. (2009). A random variable shape parameter strategy for radial basis function approximation methods. *Eng. Anal. Bound. Elem.*, 33(11):1239 – 1245.
- Schaback, R. (1995). Error estimates and condition numbers for radial basis function interpolation. *Adv. Comput. Math.*, 3(3):251–264.
- Schneider, W. (1996). Completely monotone generalised Mittag-Leffler functions. *Expo. Math.*, 14:3–16.
- Schoenberg, I. J. (1938). Metric spaces and completely monotone functions. *Ann. of Math. (2)*, 39(4):811–841.
- Shawagfeh, N. T. (1999). The decomposition method for fractional differential equations. *J. Frac. Calc.*, 16:27–33.

- Shirzadi, A., Ling, L., and Abbasbandy, S. (2012). Meshless simulations of the two-dimensional fractional-time convection-diffusion-reaction equations. *Eng. Anal. Bound. Elem.*, 36:1522–1527.
- Simmons, A., Yang, Q., and Moroney, T. (2017). A finite volume method for two-sided fractional diffusion equations on non-uniform meshes. *J. Comput. Phys.*, 335:747–759.
- Song, L. and Zhang, H. (2007). Application of homotopy analysis method to fractional KdV-Burgers-Kuramoto equation. *Phys. Lett. A*, 367(1-2):88–94.
- Sousa, E. I. (2009). Finite difference approximations for a fractional advection diffusion problem. *J. Comput. Phys.*, 228(11):4038–4054.
- Sugimoto, N. (1991). Burgers equation with a fractional derivative; hereditary effects on nonlinear acoustic waves. *J. Fluid Mech.*, 225:631–653.
- Sun, H., Liu, X., Zhang, Y., Pang, G., and Garrard, R. (2017). A fast semi-discrete Kansa method to solve the two-dimensional spatiotemporal fractional diffusion equation. *J. Comput. Phys.*, 345:74–90.
- Sweilam, N. H., Nagy, A. M., and El-Sayed, A. A. (2015). Second kind shifted Chebyshev polynomials for solving space fractional order diffusion equation. *Chaos Solitons Fractals*, 73:141–147.
- Uddin, M. and Haq, S. (2011). RBFs approximation method for time fractional partial differential equations. *Commun. Nonlinear Sci. Numer. Simul.*, 16(11):4208–4214.
- Vijesh, V. A. and Kumar, K. (2015). Wavelet based quasilinearization method for semi-linear parabolic initial boundary value problems. *Appl. Math. Comp.*, 266:1163–1176.
- Vityuk, A. and Mykhailenko, A. (2011). The Darboux problem for an implicit fractional-order differential equation. *J. Math. Sci. (N. Y.)*, 175(4):391–401.
- Wang, L., Sun, D., Li, P., and Xie, Y. (2017). Semi-analytical solution for one-dimensional consolidation of fractional derivative viscoelastic saturated soils. *Comput. Geotech.*, 83:30–39.
- Wazwaz, A. M. (1993). On the numerical solution of the Goursat problem. *Appl. Math. Comput.*, 59(1):89–95.

- West, B. J. (2015). Exact solution to fractional logistic equation. *Phys. A*, 429:103 – 108.
- West, B. J. and Nonnenmacher, T. (2001). An ant in a gurge. *Phys. Lett. A*, 278(5):255–259.
- Wright, G. B. and Fornberg, B. (2006). Scattered node compact finite difference-type formulas generated from radial basis functions. *J. Comput. Phys.*, 212(1):99–123.
- Wright, G. B. and Fornberg, B. (2017). Stable computations with flat radial basis functions using vector-valued rational approximations. *J. Comput. Phys.*, 331:137–156.
- Wu, G.-c. and Lee, E. W. M. (2010). Fractional variational iteration method and its application. *Phys. Lett. A*, 374(25):2506–2509.
- Wu, Y. L. and Shu, C. (2002). Development of RBF-DQ method for derivative approximation and its application to simulate natural convection in concentric annuli. *Comput. Mech.*, 29:477–485.
- Yakar, A. (2012). Initial time difference quasilinearization for Caputo fractional differential equations. *Adv. Difference Equ.*, pages 2012:92, 9.
- Yan, L. and Yang, F. (2015). The method of approximate particular solutions for the time-fractional diffusion equation with a non-local boundary condition. *Comput. Math. Appl.*, 70(3):254 – 264.
- Yang, J. Y., Zhao, Y. M., Liu, N., Bu, W. P., Xu, T. L., and Tang, Y. F. (2015). An implicit MLS meshless method for 2-D time dependent fractional diffusion-wave equation. *Appl. Math. Model.*, 39(3-4):1229–1240.
- Yang, Q., Turner, I., Liu, F., and Ilić, M. (2011). Novel numerical methods for solving the time-space fractional diffusion equation in two dimensions. *SIAM J. Sci. Comput.*, 33(3):1159–1180.
- Yang, Y., Huang, Y., and Zhou, Y. (2018). Numerical solutions for solving time fractional Fokker-Planck equations based on spectral collocation methods. *J. Comput. Appl. Math.*, 339:389–404.
- Zayernouri, M. and Karniadakis, G. E. (2014). Fractional spectral collocation method. *SIAM J. Sci. Comput.*, 36:A40–A62.

- Zhang, S. (2000). The existence of a positive solution for a nonlinear fractional differential equation. *J. Math. Anal. Appl.*, 252(2):804–812.
- Zhang, X., Crawford, J. W., Deeks, L. K., Stutter, M. I., Bengough, A. G., and Young, I. M. (2005). A mass balance based numerical method for the fractional advection-dispersion equation: Theory and application. *Water Resour. Res.*, 41(7).
- Zhang, Y.-F. and Li, C.-J. (2016). A Gaussian RBFs method with regularization for the numerical solution of inverse heat conduction problems. *Inverse Probl. Sci. Eng.*, 24(9):1606–1646.
- Zhu, L. and Fan, Q. (2012). Solving fractional nonlinear Fredholm integro-differential equations by the second kind Chebyshev wavelet. *Commun. Nonlinear Sci. Numer. Simul.*, 17(6):2333–2341.
- Zhu, X. G., Yuan, Z. B., Liu, F., and Nie, Y. F. (2018). Differential quadrature method for space-fractional diffusion equations on 2D irregular domains. *Numerical Algorithms*, pages 1–25.
- Zhuang, P., Liu, F., Anh, V., and Turner, I. (2008). New solution and analytical techniques of the implicit numerical method for the anomalous subdiffusion equation. *SIAM J. Numer. Anal.*, 46(2):1079–1095.

PUBLICATIONS

International Journals:

1. Chandhini, G., Prashanthi, K. S., and Vijesh, V. A. (2018). A radial basis function method for fractional Darboux problems. *Eng. Anal. Bound. Elem.*, 86:1-18.
2. Prashanthi, K. S. and Chandhini, G. Regularization of highly ill-conditioned RBF asymmetric collocation systems in fractional models. In: V. K. Singh et al. (eds.), *Advances in Mathematical Methods and High Performance Computing*, Advances in Mechanics and Mathematics, 41, Springer. *In press*.
3. Chandhini, G., Prashanthi, K. S. and Vijesh, V. A. Direct and integrated radial functions based quasilinearization schemes for nonlinear fractional differential equations. *BIT Numerical Mathematics*. *Under review*.
4. Chandhini, G., Prashanthi, K. S. On stabilization of radial functions based schemes for fractional derivatives. *Under preparation*.

BIODATA

Name : Prashanthi K. S.
Email : ksprashanthi@gmail.com
Date of Birth : 27 March 1983.
Contact No : +91-9611627987 / 9964498515
Permanent address : W/o Ramesh M.,
Lalitha Nilaya,
Gundaje (Darikere),
Karkala Post and Taluk,
Udupi District,
Karnataka

Educational Qualifications :

Degree	Year	Institution / University
B.Sc.	2003	St. Agnes Collage, Mangalore
M.Sc. (Mathematics)	2005	Mangalore University, Mangalore